COLLEGE PARK CAMPUS

STUDY OF SUPERCONVERGENCE BY A COMPUTER-BASED APPROACH

SUPERCONVERGENCE OF THE GRADIENT OF THE DISPLACEMENT, THE STRAIN AND STRESS IN FINITE ELEMENT SOLUTIONS FOR PLANE ELASTICITY

by

I. Babuška
T. Strouboulis
C. S. Upadhyay
S. K. Gangaraj

Technical Note BN-1166

and

CMC Report No. 94-02
Texas Engineering Experiment Station
The Texas A&M University System

February 1994

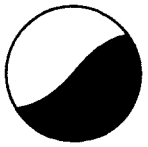

INSTITUTE FOR PHYSICAL SCIENCE AND TECHNOLOGY

SECURITY CLASSIFICATION OF THIS PAGE (When Data Entered)

REPORT DOCUMENTATION PAGE		READ INSTRUCTIONS BEFORE COMPLETING FORM
1. REPORT NUMBER Technical Note BN-1166	2. GOVT ACCESSION NO.	3. RECIPIENT'S CATALOG NUMBER
4. TITLE (and Subtitle) Study of Superconvergence by a Computer-Based Approach - Superconvergence of the Gradient of the Displacement, The Strain and Stress in Finite Element Solutions for Plane Elasticity		5. TYPE OF REPORT & PERIOD COVERED Final Life of Contract 6. PERFORMING ORG. REPORT NUMBER
7. AUTHOR(s) I. Babuska[1] - T. Strouboulis[2] - C.S. Upadhyay[2] S.K. Gangaraj[2]		8. CONTRACT OR GRANT NUMBER(s) [1]N00014-90-J-1030 ONR & [2]CCR-88-20279/NSF [2]See Page 1
9. PERFORMING ORGANIZATION NAME AND ADDRESS Institute for Physical Science and Technology University of Maryland College Park, MD 20742-2431		10. PROGRAM ELEMENT, PROJECT, TASK AREA & WORK UNIT NUMBERS
11. CONTROLLING OFFICE NAME AND ADDRESS Department of the Navy Office of Naval Research Arlington, VA 22217		12. REPORT DATE February 1994 13. NUMBER OF PAGES 41 - Figs. 1 - 14c/47 pgs.
14. MONITORING AGENCY NAME & ADDRESS(if different from Controlling Office)		15. SECURITY CLASS. (of this report) 15a. DECLASSIFICATION/DOWNGRADING SCHEDULE

16. DISTRIBUTION STATEMENT (of this Report)

Approved for public release: distribution unlimited

17. DISTRIBUTION STATEMENT (of the abstract entered in Block 20, if different from Report)

18. SUPPLEMENTARY NOTES

19. KEY WORDS (Continue on reverse side if necessary and identify by block number)

20. ABSTRACT In [1] we addressed the problem of existence of superconvergence points by a computer-based proof and we gave a detailed study of the superconvergence points for the components of the gradient in finite element solutions for Laplace's and Poisson's equations. Here we employ the same approach to study the superconvergence for the gradient of the displacement, the strain and the stress for finite element solutions of the equations of plane elasticity. We give the superconvergence points for the components of the gradient of the displacement, the strain and stress for meshes of triangles and squares of degree p, $1 \leq p \leq 4$. For the meshes of triangles we investigated the effect of the topology of the mesh by considering four mesh-patterns which typically occur in practical meshes, while in the case of squares elements we studied the effect of the element-type (tensor-product, serendipity or other).

DD FORM 1 JAN 73 1473 EDITION OF 1 NOV 65 IS OBSOLETE

S N 0102-LF-014-6601

SECURITY CLASSIFICATION OF THIS PAGE (When Data Entered)

Study of Superconvergence by a Computer-Based Approach. Superconvergence of the Gradient of the Displacement, the Strain and Stress in Finite Element Solutions for Plane Elasticity

I. Babuška*
Institute for Physical Science and Technology and Department of Mathematics,
University of Maryland, College Park, MD 20742, U.S.A.

T. Strouboulis†, C.S. Upadhyay† and S.K. Gangaraj†
Department of Aerospace Engineering, Texas A&M University,
College Station, TX 77843, U.S.A.

February 1994

*The work of this author was supported by the U.S. Office of Naval Research under Contract N00014-90-J-1030 and by the National Science Foundation under Grant CCR-88-20279.

†The work of these authors was supported by the U.S. Army Research Office under Grant DAAL03-G-028, by the National Science Foundation under Grant MSS-9025110 and by the Texas Advanced Research Program under Grant TARP-71071.

Abstract

In [1] we addressed the problem of existence of superconvergence points by a computer-based proof and we gave a detailed study of the superconvergence points for the components of the gradient in finite element solutions for Laplace's and Poisson's equations. Here we employ the same approach to study the superconvergence for the gradient of the displacement, the strain and the stress for finite element solutions of the equations of plane elasticity. We give the superconvergence points for the components of the gradient of the displacement, the strain and stress for meshes of triangles and squares of degree p, $1 \leq p \leq 4$. For the meshes of triangles we investigated the effect of the topology of the mesh by considering four mesh-patterns which typically occur in practical meshes, while in the case of square elements we studied the effect of the element-type (tensor-product, serendipity or other).

1 Introduction

In [1] we introduced a computer-based approach for finding the superconvergence points for the derivatives in finite element approximations of Laplace's and Poisson's equations. We proved a mathematical theorem which states that a superconvergence point exists if and only if it can be determined by a numerical methodology. We employed the numerical methodology to find superconvergence points for the gradient in finite element solutions of Laplace's and Poisson's equation for meshes of triangular or square elements of polynomial degree p, for $1 \leq p \leq 7$. The conclusions of the study in [1] may be summarized as follows:

1. The computer-based methodology takes directly into account the topology of the mesh, the element polynomial spaces and the type of the differential equation (homogeneous or non-homogeneous).

2. For solutions of Laplace's equation (i.e. the homogeneous equation) the superconvergence points for the derivatives always exist for any mesh-pattern and type of elements.

3. For solutions of Poisson's equation (i.e. the non-homogeneous equation) the superconvergence points may not exist depending on the mesh-pattern and the element-type.

In this paper we will employ an extension of the computer-based methodology of [1] to address the problem of existence of superconvergence points for the gradient of the displacement, strain and stress in finite element approximations of the equations of plane elasticity. We note that the majority of the classical studies on superconvergence (see [2-29] and the citations in these papers) deal primarily with Poisson's equation (with a few exceptions; see for example [18], [19], [20] and [24] which address the problem of plane elasticity).

The majority of practical computations in plane elasticity employ elements of degree p, with $1 \leq p \leq 4$ and most often $p = 2$, and involve the homogeneous case (i.e. the body-force vanishes identically). Therefore it is important to investigate in detail the superconvergence for the components of the gradient of the displacement, strain and stress for these cases (i.e. for $1 \leq p \leq 4$ and zero body-force). Similarly as in [1] we will study the superconvergence for the standard displacement finite element method and meshes of triangular and square elements.

There are two types of superconvergence (see [12]), namely:

(i). *Direct superconvergence*: By this we mean the superconvergence of pointwise values of quantities computed *directly* from the finite element solution.

(ii). *Superconvergence via averaging*: The superconvergence of post-processed values of quantities which are obtained from the finite element solution by employing a *local averaging*.

Here (as in [1]) we will address only the case of direct superconvergence. The same methodologies can be employed to study superconvergence via averaging; we will present such a study in a future paper. Further, to limit the length of the paper we show only some illustrative results. Additional results on the superconvergence of various quantities defined in terms of the stresses, the strains etc. can be easily obtained using the approach of the paper.

Following this Introduction, we introduce notations for the model problem of plane elasticity, its finite element approximation and the types of meshes employed, we outline the theoretical setting, we describe the numerical methodology for finding the superconvergence points and we report the results of the numerical study and the conclusions.

2 Preliminaries

We shall consider the vector-valued boundary-value problem

$$L_i(\boldsymbol{u}) := -\sum_{j=1}^{2} \frac{\partial}{\partial x_j}\Big(\sigma_{ij}(\boldsymbol{u})\Big) = f_i \qquad \text{in} \quad \Omega \tag{2.1a}$$

$$u_i = 0 \qquad \text{on} \quad \Gamma_D \tag{2.1b}$$

$$\sum_{j=1}^{2} \sigma_{ij}(\boldsymbol{u}) n_j = \bar{t}_i \qquad \text{on} \quad \Gamma_N \tag{2.1c}$$

where $i = 1, 2$.
Here $\Omega \subset \mathbf{R}^2$ is a bounded domain with boundary $\partial\Omega = \Gamma_D \cup \Gamma_N$;
$\boldsymbol{n} := (n_1, n_2)$ is the outward pointing unit-normal on Γ_N;
f_i, $i = 1, 2$ are the components of the load-vector (*body-force*);
$\bar{t}_i$, $i = 1, 2$ are the components of the normal-flux vector (*traction*) applied on Γ_N;
$\Gamma_D = \emptyset$, $\Gamma_D \cap \Gamma_N = \emptyset$; $\boldsymbol{u} = (u_1, u_2)$ is the solution-vector (*displacement*);

$$\epsilon_{ij}(\boldsymbol{u}) := \frac{1}{2}\Big(\frac{\partial u_i}{\partial x_j} + \frac{\partial u_j}{\partial x_i}\Big), \qquad i, j = 1, 2 \tag{2.2a}$$

$$\sigma_{ij}(\boldsymbol{u}) := \sum_{k,l=1}^{2} a_{ijkl}\,\epsilon_{kl}(\boldsymbol{u}), \qquad i,j=1,2 \tag{2.2b}$$

are the components of the strain and the stress, respectively;
a_{ijkl}, i, j, k, $l = 1, 2$, are the material-coefficients (*elastic constants*) which satisfy

$$a_{ijkl} = a_{jilk} = a_{lkij}, \qquad i,j,k,l=1,2 \tag{2.3a}$$

$$\sum_{i,j,k,l=1}^{2} a_{ijkl}\,\epsilon_{ij}\,\epsilon_{kl} \geq c \sum_{i,j=1}^{2} \epsilon_{ij}\,\epsilon_{ij}, \quad c>0, \qquad \forall\ \epsilon_{ij}=\epsilon_{ji} \tag{2.3b}$$

(Conditions (2.3a), (2.3b) are satisfied for linear anisotropic elasticity; in the case of isotropic plane elasticity $a_{ijkl} = \mu(\delta_{ij}\delta_{kl}+\delta_{il}\delta_{kj}) + \lambda\delta_{ik}\delta_{jl}$ where δ_{ij} is Kronecker's delta and λ, μ are Lamé's constants.)

Let us now cast the model problem in variational form. We will use the notations

$$\boldsymbol{H}^1 := \left\{ \boldsymbol{v} = (v_1, v_2) \ :\ v_i \in H^1(\Omega) \right\} \tag{2.4a}$$

$$\boldsymbol{H}^1_{\Gamma_D} := \left\{ \boldsymbol{v} = (v_1, v_2) \ \middle|\ v_i \in H^1(\Omega),\ v_i = 0 \ \text{ on } \ \Gamma_D \right\} \tag{2.4b}$$

$$\|\boldsymbol{v}\|_{1,\Omega} := \left(\sum_{i=1}^{2} \|v_i\|^2_{1,\Omega} \right)^{\frac{1}{2}}, \ |\boldsymbol{v}|_{1,\Omega} := \left(\sum_{i=1}^{2} |v_i|^2_{1,\Omega} \right)^{\frac{1}{2}} \tag{2.4c}$$

with $\|v_i\|_{1,\Omega}$ (resp. $|v_i|_{1,\Omega}$) being the usual $H^1(\Omega)$ Sobolev norm (resp. seminorm). The variational form of the boundary-value problem (2.1) is now posed as:

Find $\boldsymbol{u} \in \boldsymbol{H}^1_{\Gamma_D}$ such that

$$B_\Omega(\boldsymbol{u},\boldsymbol{v}) = \int_\Omega \sum_{i=1}^{2} f_i\,v_i + \int_{\Gamma_N} \sum_{i=1}^{2} \bar{t}_i\,v_i \qquad \forall\ \boldsymbol{v} \in \boldsymbol{H}^1_{\Gamma_D} \tag{2.5a}$$

where the bilinear form $B_\Omega : H^1_{\Gamma_D} \times H^1_{\Gamma_D} \longrightarrow \mathbf{R}$ is defined by

$$B_\Omega(u,v) := \int_\Omega \sum_{i,j,k,l=1}^{2} a_{ijkl} \frac{\partial u_j}{\partial x_l} \frac{\partial v_i}{\partial x_k} \tag{2.5b}$$

The energy-norm over any subdomain $S \subseteq \Omega$ is defined by

$$|||v|||_S := \sqrt{B_S(v,v)} \tag{2.5c}$$

where $B_S(u,v)$ has the obvious meaning.

Let $\mathcal{T} = \{T_h\}$ be a family of meshes of triangles or quadrilaterals with straight edges. It is assumed that the family is *regular*, namely: For the triangles the minimal angle of all the triangles is bounded below by a positive constant, the same for all the meshes. For the meshes of quadrilaterals it is assumed that the mesh can be mapped to a mesh of squares by a sufficiently smooth transformation and hence it is sufficient to study the superconvergence for a mesh of squares (see [9], [10] for details). Let us introduce the finite-element spaces

$$S^p_h := \left\{ u \in H^1 \;\middle|\; u_i \circ F_{\tau_k} \in \hat{S}^p(\hat{\tau}), \quad i = 1,2, \quad k = 1,\ldots,M(T_h) \right\} \tag{2.6}$$

where F_{τ_k} is the mapping function for the kth finite-element which maps either a standard triangular element (using a linear transformation) or a standard quadrilateral element (using a bilinear transformation) onto the kth finite element, $\hat{\tau}$ denotes a standard element, $M(T_h)$ is the number of elements in the mesh T_h, $\hat{S}^p(\hat{\tau})$ denotes the element-space over $\hat{\tau}$.

As in [1] we will consider the following choices for the element-space $\hat{S}^p(\hat{\tau})$:

a. Complete polynomial space up to degree p.

For the triangular elements we let $\hat{S}_p(\hat{\tau}) = \hat{\mathcal{P}}_p(\hat{\tau})$ where

$$\hat{\mathcal{P}}_p(\hat{\tau}) := \left\{ \hat{P} \;\middle|\; \hat{P}(\hat{x}_1,\hat{x}_2) = \sum_{\substack{i,j \\ 0 \le i+j \le p}} \alpha_{i,j}\, \hat{x}_1^i\, \hat{x}_2^j \right\}. \tag{2.7}$$

For the square elements we consider the following choices for the definition of the polynomial space $\hat{S}_p(\hat{\tau})$ (see also [32]).

b. Tensor-product (bi-p) polynomial space of degree p.

$$\hat{\mathcal{S}}^{(p,p)}(\hat{\tau}) := \left\{ \hat{P} \,\middle|\, \hat{P}(\hat{x}_1, \hat{x}_2) = \sum_{\substack{i,j \\ 0 \le i,j \le p}} \alpha_{i,j}\, \hat{x}_1^i\, \hat{x}_2^j \right\} \tag{2.8}$$

c. Serendipity (trunc) polynomial space of degree p.

$$\hat{\mathcal{S}}^{p}(\hat{\tau}) := \left\{ \hat{P} \,\middle|\, \hat{P}(\hat{x}_1, \hat{x}_2) = \sum_{\substack{i,j \\ 0 \le i+j \le p}} \alpha_{i,j}\, \hat{x}_1^i\, \hat{x}_2^j + \alpha_{p,1}\, \hat{x}_1^p\, \hat{x}_2 + \alpha_{1,p}\, \hat{x}_1\, \hat{x}_2^p \right\} \tag{2.9}$$

d. Intermediate polynomial space of degree p.

$$\hat{\mathcal{S}}^{\prime p}(\hat{\tau}) := \left\{ \hat{P} \,\middle|\, \hat{P}(\hat{x}_1, \hat{x}_2) = \sum_{\substack{i,j \\ 0 \le i+j \le p}} \alpha_{i,j}\, \hat{x}_1^i\, \hat{x}_2^j + \sum_{k=0}^{p-1} \alpha_{p-k,k+1}\, \hat{x}_1^{p-k}\, \hat{x}_2^{k+1} \right\} \tag{2.10}$$

We let

$$S^p_{h,\Gamma_D} := S^p_h \cap H^1_{\Gamma_D} \tag{2.11}$$

The finite element solution u^h of the elasticity problem satisfies:

Find $u_h \in S^p_{h,\Gamma_D}$ such that

$$\mathcal{B}_\Omega(u_h, v_h) = \int_\Omega \sum_{i=1}^{2} f_i\, v_{hi} + \int_{\Gamma_N} \sum_{i=1}^{2} g_i\, v_{hi} \qquad \forall\ v_h \in S^p_{h,\Gamma_D} \tag{2.12}$$

The error is $e_h := u - u_h$.

3 Definition of the superconvergence quantities

Let $T_h \in \mathcal{T}$ be a finite element grid, $u_h \in S^p_{h,\Gamma_D}$ the corresponding finite element solution and let $\tau \in T_h$ be any element. Let $F(u)$ be the solution quantity of interest, for example $F(u) = \dfrac{\partial u_i}{\partial x_j}$ or $\epsilon_{ij}(u)$ or $\sigma_{ij}(u)$, $i,j = 1, 2$. We are interested in the values of the relative error in $F(u)$ at points $\bar{x}_\tau \in \tau$,

$$\Theta(\bar{x}_\tau; F; u, u_h, h, \tau) := \begin{cases} \dfrac{|F(u-u_h)(\bar{x}_\tau)|}{\Psi(u-u_h)} & , \quad \text{if } \Psi(u-u_h) \neq 0 \\ 0 & , \quad \text{if } \Psi(u-u_h) = 0 \end{cases} \tag{3.1a}$$

where

$$\Psi(u-u_h) := \max_{x \in \tau} |F(u-u_h)(x)| \tag{3.1b}$$

Let us assume that τ is an element of fixed geometry (but not of fixed size) which appears in all the meshes T_h of the sequence $\mathcal{T}$. If there exists a point $\bar{x}_\tau$, which is fixed with respect to the element τ, such that

$$\lim_{h \to 0} \Theta(\bar{x}_\tau; F; u, u_h, h, \tau) \leq \frac{\eta}{100}, \qquad 0 \leq \eta \leq 100 \tag{3.2}$$

we will say that $\bar{x}_\tau$ is a $u-\eta\%$-*superconvergence point* in element τ. Further, we will call $\bar{x}_\tau$ a $\mathcal{U}-\eta\%$-superconvergence point if it is $u-\eta\%$-superconvergence point for every $u \in \mathcal{U}$. Note that $\Theta(\bar{x}; F; u, u_h, h, \tau) \leq 1$ and thus all points in every element τ are 100%-superconvergence points. If there exists a point $\bar{x}_\tau$ such that (3.2) holds for a given solution u (resp. class of solutions $\mathcal{U}$) with $\eta = 0$ then $\bar{x}_\tau$ is a u-superconvergence (resp. $\mathcal{U}$-superconvergence) point in the classical sense.

Let us now define the following geometrical quantities which will be employed in the study of superconvergence below. For a given η, $0 \leq \eta \leq 100$ we define

1. $\eta\%$-contour of $F(u)$ in the element τ of the mesh T_h for the exact solution u:

$$C^{\eta\%}_{F(u)}(u; \tau, T_h) := \left\{ x \in \tau \;\middle|\; \Theta(x; F; u, u_h, h, \tau) = \frac{\eta}{100} \right\} \tag{3.3}$$

2. Superconvergence points of $F(u)$ in the element τ of the mesh T_h for the class of exact solutions $\mathcal{U}$:

$$\mathcal{X}^{\text{sup}}_{F(u)}(\mathcal{U}; \tau, T_h) := \bigcap_{u \in \mathcal{U}} C^{0\%}_{F(u)}(u; \tau, T_h) \tag{3.4}$$

3. η%-band of $F(u)$ in the element τ of the mesh T_h for the exact solution u:

$$\mathcal{B}^{\eta\%}_{F(u)}(u;\tau,T_h) := \left\{ x \in \tau \;\middle|\; \Theta(x;F;u,u_h,h,\tau) < \frac{\eta}{100} \right\} \tag{3.5}$$

4. η%-superconvergence regions of $F(u)$ in the element τ of the mesh T_h for the class of exact solutions $\mathcal{U}$:

$$\mathcal{R}^{\eta\%}_{F(u)}(\mathcal{U};\tau,T_h) := \bigcap_{u\in\mathcal{U}} \mathcal{B}^{\eta\%}_{F(u)}(u;\tau,T_h) \tag{3.6}$$

Remark 3.1. We could be interested in the points which are superconvergent simultaneously for several functionals e.g. all the stress components. We can formalize this by assuming a vector functional; the meaning of the η%-superconvergence point for the vector functional is obvious.

4 The class of locally periodic meshes

In this paper we will study the superconvergence of finite element solutions for the equations of plane elasticity for a special class of locally periodic meshes which are defined as follows. Let $0 < H < H^0$, $x^0 = (x_1^0, x_2^0) \in \Omega$,

$$S(x^0,H) := \left\{ x = (x_1,x_2) \middle|\; |x_i - x_i^0| < H, \quad i = 1,2 \right\} \tag{4.1}$$

and assume H^0 is sufficiently small such that $\bar{S}(x^0,H^0) \subset \Omega$. Further, let γ be a set of multi-indices (i,j), $x^{(i,j)} = (x_1^{(i,j)}, x_2^{(i,j)}) \in \Omega$ and

$$c(x^{(i,j)},h) := S(x^{(i,j)},h) \subset S(x^0,H), \qquad (i,j) \in \gamma \tag{4.2}$$

be the set of the h-cells (or cells) which cover exactly $S(x^0,H)$ i.e.

$$\bigcup_{(i,j)\in\gamma} \bar{c}(x^{(i,j)},h) = \bar{S}(x^0,H) \tag{4.3a}$$

$$c(x^{(i_1,j_1)},h) \bigcap c(x^{(i_2,j_2)},h) = \emptyset \;\text{ for }\; (i_1,j_1) \neq (i_2,j_2) \tag{4.3b}$$

We will refer to $S(\boldsymbol{x}^0, H)$ as *the subdomain of periodicity of the mesh centered at* $\boldsymbol{x}^0$. We will denote by

$$\tilde{c} := S(\mathbf{0}, 1) := \left\{ (\tilde{x}_1, \tilde{x}_2) \middle| \ |\tilde{x}_1| < 1 \,,\ |\tilde{x}_2| < 1 \right\} \tag{4.4}$$

the *unit-* (*master-*) cell $\tilde{c}$, the h-cell is an h-scaled and translated master-cell.

Let $\tilde{T}$ be a mesh of triangles or squares on the master-cell (the master-mesh) and $\tilde{T}_h^{(i,j)}$ be the mesh on $c(\boldsymbol{x}^{(i,j)}, h)$ which is the scaled and translated image of $\tilde{T}$. We will consider the family $\mathcal{T}$ of locally periodic meshes. Let $T_h \in \mathcal{T}$ and $T_h(\boldsymbol{x}^0, H)$ be the restriction of T_h on $S(\boldsymbol{x}, H)$ and $T_h^{(i,j)}$ the restriction of $T_h(\boldsymbol{x}^0, H)$ on $c(\boldsymbol{x}^{(i,j)}, h)$. We assume that $T_h^{(i,j)} = \tilde{T}_h^{(i,j)}$, $(i,j) \in \gamma$ i.e. $T_h(\boldsymbol{x}^0, H)$ is made by the periodic repetition of the h-scaled master mesh.

The type of meshes under consideration is depicted in Fig. 1, where the periodic-mesh subdomain $S(\boldsymbol{x}^0, H)$ is shown with thick perigram. Outside the subdomain $S(\boldsymbol{x}^0, H)$ the mesh is arbitrary; it could have curved elements, refinements, etc.

5 Outline of the theoretical setting

Let $\boldsymbol{Q}$ be a vector-valued function with components which are polynomials of degree $(p+1)$ defined over the master-cell $\tilde{c}$ and let $\tilde{T}$ be the master-mesh. Then denote

$$\boldsymbol{\rho} := \boldsymbol{Q} - \boldsymbol{Q}_1^{\mathrm{INT}} \tag{5.1}$$

where $\boldsymbol{Q}_1^{\mathrm{INT}}$ is the interpolant of degree p of the function $\boldsymbol{Q}$ defined over the master-mesh $\tilde{T}$ (for which $h = 1$). Any vector-valued function with components which are polynomials of degree p on an element τ_k belongs to $\boldsymbol{S}_1^p(\tau_k)$ and hence any polynomial of degree p on $S(\boldsymbol{x}^0, H)$ belongs to $\boldsymbol{S}_1^p(S(\boldsymbol{x}^0, H))$. It follows that $\boldsymbol{\rho}$ defined in (5.1) is $\tilde{c}$-periodic; this can be shown exactly as in [40]. We have

$$\boldsymbol{\rho}(1, \tilde{x}_2) = \boldsymbol{\rho}(-1, \tilde{x}_2)\,, \qquad |\tilde{x}_2| < 1 \tag{5.2a}$$

$$\boldsymbol{\rho}(\tilde{x}_1, 1) = \boldsymbol{\rho}(\tilde{x}_1, -1)\,, \qquad |\tilde{x}_1| < 1 \tag{5.2b}$$

Let

$$(5.3) \qquad \boldsymbol{H}^1_{\mathrm{PER}}(\tilde{c}) := \left\{ \boldsymbol{u} \in \boldsymbol{H}^1(\tilde{c}) \;\middle|\; \boldsymbol{u} \text{ satisfies (5.2)} \right\}$$

and

$$(5.4) \qquad \boldsymbol{S}^p_{1,\mathrm{PER}}(\tilde{c}) := \left\{ \boldsymbol{u} \in \boldsymbol{H}^1_{\mathrm{PER}}(\tilde{c}) \middle|\; \boldsymbol{u}|_{\tilde{\tau}} \in \boldsymbol{S}^p_1(\tilde{\tau}),\ i = 1,2, \quad \forall\ \tilde{\tau} \in \tilde{T} \right\}$$

Further let $\boldsymbol{z}^\rho \in \boldsymbol{S}^1_{\mathrm{PER}}(\tilde{c})$ such that

$$(5.5a) \qquad B_{\tilde{c}}(\tilde{\boldsymbol{z}}^\rho, \tilde{\boldsymbol{v}}) = B_{\tilde{c}}(\rho, \tilde{\boldsymbol{v}}) \qquad \forall\ \tilde{\boldsymbol{v}} \in \boldsymbol{S}^p_{1,\mathrm{PER}}(\tilde{c})$$

and

$$(5.5b) \qquad \int_{\tilde{c}} (\rho - \tilde{\boldsymbol{z}}^\rho) = \boldsymbol{0}$$

Note that the function $\tilde{\boldsymbol{z}}^\rho$ exists and is uniquely determined (we will compute it numerically in the examples). Let us also define $\psi \in \boldsymbol{H}^1(\tilde{c})$ by

$$(5.6) \qquad \psi := \rho - \tilde{\boldsymbol{z}}^\rho = \boldsymbol{Q} - \tilde{\boldsymbol{w}} \quad \text{where} \quad \tilde{\boldsymbol{w}} := \boldsymbol{Q}_1^{\mathrm{INT}} + \tilde{\boldsymbol{z}}^\rho$$

Let $\psi_h \in H^1_{\mathrm{PER}}(c(\boldsymbol{x}^{(i,j)}, h))$ be the function ψ, defined above, scaled and translated onto the cell $c(\boldsymbol{x}^{(i,j)}, h)$ of the mesh in $S(\boldsymbol{x}^0, H)$ i.e.

$$(5.7) \qquad \psi_h(\boldsymbol{x}) := h^{p+1}\, \psi(\tilde{\boldsymbol{x}}), \qquad \frac{\partial \psi_h}{\partial x_i}(\boldsymbol{x}) = h^p \frac{\partial \psi}{\partial \tilde{x}_i}(\tilde{\boldsymbol{x}}), \quad i = 1,2,$$

where $\tilde{\boldsymbol{x}} = \dfrac{1}{h}(\boldsymbol{x} - \boldsymbol{x}^{(i,j)}), \quad \boldsymbol{x} \in c(\boldsymbol{x}^{(i,j)}, h)$. It is easy to see that ψ_h can be periodically extended over $S(\boldsymbol{x}^0, H_1)$.

In [1] we proved the following theorem for Poisson's equation based on the theory of interior estimates (see [33]-[39]):

Theorem 1. (Poisson's equation; see [1]) Let $H_1 < H < H^0$ and assume that the following assumptions hold with

$$(5.8) \qquad \alpha = \frac{6p+1}{6p}, \qquad \beta = p + 1 - \epsilon, \qquad \epsilon = \sigma_0 = \frac{1}{6(6p+1)}$$

Assume that the exact solution u satisfies

$$\|D^\alpha u\|_{L^\infty(S(x^0,H))} \le K < \infty, \qquad 0 \le |\alpha| \le p+2 \tag{5.9a}$$

where $\alpha := (\alpha_1, \alpha_2)$, $D^\alpha u := \dfrac{\partial^{|\alpha|} u}{\partial x_1^{\alpha_1}\, \partial x_2^{\alpha_2}}$, $|\alpha| := \alpha_1 + \alpha_2$, and

$$R^2 = \sum_{|\alpha|=p+1} a_\alpha^2 > 0 \qquad \text{where} \qquad a_\alpha := (D^\alpha u)(x^0) \tag{5.9b}$$

Further assume that the mesh T_h is such that

$$\|e_h\|_{L^2(S(x^0,H_1))} \le C h^\beta H_1, \qquad \text{with} \quad \beta \ge (p+1) - \epsilon \tag{5.10}$$

Moreover assume that the meshes T_h in $S(x^0, H)$ are such that

$$C_1 H_1^\alpha \le h \le C_2 H_1^\alpha \tag{5.11}$$

Then for any $x \in S(x^0, H_1)$

$$\left|\frac{\partial e_h}{\partial x_i}(x)\right| = \left|\frac{\partial \psi_h}{\partial x_i}(x)\right| + \lambda C h^{p+\sigma_0} \tag{5.12}$$

with $|\lambda| \le 1$ and C independent of h.

Remark 5.1. The theorem assumes that the mesh is periodic in a small subdomain (i.e. $S(x^0, H)$) in the interior of the domain and that the solution is smooth in the neighborhood of the subdomain. Outside the subdomain we assume neither periodicity of the mesh nor smoothness of the solution. The solution may have algebraic-type singularities at a finite number of corner points or points of abrupt change in the type of boundary-condition. Here it is only assumed that the pollution-error in a shrinking mesh-patch (i.e. $T_h(x^0, H_1)$) in the interior of the subdomain is controlled; this implies that the mesh has been adequately refined in the neighborhood of all singular points.

Remark 5.2. If we further assume that

$$\left\|\frac{\partial e_h}{\partial x_i}\right\|_{L^\infty(\tau)} \ge \bar{c} \max_{j=1,2} \left\|\frac{\partial e_h}{\partial x_j}\right\|_{L^\infty(\tau)} \ge C h^p, \quad i = 1,2, \quad \bar{c} > 0 \tag{5.13}$$

theorem 1 implies that: A point $\boldsymbol{x}_\tau$ in the element τ is a superconvergence point for $F(u) = \dfrac{\partial u}{\partial x_i}$ in the element τ if and only if $\dfrac{\partial \psi}{\partial x_i}(\boldsymbol{x}_\tau) = 0$. Assumption (5.13) can be realized by imposing additional restrictions on the values a_α of the $(p+1)$-derivatives of the solution at $\boldsymbol{x}_0$. This assumption is reasonable because we are interested in a sufficiently large class of solutions $\mathcal{U}$.

Remark 5.3. Under assumption (5.13) Theorem 1 also states that: *A point $\boldsymbol{x}_{\tilde{\tau}}$ in the element $\tilde{\tau}$ is an asymptotically η%-superconvergence point for $F(u) = \dfrac{\partial u}{\partial x_i}$, $i = 1,2$, if and only if* $\tilde{\Theta}(\boldsymbol{x}_{\tilde{\tau}}; F; Q, \tilde{w}, 1, \tilde{\tau}) \leq \dfrac{\eta}{100}$ where

$$(5.14) \qquad \tilde{\Theta}(\boldsymbol{x}_{\tilde{\tau}}; F; Q, \tilde{w}, 1, \tilde{\tau}) := \begin{cases} \dfrac{|\tilde{F}(\psi)(\boldsymbol{x}_{\tilde{\tau}})|}{\tilde{\Psi}(\psi)} & , \quad \text{if } \tilde{\Psi}(\psi) := \|\psi\|_{L^\infty(\tilde{\tau})} \neq 0 \\ 0 & , \quad \text{if } \|\psi\|_{L^\infty(\tilde{\tau})} = 0 \end{cases}$$

Remark 5.4. The proof of theorem 1 in [40] was based on various interior estimates for the error in finite element approximations of Poisson's equation, especially the results given in [38] and [39]. It is very plausible that analogs of these results hold for finite element approximations of the elasticity equations and more general elliptic-systems because the main ideas of the proofs of these results carry to the general case. To our knowledge the precise details are not available for the elasticity equations. Nevertheless we will assume the validity of the analog of Theorem 1 for the equations of elasticity.

6 The methodology for determining the superconvergence points

In order to study the superconvergence of finite element solutions in uniform mesh-patches in the interior of a subdomain $S(\boldsymbol{x}^0, H)$, we let

$$(6.1) \quad \mathcal{U}^G := \left\{ \boldsymbol{u} \in \boldsymbol{H}^1(\Omega) \middle| \ \|D^\alpha u_i\|_{L^\infty(S(\boldsymbol{x}^0, H))} < K \ , \ i = 1,2, \ 0 \leq |\alpha| \leq p+2 \right\}$$

the class of solutions which are locally smooth in $S(\boldsymbol{x}^0, H)$, where $S(\boldsymbol{x}^0, H)$ denotes an interior subdomain of interest in which the mesh is locally periodic as described above (the subdomain must be a finite distance away from the boundary and points of roughness of the body-force; see Fig. 1). In the majority of the applications one is only interested in the subclass of solutions in $\mathcal{U}^G$ which are "harmonic", namely,

$$(6.2) \qquad \mathcal{U}^{"H"} := \left\{ u \in \mathcal{U}^G \;\middle|\; L_i(u) = 0, \quad i = 1,2, \quad \text{in} \quad \Omega \right\}$$

We may also assume that the functions are "harmonic" in a subdomain which is slightly bigger than $S(x^0, H)$ and which includes $S(x^0, H)$ in its interior.

For a given locally periodic grid with corresponding periodic master-mesh $\tilde{T}$, given material orthotropy and given class of smooth solutions $\mathcal{U}$ we let

$$(6.3) \qquad \mathcal{Q} := \left\{ Q \;\middle|\; Q(x_1, x_2) = \sum_{k=1}^{nd} \alpha_k Q_k(x_1, x_2) \right\}$$

denote the class of $(p+1)$-degree monomials which occur in all $(p+1)$-degree Taylor-series expansions of functions from $\mathcal{U}$. Here Q_k, $k = 1, \ldots, nd$ denotes a set of linearly independent monomials which form a basis for $\mathcal{Q}$. For example, let us assume that $\mathcal{U}$ is the class of smooth solutions $\mathcal{U}^G$ given in (6.1); in this case $\mathcal{Q}$ is the $2(p+2)$ dimensional space of vector-valued functions with components which are monomials of degree $(p+1)$. The set $\mathcal{Q}$ which corresponds to the class of "harmonic" solutions $\mathcal{U}^{"H"}$ is the four-dimensional linear space of "harmonic" monomials of degree $(p+1)$ denoted by $\mathcal{Q}^{"H"}$. The "harmonic" basis monomials of degree $(p+1)$ for $1 \le p \le 4$, which were employed in the computations, are given in the Appendix.

The asymptotic values of the error for any smooth solution u in the interior of a periodic mesh-subdomain can be obtained by solving the periodic boundary-value problem (5.5), using the master-mesh $\tilde{T}$ over the master-cell $\tilde{c}$, with data obtained from the local $(p+1)$-degree Taylor-series expansion Q of the exact solution. The asymptotic η%-contours for a given solution u can be obtained by contouring the function $F(\psi)$, with ψ defined as in (5.6) corresponding to the local Taylor-series expansion Q of the solution u. The superconvergence points $\tilde{\tilde{x}}$ for a given class of solutions $\mathcal{U}$ satisfy

$$(6.4) \qquad F(\psi_i)(\tilde{\tilde{x}}) = 0, \qquad 1 \le i \le nd$$

Therefore $\tilde{\tilde{x}}$ is a superconvergence point if and only if the zero-contours of $F(\psi_i)$ intersect at $\tilde{\tilde{x}}$ for $1 \le i \le nd$. Here $\psi_i := \rho_i - z^{\rho_i}$ which is obtained from (5.6) for $\rho_i = Q_i - (Q_i)_1^{\text{INT}}$ where Q_i is the i-th basis monomial of the nd-dimensional monomial space $\mathcal{Q}$ corresponding to the class $\mathcal{U}$. We also let $\tilde{w}_i := (Q_i)_1^{\text{INT}} + z^{\rho_i}$.

The asymptotic η%-superconvergence regions for a class of solutions $\mathcal{U}$ can be determined by using numerical optimization. In particular, let us consider the

uniform subdivision of the element τ into subtriangles with vertices at the set of points $\Xi := \{\xi_k\}_{k=1}^{np}$. We will define the function

$$(6.5)\quad \tilde{\mathcal{H}}^{\Xi}_{F(u)}(\xi_k; F; \mathcal{Q}, \{\tilde{w}_i\}_{i=1}^{nd}, 1, \tilde{\tau}) := \max_{\alpha_i} \left(\frac{|\sum_{i=1}^{nd} \alpha_i F(\psi_i)(\xi_k)|}{\max_{j=1,\ldots,np} |\sum_{i=1}^{nd} \alpha_i F(\psi_i)(\xi_j)|} \right) 100,$$

at the points in Ξ. The function $\tilde{\mathcal{H}}^{\Xi}_{F(u)}(\tilde{x}; F; \mathcal{Q}, \{\tilde{w}_i\}_{i=1}^{nd}, 1, \tilde{\tau})$ will be defined for any point $\tilde{x} \in \tilde{\tau}$ by using linear interpolation in the subtriangles. The asymptotic $\eta\%$-superconvergence regions in the element τ can be approximated using the level-sets of the functions $\tilde{\mathcal{H}}^{\Xi}_{F(u)}(\tilde{x}; F; \mathcal{Q}, \{\tilde{w}_i\}_{i=1}^{nd}, 1, \tilde{\tau})$ i.e.

$$(6.6)\quad \tilde{\mathcal{R}}^{\eta\%}_{F(u)}(\mathcal{Q}; \tilde{\tau}, \tilde{T}) \approx \left\{ \tilde{x} \in \tilde{\tau} \;\middle|\; \tilde{\mathcal{H}}^{\Xi}_{F(u)}(\tilde{x}; F; \mathcal{Q}, \{\tilde{w}_i\}_{i=1}^{nd}, 1, \tilde{\tau}) < \eta\% \right\}$$

We will call the above approach the *direct approach*. It is also possible to use a *simplified approach* which avoids the use of numerical optimization at every point. Let us define (see also [30, 31])

$$(6.7)\quad \widehat{\tilde{\mathcal{H}}}^{\Xi}_{F(u)}(\tilde{x}; F; \mathcal{Q}, \{\tilde{w}_i\}_{i=1}^{nd}, 1, \tilde{\tau}) := \frac{1}{Z_{\Xi}} \sqrt{\sum_{i=1}^{nd} \big(F(\psi_i)(\tilde{x})\big)^2},$$

where

$$(6.8)\quad Z_{\Xi} := \min_{\alpha_i} \left(\frac{\max_{j=1,\ldots,np} |\sum_{i=1}^{nd} \alpha_i F(\psi_i)(\xi_j)|}{(\sum_{i=1}^{nd} \alpha_i^2)^{\frac{1}{2}}} \right)$$

The quantity Z_{Ξ} can be computed using numerical optimization. Then

$$(6.9)\quad \widehat{\tilde{\mathcal{R}}}^{\eta\%}_{F(u)}(\mathcal{Q}; \tau, \tilde{T}) := \left\{ \tilde{x} \in \tau \;\middle|\; \widehat{\tilde{\mathcal{H}}}^{\Xi}_{F(u)}(\tilde{x}; F; \mathcal{Q}, \{\tilde{w}_i\}_{i=1}^{nd}, 1, \tilde{\tau}) < \frac{\eta}{100} \right\}$$

are the approximate regions of $\eta\%$-superconvergence for the class of solutions $\mathcal{Q}$.

Remark 6.1. Note that

$$(6.10)\quad \widehat{\tilde{\mathcal{R}}}^{\eta\%}_{F(u)}(\mathcal{Q}; \tilde{\tau}, \tilde{T}) \subseteq \tilde{\mathcal{R}}^{\eta\%}_{F(u)}(\mathcal{Q}; \tilde{\tau}, \tilde{T}) .$$

Therefore the simplified approach results to a conservative estimate for the $\eta\%$-superconvergence regions.

Remark 6.2. The functions defined in (6.5), (6.7) depend on the set of points Ξ. To ensure good accuracy in the approximation of the $\eta\%$-superconvergence regions a sufficient number of points must be employed.

7 Numerical study of superconvergence for periodic meshes of triangles and squares

We will now use the methodology of the previous Section to find the superconvergence points or the $\eta\%$-superconvergence regions for the components of the gradient of the displacement, strain and stress for finite element solutions of the equations of elasticity in the interior of periodic meshes of triangular and square elements. In the numerical examples we addressed the following questions:

1. For periodic meshes of triangles with various mesh-topologies, and elements of degree p, where are the superconvergence points for the various solution quantities for the class of "harmonic" solutions? Are these points superconvergence points for the class of general solutions?

2. For meshes of squares of degree p, where are the superconvergence points for the various quantities for the tensor-product space $\hat{S}^{(p,p)}(\hat{\tau})$, the serendipity space $\hat{S}^{p}(\hat{\tau})$ and the intermediate space $\hat{S}^{\prime p}(\hat{\tau})$?

3. In the cases that there are no superconvergence points (i.e. 0%-superconvergence points) where are $\eta\%$-superconvergence points for small values of $\eta\%$?

We will answer these questions using the computer-based approach of Section 6.

7.1 Determination of the superconvergence points for the periodic meshes of triangles

The majority of the results for the superconvergence points for the triangular elements in the literature are given exclusively for the Regular pattern (which is also known as *the three-directional mesh* and is shown in Fig. 2a), for linear and quadratic elements and for the Poisson's equation. In [1] we determined the superconvergence points for Laplace's and Poisson's equations, for all the mesh patterns shown in Fig. 2 and elements of degree p, $1 \leq p \leq 7$. Here, we employed the numerical methodology of Section 6 to find the superconvergence points, for the same mesh-patterns, for $\dfrac{\partial u_1}{\partial x_1}$ for the class of "harmonic" solutions of the equations of plane-elasticity and $1 \leq p \leq 4$.

In Fig. 3 (resp. Fig. 4) we give examples of how the superconvergence points for the class of "harmonic" solutions, for $p = 1, 2, 3$, were obtained for the Regular (resp. Criss-Cross) pattern from the intersection of the zero-contours $C^{0\%}_{\frac{\partial u_1}{\partial x_1}}(Q_i^{"H"}; \tilde{\tau}, \tilde{T})$, of the error functions ψ_i, $i = 1, \ldots, 4$, which correspond to the basis "harmonic" monomials of degree $(p+1)$. From the numerical results we observe that:

(i) In the Regular, Chevron and Criss-Cross patterns for linear or cubic elements ($p = 1$ or 3), there exists one superconvergence point for $\frac{\partial u_1}{\partial x_1}$ in the elements with an edge parallel to the x_1-axis. This point is located at the midside of the edge parallel to the x_1-axis.

(ii) In the Regular, Criss-Cross patterns for quadratic elements ($p = 2$) there are two superconvergence points for $\frac{\partial u_1}{\partial x_1}$ in the elements with an edge parallel to the x_1-axis. These points are located at the Gauss-points of the edge parallel to the x_1-axis.

(iii) In the Chevron pattern, the Union-Jack pattern and element τ_2 of the Criss-Cross pattern (shown in Fig. 2d) for quadratic elements ($p = 2$) there are no superconvergence points for $\frac{\partial u_1}{\partial x_1}$.

(iv) The superconvergence points for the components of the gradient of the displacement for the class of general solutions coincide with the superconvergence points for the class of "harmonic" solutions.

(v) There are no superconvergence points for the stress in any of the mesh-patterns except for the special case that the Poisson's ratio is equal to zero. In this case the normal stress components σ_{11}, σ_{22} are superconvergent at the superconvergence points for $\frac{\partial u_1}{\partial x_1}$, $\frac{\partial u_2}{\partial x_2}$, respectively (if such points exist in the mesh-pattern).

(vi) There are no superconvergence points for the shear-stress in any of the mesh-patterns.

(vii) For $p = 4$ there are no superconvergence points in any of the mesh-patterns for any of the quantities and for all values of Poisson's ratio.

7.2 η%-superconvergence regions for the components of the gradient and stress for the periodic meshes of triangles

For $p \geq 3$ there are very few (if any) superconvergence points for any of the solution-quantities for the problem of plane isotropic elasticity. In these cases suitable sampling points (i.e. points where the error in the solution-quantity is small, asymptotically, with respect to the error in other points in the element) can be determined from the η%-superconvergence regions. In the Figs. 5-7 below we give the regions $\tilde{\mathcal{R}}^{\eta\%}_{\frac{\partial u_1}{\partial x_1}}(Q^{"H"};\tilde{\tau};\tilde{T})$, for the Regular, Chevron and Criss-Cross patterns for $p = 1$, 2, 3 and Poisson's ratio = 0.3. (It should be noted that the η%-scale employed varies in the Figures.) From the numerical results we observe that:

(i) The regions $\tilde{\mathcal{R}}^{\eta\%}_{\frac{\partial u_1}{\partial x_1}}(Q^{"H"};\tilde{\tau};\tilde{T})$ exist for small η for almost all the cases (note however that $\eta\% = 100\%$ everywhere in the element τ_2 of the Criss-Cross pattern for linear elements, as shown in Fig. 7a).

(ii) For $p = 2$, in the Chevron pattern there exist η%-superconvergence regions with minimum $\eta \approx 34\%$ (as shown in Fig. 6b).

(iii) For $p = 2$, 3, in the element τ_2 of the Criss-Cross pattern there exist η%-superconvergence regions of significant size (although η may be relatively large), as shown in Figs. 7b, 7c, respectively.

From the engineering point of view one is mostly interested in determining optimal sampling points for the stress-components. Except for the special case of zero Poisson's ratio there are no superconvergence points for any of the stress-components in any of the mesh-patterns and for elements of any degree p. Here we show that for elements of degree $p \geq 2$ there exist η%-superconvergence points for the stress-components in all the mesh-patterns for relatively small values of η; these points may be employed as sampling-points for the corresponding stress-components. In Figs. 8, 9, 10 we give the η%-superconvergence regions for σ_{11} and σ_{12}, for $p = 2$ and 3, for the Regular, Chevron and Criss-Cross patterns. (The regions for the Union-Jack are similar and will not be given here; note that the Union-Jack pattern is obtained by a 45°-rotation of the Criss-Cross pattern.) We did not give the regions for $p = 1$ because the minimal values of η% for which the regions exist are close to 100% for all the mesh-patterns (in other words for meshes of linear triangles there is not a preferable set of sampling points for the stress-components, unless the Poisson's ratio is equal to zero).

The minimal value of η% in the η%-superconvergence regions shown in Figs. 8-10 are given in Table 1. (We did not report the points where these minima occur but these can be easily found.) In summary we observed that:

(i) The regions $\tilde{\mathcal{R}}^{\eta\%}_{F(u)}(\mathcal{Q}^{"H"};\tilde{\tau};\tilde{T})$ for $F(u) = \sigma_{11}$ or σ_{12} exist (resp. do not exist) for $p = 2, 3$ (resp. for $p = 1$) for relatively small values of $\eta\%$.

(ii) The minimal values of $\eta\%$ and their locations depend on the mesh-pattern, the degree p of the elements, the stress-component and the orientation of the coordinate-axes with respect to the mesh-pattern.

7.3 Superconvergence points for periodic meshes of squares

We also used the computer-based approach to determine the superconvergence points for meshes of square elements. Here we investigated the effect of the choice of the finite-element space (tensor-product, serendipity and intermediate element-space) on the superconvergence points for the components of the gradient of displacement, strain and stress. In the cases where there are no superconvergence points (for example, in the quartic serendipity element) we reported the element-coordinates of $\eta\%$-superconvergence points for minimal values of $\eta\%$.

a. Tensor-product and intermediate family

The superconvergence points for $\frac{\partial u_1}{\partial x_1}$ and $\frac{\partial u_2}{\partial x_1}$ are located on the Gauss-lines which are parallel to the $\hat{x}_2$-axis and are intersecting the $\hat{x}_1$-axis at the Gauss-Legendre points of degree p. The $(p \times p)$ Gauss-Legendre points are superconvergence points for all the components of strain and stress for all Poisson's ratios for both the "harmonic" and general class of solutions.

b. Serendipity family

For $p = 1$ and $p = 2$, the superconvergence points for all the quantities are exactly the same as the corresponding superconvergence points for the tensor-product and the intermediate family i.e. the $p \times p$ Gauss-Legendre points in the element.

In the cubic serendipity element ($p = 3$) there exist four superconvergence points and one superconvergence line for the components of the gradient of the solution for the class of "harmonic" solutions. The superconvergence points for $\frac{\partial u_1}{\partial x_1}$ are given in Table 2 and are shown in Fig. 11a. The four superconvergence points and the superconvergence line for $\frac{\partial u_1}{\partial x_2}$ are shown in Fig. 11b. For ϵ_{12} (and σ_{12}) and σ_{11} (and σ_{22}) there is only one superconvergence point, at the center of the element, as shown in Figs. 11c and 11d, respectively. All points given above are also superconvergence points for the class of general solutions and all admissible values of Poisson's ratio. In the special case of zero value for the Poisson's ratio the superconvergence points for σ_{11} (resp. σ_{22}) coincide with the superconvergence points for $\frac{\partial u_1}{\partial x_1}$ (resp. $\frac{\partial u_2}{\partial x_2}$).

For the cubic serendipity element we also determined the $\eta\%$-superconvergence regions $\tilde{\mathcal{R}}^{\eta\%}_{F(u)}(\mathcal{Q}^{"H"};\tilde{\tau},\tilde{T})$ for $F(u) = \dfrac{\partial u_1}{\partial x_1}$, $\dfrac{\partial u_1}{\partial x_2}$, σ_{11} and σ_{12}; these are given in Figs. 12a, 12b, 12c, 12d, respectively, for Poisson's ratio equal to 0.3. From Fig. 12c we observe that some of the points of the 3×3 Gauss-Legendre product rule (these points are often employed to sample the stresses in the cubic serendipity element) correspond to $\eta\%$-superconvergence points for the normal stress components with $\eta\% > 75\%$. From the same Figure it is clear that it is possible to find sets of sampling points for the normal stresses with $\eta\% < 50\%$.

In the quartic serendipity element ($p = 4$) there are no 0%-superconvergence points for any of the solution quantities. We found however that there exist $\eta\%$-superconvergence points and regions for the components of the gradient, strain and the stress (for $\nu = 0.3$) for small values of η, namely $\eta\% < 2.5\%$. In Figs. 13a and 13b we give the $\eta\%$-superconvergence regions $\widehat{\tilde{\mathcal{R}}}^{\eta\%}_{\frac{\partial u_1}{\partial x_1}}(\mathcal{Q}^{"H"};\tau,\tilde{T})$ and $\widehat{\tilde{\mathcal{R}}}^{\eta\%}_{\frac{\partial u_1}{\partial x_2}}(\mathcal{Q}^{"H"};\tau,\tilde{T})$, respectively, for Poisson's ratio equal to 0.3. In Tables 3b and 3c we give the master-element coordinates of sampling-points for ϵ_{12} and σ_{11} with $\eta\% \leq 2.5\%$. The $\eta\%$-superconvergence regions for ϵ_{12}, σ_{11} for $\eta \leq 25$ are shown in Figs. 13c, 13d, respectively. We also determined the common $\eta\%$-superconvergence regions for a class of Poisson's ratios ($0 \leq \nu \leq 0.35$). In Figs. 14a, 14b and 14c we show the regions $\bigcap_{0\leq\nu\leq 0.35} \widehat{\tilde{\mathcal{R}}}^{25\%}_{F(u)}(\mathcal{Q}^{"H"};\tilde{\tau};\tilde{T})$ for $F(u) = \dfrac{\partial u_1}{\partial x_1}$, σ_{11} and ϵ_{12}, respectively, for $p = 4$ and the class of "harmonic" solutions (the Poisson's ratio was varied from 0 to 0.35 in steps of 0.05). From Fig. 14b it can be seen that there is a very small common 25%-superconvergence region for σ_{11} for all the Poisson's ratios ($0 \leq \nu \leq 0.35$).

7.4 Rate of convergence at the superconvergence points

We checked the rate of convergence of $\dfrac{\partial u_{h1}}{\partial x_1}$ at the superconvergence points (given in Sections 7.1 and 7.3) in model computations using relatively coarse meshes. We considered the Dirichlet problem with data consistent with the exact solution $u_1(x_1,x_2) = u_2(x_1,x_2) = \sin(\pi x_1)\sin(\pi x_2)$ (note that $\boldsymbol{u} \notin \mathcal{U}^{"H"}$) in the domain $\Omega = (0,1)^2$ which was meshed by a uniform grid of elements (of triangles in the Regular-pattern or squares). We computed the quantity:

$$E = \max_{x_\tau^{sup}\in\Omega_0} \left| \left(\frac{\partial u_1}{\partial x_1} - \frac{\partial u_{h1}}{\partial x_1} \right)(x_\tau^{sup}) \right|, \tag{7.1}$$

where x_τ^{sup} denotes the superconvergence points in the elements in the subdomain $\Omega_0 = (0.25, 0.75)^2$. We computed the values of E in meshes with mesh-sizes $h =$

$\frac{1}{4}, \frac{1}{8}, \frac{1}{16}$. We will say that the values of E are superconvergent with rate $(p+\sigma_0)$ if there exists $\sigma_0 > 0$ s.t. $\lim_{h\to 0}(h^{-(p+\sigma_0)}E) = \text{constant}$.

In Table 4a (resp. Table 4b) we give the values of E and $h^{-3}E$ (resp. $h^{-4}E$) computed using a uniform mesh of triangles of Regular pattern with $p = 2$ (resp. $p = 3$). We note that as the element size h is decreased, the values of $h^{-(p+1)}E$ converge to constants; therefore the quantity E converges at the rate of $(p+1)$ i.e. $\sigma_0 = 1$. In Table 4c we give the values of E and $h^{-4}E$ computed using a uniform mesh of cubic serendipity squares of size h. We computed the values of E using the points given in Table 2 in the subdomain Ω_0. It can be observed that the values of the quantity E converge with rate equal to 4. Hence the points given in Sections 7.1 and 7.3 are superconvergence points with rate equal to $(p+1)$.

We also checked the value of relative error at the η%-superconvergence points for the quartic serendipity element which are given in Table 3a. We considered the Dirichlet problem in $\Omega = (0,1)^2$ with data consistent with the exact solution $u_1(x_1,x_2) = u_2(x_1,x_2) = \sin(\pi x_1)\sin(\pi x_2)$ and computed its finite elements solution on a 9×9 uniform grid of serendipty squares. For this finite element solution we computed the values of the relative error $\Theta(x_\tau; \frac{\partial u}{\partial x_1}; u, u_h; \frac{1}{9}, \tau)$ at the (4×4) Gauss-Legendre points and at the η%-superconvergence points given in Table 3a for the central element of the (9×9) square mesh which coincides with the square $\left(\frac{4}{9}, \frac{5}{9}\right)^2$. In Table 6a we give the values of the relative error at the (4×4) Gauss-Legendre points while in Table 6b we give the values of the error at the η%-superconvergence points given in Table 3a. It can be seen that the relative error at several of the (4×4) Gauss-Legendre points is nearly 47% while at the η%-superconvergence points from Table 3a the relative error does not exceed 3%. Thus, the η%-superconvergence points of Table 3a should be used as sampling points in the quartic serendipity element instead of the points of the 3×3 Gauss-Legendre product-rule.

8 Summary of conclusions

1. We presented a study of superconvergence for finite element approximations of plane elasticity. We employed a computer-based methodology which takes directly into account the topology of the grid, the element-space, the class of solutions and the value of Poisson's ratio.

2. We determined the superconvergence points for the components of the gradient of the displacement, the strain and the stress. We observed the following:

   a. For meshes of triangles of degree p, $1 \leq p \leq 4$.

(i) For some mesh-patterns (Regular, Criss-Cross, Chevron) there exist superconvergence points for the components of the gradient of the displacement. These points are the same as the superconvergence points for the components of the gradient for finite element solutions of Poisson's equation given in [1]. The location of the points does not depend on the value of Poisson's ratio.

(ii) There are no superconvergence points for any of the stress-components (except for the normal stress-components when the Poisson's ratio is equal to zero) or the shear strain in any of the mesh-pattern.

(iii) For $p = 4$ there are no superconvergence points for any of the quantities in any of the patterns:

(iv) Suitable sampling points for the stresses can be obtained by locating minimal $\eta\%$-superconvergence points in each pattern for each stress-components, for each element-degree p.

b. For meshes of squares of degree p, $1 \leq p \leq 4$.

(i) For elements of the tensor-product or the intermediate family for $1 \leq p \leq 4$ and elements of the serendipity family for $p = 1$ and 2 the points of the $p \times p$ Gauss-Legendre product-rule are superconvergence points simultaneously for the components of the gradient of the displacement, the strain and the stress.

(ii) For the cubic serendipity square there exist four superconvergence points and one superconvergence line the components of the gradient of the displacement. For the normal components of stress (for non-zero values of Poisson's ratio) and the shear-strain there is only one superconvergence point located at the center of the element.

(iii) For the quartic serendipity square there are no 0%-superconvergence points for any of the solution quantities. However it is possible to locate $\eta\%$-superconvergence points, for the components of the gradient and the stress, for small values of $\eta\%$ ($\eta\% < 2.5\%$). The values of the solution quantities are much more accurate, asymptotically, at the corresponding $\eta\%$-superconvergence points than the values of the quantities at the 4×4 points of the Gauss-Legendre product-rule.

Acknowledgments

The first author was partially supported by the Office of Naval Research under Grant N00014-90-J-1030 and the National Science Foundation under Grant CCR-88-20279.

The second, third and fourth authors acknowledge the support of the National Science Foundation under grant MSS-9025110, the Army Research Office under grant DAAL03-92-G-0268 and the Texas Advanced Research Program under grant TARP-71071.

References

1. I. BABUŠKA, T.S. STROUBOULIS, C.S. UPADHYAY AND S.K. GANGARAJ, *Study of superconvergence by a computer-based approach. Superconvergence of the gradient in finite element solutions of Laplace's and Poisson's equations*, Technical Note BN-1155, Institute for Physical Science and Technology, University of Maryland, College Park, November 1993.

2. L.A. OGANESYAN AND L.A. RUKHOVETS, *Study of the rate of convergence of variational difference schemes for second-order elliptic equations in a two-dimensional field with a smooth boundary*, U.S.S.R. Comput. Math. Math. Phys., 9 (1968), pp. 153-183.

3. J. DOUGLAS, JR., AND T. DUPONT, *Superconvergence for Galerkin methods for the two point boundary problem via local projections*, Numer. Math., 21 (1973), pp. 270-278.

4. J. DOUGLAS, JR., AND T. DUPONT, *Galerkin approximations for the two point boundary problem using continuous piecewise polynomial spaces*, Numer. Math., 22 (1974), pp. 99-109.

5. J. DOUGLAS, JR., T. DUPONT AND M.F. WHEELER, *An L^∞ estimate and a superconvergence result for a Galerkin method for elliptic equations based on tensor products of piecewise polynomials*, RAIRO Anal. Numér., 8 (1974), pp. 61-66.

6. T. DUPONT, *A unified theory of superconvergence for Galerkin methods for two-point boundary problems*, SIAM J. Numer. Anal., 13 (1976), pp. 362-368.

7. J.H. BRAMBLE and A.H. SCHATZ, *Higher order local accuracy by averaging in the finite element method*, Math. Comp., 31 (1977), pp. 94-111.

8. V. THOMÉE *High order local approximations to derivatives in the finite element method*, Math. Comp. 31 (1977), pp. 652-660.

9. M. ZLÁMAL, *Superconvergence and reduced integration in the finite element method*, Math. Comp., 32 (1978), pp. 663-685.

10. P. LESAINT AND M. ZLÁMAL, *Superconvergence of the gradient of finite element solutions*, RAIRO Anal. Numér., 13 (1979), pp. 139-166.

11. R.Z. DAUTOV, A.V. LAPIN AND A.D. LYASHKO, *Some mesh schemes for quasilinear elliptic equations*, U.S.S.R. Comput. Math. Math. Phys., 20 (1980), pp. 62-78.

12. M. KŘÍŽEK AND P. NEITTAANMÄKI, *Superconvergence phenomenon in the finite element method arising from averaging gradients*, Numer. Math., 45 (1984), pp. 105-116.

13. N. LEVINE, *Superconvergent recovery of the gradient from piecewise linear finite-element approximations*, IMA J. Numer. Anal., 5 (1985), pp. 407-427.

14. M.F. WHEELER AND J.R. WHITEMAN, *Superconvergent recovery of gradients on subdomains from piecewise linear finite-element approximations*, Numer. Methods for PDEs, 3 (1987), pp. 65-82.

15. M.T. NAKAO, *Superconvergence of the gradient of Galerkin approximations for elliptic problems*, RAIRO Math. Model. Numer. Anal., 21 (1987), pp. 679-695.

16. M. KŘÍŽEK AND P. NEITTAANMÄKI, *On superconvergence techniques*, Acta Applic. Math., 9 (1987), pp. 175-198.

17. M. KŘÍŽEK AND P. NEITTAANMÄKI, *On a global superconvergence of the gradient of linear triangular elements*, J. Comput. Appl. Math., 18 (1987), pp. 221-233.

18. I. HLAVÁČEK AND M. KŘÍŽEK, *On a superconvergent finite element scheme for elliptic systems. I. Dirichlet boundary condition*, Aplik. Mat., 32 (1987), pp. 131-154.

19. I. HLAVÁČEK AND M. KŘÍŽEK, *On a superconvergent finite element scheme for elliptic systems. II. Boundary conditions of Newton's or Neumann's type*, Aplik. Mat., 32 (1987), pp. 200-213.

20. I. HLAVÁČEK AND M. KŘÍŽEK, *On a superconvergent finite element scheme for elliptic systems. III. Optimal interior estimates*, Aplik. Mat., 32 (1987), pp. 276-289.

21. A.B. ANDREEV AND R.D. LAZAROV, *Superconvergence of the gradient for quadratic triangular finite elements*, Numer. Methods for PDEs, 4 (1988), pp. 15-32.

22. Q.D. ZHU AND Q. LIN, *Superconvergence Theory of FEM*, Hunan Science Press, 1989.

23. G. GOODSELL AND J.R. WHITEMAN, *A unified treatment of superconvergent recovered gradient functions for piecewise linear finite element approximations*, Internat. J. Numer. Methods Engrg., 27 (1989), pp. 469-481.

24. G. GOODSELL AND J.R. WHITEMAN, *Pointwise superconvergence of recovered gradients for piecewise linear finite element approximations to problems of planar linear elasticity*, Numer. Methods for PDEs, 6 (1990), pp. 59-74.

25. G. GOODSELL AND J.R. WHITEMAN, *Superconvergence of recovered gradients of piecewise quadratic finite element approximations. Part I: L_2-error estimates*, Numer. Methods for PDEs, 7 (1991), pp. 61-83.

26. G. GOODSELL AND J.R. WHITEMAN, *Superconvergence of recovered gradients of piecewise quadratic finite element approximations. Part II: L_∞-error estimates*, Numer. Methods for PDEs, 7 (1991), pp. 85-99.

27. R. DURÁN, M.A. MUSCHIETTI AND R. RODRÍGUEZ, *On the asymptotic exactness of error estimators for linear triangular finite elements*, Numer. Math., 59 (1991), pp. 107-127.

28. R. DURÁN, M.A. MUSCHIETTI AND R. RODRÍGUEZ, *Asymptotically exact error estimators for rectangular finite elements*, SIAM J. Numer. Anal., 29 (1992), pp. 78-88.

29. A.H. SCHATZ, I.H. SLOAN AND L.B. WAHLBIN, *Superconvergence in finite element methods and meshes which are symmetric with respect to a point*, preprint.

30. I. BABUŠKA, T. STROUBOULIS AND C.S. UPADHYAY, *η%-superconvergence of finite element approximations in the interior of general meshes of triangles*, Technical Note BN-1160, Institute for Physical Science and Technology, University of Maryland, College Park, December 1993.

31. I. BABUŠKA, T. STROUBOULIS, S.K. GANGARAJ AND C.S. UPADHYAY, *η%-superconvergence in the interior of locally refined meshes of quadrilaterals. Superconvergence of the gradient in finite element solutions of Laplace's and Poisson's equations*, Technical Note BN-1161, Institute for Physical Science and Technology, University of Maryland, College Park, January 1994.

32. B.A. SZABÓ AND I. BABUŠKA, *Finite Element Analysis*, John Wiley & Sons, Inc., New York, 1991.

33. J.A. NITSCHE AND A.H. SCHATZ, *Interior estimates for Ritz-Galerkin methods*, Math. Comp. 28 (1974), pp. 937-958.

34. J.H. BRAMBLE, J.A. NITSCHE AND A.H. SCHATZ, *Maximum-norm estimates for Ritz-Galerkin methods*, Math. Comp. 29 (1975), pp. 677-688.

35. A.H. SCHATZ AND L.B. WAHLBIN, *Interior maximum norm estimates for finite element methods*, Math. Comp. 31 (1977), pp. 414-442.

36. A.H. SCHATZ AND L.B. WAHLBIN, *Maximum norm estimates in the finite element method on plane polygonal domains. Part 1*, Math. Comp. 32 (1978), pp. 73-109.

37. A.H. SCHATZ AND L.B. WAHLBIN, *Maximum norm estimates in the finite element method on plane polygonal domains. Part 2*, refinements, Math. Comp. 33 (1979), pp. 465-492.

38. L.B. WAHLBIN, *Local behavior in finite element methods*, in: P.G. Ciarlet and J.L. Lions, eds., Handbook of Numerical Analysis, Vol. II (North-Holland, Amsterdam, 1991), pp. 357-522.

39. A.H. SCHATZ AND L.B. WAHLBIN, *Interior maximum norm estimates for finite element methods. Part II*, preprint.

40. I. BABUŠKA, T. STROUBOULIS AND C.S. UPADHYAY, *A model study of the quality of a posteriori error estimators for linear elliptic problems: Error estimation in the interior of patchwise uniform grids of triangles*, Comput. Methods Appl. Mech. Engrg. (1994), to appear.

Appendix
"Harmonic" monomials of degree $p+1$ $(1 \leq p \leq 4)$

Below we give the "harmonic" basis monomials of degree $(p+1)$, for the space $Q^{"H"}$ defined in Section 6, for the equations of plane elasticity and $1 \leq p \leq 4$.

a. Quadratic "harmonic" monomials

$$Q_1^{"H"}(x_1, x_2; a_1, a_3, b_2, b_3) = a_1 x_1^2 + a_2 x_2^2 + a_3 x_1 x_2$$

$$Q_2^{"H"}(x_1, x_2, a_1, a_3, b_2, b_3) = b_1 x_1^2 + b_2 x_2^2 + b_3 x_1 x_2$$

where

$$a_2 = -\frac{\lambda+2\mu}{\mu} a_1 - \frac{\lambda+\mu}{2\mu} b_3, \qquad b_1 = -\frac{\lambda+2\mu}{\mu} b_2 - \frac{\lambda+\mu}{2\mu} a_3$$

b. Cubic "harmonic" monomials

$$Q_1^{"H"}(x_1, x_2; a_3, a_4, b_3, b_4) = a_1 x_1^3 + a_2 x_2^2 + a_3 x_1^2 x_2 + a_4 x_1 x_2^2$$

$$Q_2^{"H"}(x_1, x_2; a_3, a_4, b_3, b_4) = b_1 x_1^3 + b_2 x_2^3 + b_3 x_1 x_2^2 + b_4 x_1^2 x_2$$

where

$$a_1 = -\frac{\lambda+\mu}{3(\lambda+2\mu)} b_4 - \frac{\mu}{3(\lambda+2\mu)} a_4, \qquad b_2 = -\frac{\lambda+\mu}{3(\lambda+2\mu)} a_4 - \frac{\mu}{3(\lambda+2\mu)} b_4$$

$$a_2 = -\frac{\lambda+2\mu}{3\mu} a_3 - \frac{\lambda+\mu}{3\mu} b_3, \qquad b_1 = -\frac{\lambda+2\mu}{3\mu} b_3 - \frac{\lambda+\mu}{3\mu} a_3$$

c. Quartic "harmonic" monomials

$$Q_2^{"H"}(x_1, x_2; a_3, a_5, b_3, b_5) = a_1 x_1^4 + a_2 x_2^4 + a_3 x_1^3 x_2 + a_4 x_1^2 x_2^2 + a_5 x_1 x_2^3$$

$$Q_2^{"H"}(x_1, x_2; a_3, a_5, b_3, b_5) = b_1 x_1^4 + b_2 x_2^4 + b_3 x_1 x_2^3 + b_4 x_1^2 x_2^2 + b_5 x_1^3 x_2$$

where

$$b_4 = -\frac{3\mu}{2(\lambda+\mu)}a_5 - \frac{3(\lambda+2\mu)}{2(\lambda+\mu)}a_3, \qquad a_4 = -\frac{3\mu}{2(\lambda+\mu)}b_5 - \frac{3(\lambda+2\mu)}{2(\lambda+\mu)}b_3$$

$$a_1 = -\frac{\lambda+\mu}{4(\lambda+2\mu)}b_5 - \frac{\mu}{6(\lambda+2\mu)}a_4, \qquad b_2 = -\frac{\lambda+\mu}{4(\lambda+2\mu)}a_5 - \frac{\mu}{6(\lambda+2\mu)}b_4$$

d. Quintic "harmonic" monomials

$$Q_1^{"H"}(x_1, x_2; a_4, a_5, b_4, b_5) = a_1 x_1^5 + a_2 x_2^5 + a_3 x_1^4 x_2 + a_4 x_1^3 x_2^2 + a_5 x_1^2 x_2^3 + a_6 x_1 x_2^4$$

$$Q_2^{"H"}(x_1, x_2; a_4, a_5, b_4, b_5) = b_1 x_1^5 + b_2 x_2^5 + b_3 x_1 x_2^4 + b_4 x_1^2 x_2^3 + b_5 x_1^3 x_2^2 + b_6 x_1^4 x_2$$

where

$$a_3 = -\frac{\lambda+\mu}{2(\lambda+2\mu)}b_5 - \frac{\mu}{2(\lambda+2\mu)}a_5, \qquad b_3 = -\frac{\lambda+\mu}{2(\lambda+2\mu)}a_5 - \frac{\mu}{2(\lambda+2\mu)}b_5$$

$$a_6 = -\frac{\lambda+2\mu}{2\mu}a_4 - \frac{\lambda+\mu}{2\mu}b_4, \qquad b_6 = -\frac{\lambda+2\mu}{2\mu}b_4 - \frac{\lambda+\mu}{2\mu}a_4$$

$$a_1 = -\frac{(\lambda+\mu)}{5(\lambda+2\mu)}b_6 - \frac{\mu}{10(\lambda+2\mu)}a_4, \qquad b_2 = -\frac{(\lambda+\mu)}{5(\lambda+2\mu)}a_6 - \frac{\mu}{10(\lambda+2\mu)}b_4$$

$$a_2 = -\frac{(\lambda+2\mu}{10\mu}a_5 - \frac{(\lambda+\mu)}{5\mu}b_3, \qquad b_1 = -\frac{(\lambda+2\mu}{10\mu}b_5 - \frac{(\lambda+\mu)}{5\mu}a_3.$$

Minimal values of $\eta\%$ for the stress-components						
Degree of the elements	Regular pattern		Chevron pattern		Criss-Cross pattern	
	σ_{11}	σ_{12}	σ_{11}	σ_{12}	σ_{11}	σ_{12}
$p = 2$	18.17%	5.75%	11.79%	12.19%	5.53%(τ_1) 30.50%(τ_2)	28.75%(τ_1) 24.51%(τ_2)
$p = 3$	8.71%	13.33%	11.5%	3.88%	10.77%(τ_1) 1.07%(τ_2)	6.91%(τ_1) 6.07%(τ_2)

Table 1. *$\eta\%$-superconvergence of stress-components in the meshes of triangles: Minimal values of $\eta\%$ for the σ_{11}, σ_{12} components in the Regular, Chevron and Criss-Cross mesh-patterns.*

Cubic serendipity square elements		
Superconvergence points for $\frac{\partial u_1}{\partial x_1}, \frac{\partial u_2}{\partial x_2}$		
Points	$\hat{x}_1$	$\hat{x}_2$
1	.000000000000	[-1, 1]
2	.774596669175	.577350269112
3	-.774596669175	.577350269112
4	-.774596669175	-.577350269112
5	.774596669175	-.577350269112

Table 2. *Superconvergence points for cubic serendipity square elements: Superconvergence points for* $\frac{\partial u_1}{\partial x_1}, \frac{\partial u_2}{\partial x_1}$. Note that there are four superconvergence points and one superconvergence line and are valid also for the class of general solutions and all values of Poisson's ratio.

Quartic serendipity square elements			
η%-superconvergence points for $\frac{\partial u_1}{\partial x_1}$			
Point	$\hat{x}_1$	$\hat{x}_2$	η%
1	-0.6000	-1.0000	2.154
2	0.6000	-1.0000	2.154
3	0.0000	-0.6364	0.952
4	-0.5273	0.0000	0.150
5	0.5273	0.0000	0.150
6	0.0000	0.6364	0.952
7	-0.6000	1.0000	2.154
8	0.6000	1.0000	2.154

Table 3a. *η%-superconvergence points for quartic serendipity square elements: Sampling points for $\frac{\partial u_1}{\partial x_1}$ with $\eta\% < 2.5\%$ for Poisson's ratio $\nu = 0.30$.*

Quartic serendipity square elements			
η%-superconvergence points for ϵ_{12}			
Point	$\hat{x}_1$	$\hat{x}_2$	η%
1	0.0000	-0.6727	0.724
2	-0.4909	0.0000	0.499
3	0.4909	0.0000	0.499
4	0.0000	0.6727	0.724

Table 3b. *η%-superconvergence points for quartic serendipity square elements: Sampling points for ϵ_{12} with $\eta\% < 0.75\%$ for Poisson's ratio $\nu = 0.30$.*

Quartic serendipity square elements			
η%-superconvergence points for σ_{11}			
Point	$\hat{x}_1$	$\hat{x}_2$	η%
1	0.0000	-0.5818	1.334
2	-0.5636	0.0000	0.815
3	0.5636	0.0000	0.815
4	0.0000	0.5818	1.334

Table 3c. *η%-superconvergence points for quartic serendipity square elements: Sampling points for σ_{11} with $\eta\% < 1.5\%$ for Poisson's ratio $\nu = 0.30$.*

Rate of convergence at the superconvergence points		
Regular pattern; quadratic triangles		
h	$\max_{x_\tau^{sup}\in\Omega_0} \left\lvert \left(\frac{\partial u_1}{\partial x_1} - \frac{\partial u_{h1}}{\partial x_1}\right)(x_\tau^{sup}) \right\rvert$	$h^{-3} \max_{x_\tau^{sup}\in\Omega_0} \left\lvert \left(\frac{\partial u_1}{\partial x_1} - \frac{\partial u_{h1}}{\partial x_1}\right)(x_\tau^{sup}) \right\rvert$
.25	0.032184	2.057
.125	0.003927	2.011
.0625	0.000488	1.999
.03125	0.000061	1.996

Table 4a. *Rate of convergence at the superconvergence points: Values of* $\max_{x_\tau^{sup}\in\Omega_0} \left\lvert \left(\frac{\partial u_1}{\partial x_1} - \frac{\partial u_{h1}}{\partial x_1}\right)(x_\tau^{sup}) \right\rvert$ and $h^{-3} \max_{x_\tau^{sup}\in\Omega_0} \left\lvert \left(\frac{\partial u_1}{\partial x_1} - \frac{\partial u_{h1}}{\partial x_1}\right)(x_\tau^{sup}) \right\rvert$. Dirichlet problem in $\Omega = (0,1)^2$ with data consistent with the exact solution, $u_1(x_1,x_2) = u_2(x_1,x_2) = \sin(\pi x_1)\sin(\pi x_2)$, $\Omega_0 := (0.25, 0.75)^2$. Grids of quadratic triangular elements in the Regular pattern. Note that the values of $\frac{\partial u_1}{\partial x_1}$ at the superconvergence points are superconvergent with rate of convergence equal to 3.

Rate of convergence at the superconvergence points		
Regular pattern; Cubic triangles		
h	$\max_{x_\tau^{sup}\in\Omega_0} \left\lvert \left(\frac{\partial u_1}{\partial x_1} - \frac{\partial u_{h1}}{\partial x_1}\right)(x_\tau^{sup}) \right\rvert$	$h^{-4} \max_{x_\tau^{sup}\in\Omega_0} \left\lvert \left(\frac{\partial u_1}{\partial x_1} - \frac{\partial u_{h1}}{\partial x_1}\right)(x_\tau^{sup}) \right\rvert$
.25	0.0007548	0.193
.125	0.0000525	0.215
.0625	0.0000035	0.226
.03125	0.0000002	0.231

Table 4b. *Rate of convergence at the superconvergence points: Values of* $\max_{x_\tau^{sup}\in\Omega_0} \left\lvert \left(\frac{\partial u_1}{\partial x_1} - \frac{\partial u_{h1}}{\partial x_1}\right)(x_\tau^{sup}) \right\rvert$ and $h^{-4} \max_{x_\tau^{sup}\in\Omega_0} \left\lvert \left(\frac{\partial u_1}{\partial x_1} - \frac{\partial u_{h1}}{\partial x_1}\right)(x_\tau^{sup}) \right\rvert$. Dirichlet problem in $\Omega = (0,1)^2$ with data consistent with the exact solution, $u_1(x_1,x_2) = u_2(x_1,x_2) = \sin(\pi x_1)\sin(\pi x_2)$, $\Omega_0 := (0.25, 0.75)^2$. Grids of cubic triangular elements in the Regular pattern. Note that the values of $\frac{\partial u_1}{\partial x_1}$ at the superconvergence points are superconvergent with rate of convergence equal to 4.

Quartic serendipity square elements		
η%-superconvergence for $\dfrac{\partial u_1}{\partial x_1}$		
h	$\max\limits_{x_\tau^{sup}\in\Omega_0} \left\lvert \left(\dfrac{\partial u_1}{\partial x_1} - \dfrac{\partial u_{h1}}{\partial x_1}\right)(x_\tau^{sup}) \right\rvert$	$h^{-4} \max\limits_{x_\tau^{sup}\in\Omega_0} \left\lvert \left(\dfrac{\partial u_1}{\partial x_1} - \dfrac{\partial u_{h1}}{\partial x_1}\right)(x_\tau^{sup}) \right\rvert$
0.2500	.12053504E+00	30.8570
0.1250	.70559307E-02	28.9011
0.0625	.43019091E-03	28.1930

Table 5. *Rate of convergence at the superconvergence points: Values of* $\max\limits_{x_\tau^{sup}\in\Omega_0} \left\lvert \left(\dfrac{\partial u_1}{\partial x_1} - \dfrac{\partial u_{h1}}{\partial x_1}\right)(x_\tau^{sup}) \right\rvert$ *and* $h^{-4} \max\limits_{x_\tau^{sup}\in\Omega_0} \left\lvert \left(\dfrac{\partial u_1}{\partial x_1} - \dfrac{\partial u_{h1}}{\partial x_1}\right)(x_\tau^{sup}) \right\rvert$. Dirichlet problem in $\Omega = (0,1)^2$ with data consistent with the exact solution, $u_1(x_1,x_2) = u_2(x_1,x_2) = \sin(\pi x_1)\sin(\pi x_2)$, $\Omega_0 := (0.25, 0.75)^2$. Meshes of cubic serendipity squares. Note that the values of $\dfrac{\partial u_1}{\partial x_1}$ at the superconvergence points are superconvergent with rate equal to 4.

Relative error at the 4×4 Gauss-Legendre points			
Point	$\hat{x}_1$	$\hat{x}_2$	$\Theta(x_\tau; \frac{\partial u_1}{\partial x_1}; u, u_h, h, \tau)$
1	-.861136311600	-.861136311600	30.5947
2	-.861136311600	.861136311600	30.5948
3	-.861136311600	-.339981043600	30.4170
4	-.861136311600	.339981043600	30.4171
5	.861136311600	-.861136311600	30.5948
6	.861136311600	.861136311600	30.5947
7	.861136311600	-.339981043600	30.4171
8	.861136311600	.339981043600	30.4170
9	-.339981043600	-.861136311600	6.1581
10	-.339981043600	.861136311600	6.1580
11	-.339981043600	-.339981043600	46.5763
12	-.339981043600	.339981043600	46.5762
13	.339981043600	-.861136311600	6.1580
14	.339981043600	.861136311600	6.1581
15	.339981043600	-.339981043600	46.5762
16	.339981043600	.339981043600	46.5763

Table 6a. *Values of the relative error* $\Theta(x_\tau; \frac{\partial u_1}{\partial x_1}; u, u_h, h, \tau)$ *at the 4×4 Gauss-Legendre points: Quartic serendipity square element.* Dirichlet problem in $\Omega = (0,1)^2$ with data consistent with the exact solution $u_1(x_1, x_2) = u_2(x_1, x_2) = \sin(\pi x_1)\sin(\pi x_2)$. The domain Ω was discretized using a 9×9 uniform mesh of quartic serendipity elements. The relative errors are reported for the element at the center at the center of the mesh. Note that the values of the relative error at some of the Gauss-Legendre points exceeds 45%.

Relative error at the points from Table 3a			
Point	$\hat{x}_1$	$\hat{x}_2$	$\Theta(x_\tau; \frac{\partial u_1}{\partial x_1}; u, u_h, h, \tau)$
1	-.6000	-1.00000	.5797
2	.6000	-1.00000	.5797
3	.0000	-.63640	.0001
4	-.5273	.00000	2.8799
5	.5273	.00000	2.8799
6	.0000	.63640	.0001
7	-.6000	1.00000	.5797
8	.6000	1.00000	.5797

Table 6b. *Values of the relative error* $\Theta(x_\tau; \frac{\partial u_1}{\partial x_1}; u, u_h, h, \tau)$ *at the* η*%-superconvergence points (from Table 3): Quartic serendipity square element.* Dirichlet problem in $\Omega = (0,1)^2$ with data consistent with the exact solution $u_1(x_1, x_2) = u_2(x_1, x_2) = \sin(\pi x_1)\sin(\pi x_2)$. The domain Ω was discretized using a 9×9 uniform mesh of quartic serendipity elements. The relative errors are reported for the element at the center at the center of the mesh. Note that the values of the relative error do not exceed 3%.

List of Figures

Fig. 1. *An example of a locally periodic grid of squares: An adaptive grid with a periodic mesh-subdomain.* The mesh outside the subdomain was refined in order to control the pollution-error in the interior of the subdomain.

Fig. 2 *Periodic meshes of triangles.* (a) Regular pattern; (b) Chevron pattern; (c) Union-Jack pattern; (d) Criss-Cross pattern.

Fig. 3. *Superconvergence points for* $\frac{\partial u_1}{\partial x_1}$ *for the class of "harmonic" solutions of the equations of plane elasticity: Triangular elements in the Regular pattern.* The superconvergence points are located at the intersection of the contours $C^{0\%}_{\frac{\partial u_1}{\partial x_1}}(Q_i^{"H"}; \tilde{\tau}, \tilde{T})$, $i = 1, \ldots, 4$. In the Figures the 0%-contours of the error corresponding to the various monomials were drawn with different thicknesses and the element boundaries were drawn with dashed lines. The 0%-contours and the superconvergence points are given for: (a) Linear elements ($p = 1$); (b) Quadratic elements ($p = 2$); (c) Cubic elements ($p = 3$). Note that the superconvergence points are shown in each Figure by a solid circle and are also superconvergence points for the class of general solutions and for all values of Poisson's ratio.

Fig. 4. *Superconvergence points for* $\frac{\partial u_1}{\partial x_1}$ *for the class of "harmonic" solutions of the equations of plane elasticity: Triangular elements in the Criss-Cross pattern.* The superconvergence points are located at the intersection of the contours $C^{0\%}_{\frac{\partial u_1}{\partial x_1}}(Q_i^{"H"}; \tilde{\tau}, \tilde{T})$, $i = 1, \ldots, 4$. In the Figures the 0%-contours of the error corresponding to the various monomials were drawn with different thicknesses and the element boundaries were drawn with dashed lines. The 0%-contours and the superconvergence points are given for: (a) Linear elements ($p = 1$); (b) Quadratic elements ($p = 2$); (c) Cubic elements ($p = 3$). Note that the superconvergence points are shown in each Fig. by a solid circle and are also superconvergence points for the class of general solutions and for all values of Poisson's ratio.

Fig. 5. *η%-superconvergence regions for* $\frac{\partial u_1}{\partial x_1}$ *for the class of "harmonic" solutions of the equations of plane elasticity: Triangular elements in the Regular pattern.* The regions $\tilde{\mathcal{R}}^{\eta\%}_{\frac{\partial u_1}{\partial x_1}}(Q^{"H"}; \tilde{\tau}; \tilde{T})$ are given for: (a) Linear elements ($p = 1$); (b) Quadratic elements ($p = 2$); (c) Cubic elements ($p = 3$). The η%-levels 5%, 15%, 30% (dark, light, lighter gray) were employed.

Fig. 6. *η%-superconvergence regions for* $\frac{\partial u_1}{\partial x_1}$ *for the class of "harmonic" solutions of the equations of plane elasticity: Triangular elements in the Chevron pattern.*

The regions $\tilde{\mathcal{R}}^{\eta\%}_{\frac{\partial u_1}{\partial x_1}}(\mathcal{Q}^{\text{"}H\text{"}};\tilde{\tau};\tilde{T})$ are given for: (a) Linear elements ($p=1$) (η%-levels: 5%, 15%, 30%); (b) Quadratic elements ($p=2$) (η%-levels: 40%, 50%, 60%); (c) Cubic elements, ($p=3$) (η%-levels: 5%, 15%, 30%).

Fig. 7. *η%-superconvergence regions for $\dfrac{\partial u_1}{\partial x_1}$ for the class of "harmonic" solutions of the equations of plane elasticity: Triangular elements in the Criss-Cross pattern.* The regions $\tilde{\mathcal{R}}^{\eta\%}_{\frac{\partial u_1}{\partial x_1}}(\mathcal{Q}^{\text{"}H\text{"}};\tilde{\tau};\tilde{T})$ are given for: (a) Linear elements ($p=1$) (η%-levels: 5%, 15%, 30%); (b) Quadratic elements ($p=2$) (η%-levels: 10%, 30%, 50%); (c) Cubic elements ($p=3$) (η%-levels: 5%, 15%, 30%).

Fig. 8. *η%-superconvergence regions for σ_{11} and σ_{12} for the class of "harmonic" solutions of the equations of plane elasticity: Triangular elements in the Regular pattern.* (a) $\mathcal{R}^{\eta\%}_{\sigma_{11}}(\mathcal{Q}^{\text{"}H\text{"}};\tilde{\tau},\tilde{T})$, $p=2$, min η%= 18.17%; (b) $\mathcal{R}^{\eta\%}_{\sigma_{12}}(\mathcal{Q}^{\text{"}H\text{"}};\tilde{\tau},\tilde{T})$, $p=2$, min $\eta\%=5.75\%$; (c) $\mathcal{R}^{\eta\%}_{\sigma_{11}}(\mathcal{Q}^{\text{"}H\text{"}};\tilde{\tau},\tilde{T})$, $p=3$, min $\eta\%=8.71\%$; (d) $\mathcal{R}^{\eta\%}_{\sigma_{12}}(\mathcal{Q}^{\text{"}H\text{"}};\tilde{\tau},\tilde{T})$, $p=3$, min $\eta\%=13.33\%$. The η%-levels 10%, 30%, 60% (dark, light, lighter gray) were employed.

Fig. 9. *η%-superconvergence regions for σ_{11} and σ_{12} for the class of "harmonic" solutions of the equations of plane elasticity: Triangular elements in the Chevron pattern.* (a) $\mathcal{R}^{\eta\%}_{\sigma_{11}}(\mathcal{Q}^{\text{"}H\text{"}};\tilde{\tau},\tilde{T})$, $p=2$, min $\eta\%=11.79\%$; (b) $\mathcal{R}^{\eta\%}_{\sigma_{12}}(\mathcal{Q}^{\text{"}H\text{"}};\tilde{\tau},\tilde{T})$, $p=2$. min $\eta\%=12.19\%$; (c) $\mathcal{R}^{\eta\%}_{\sigma_{11}}(\mathcal{Q}^{\text{"}H\text{"}};\tilde{\tau},\tilde{T})$, $p=3$, min $\eta\%=11.50\%$; (d) $\mathcal{R}^{\eta\%}_{\sigma_{12}}(\mathcal{Q}^{\text{"}H\text{"}};\tilde{\tau},\tilde{T})$, $p=3$, min $\eta\%=3.88\%$. The η%-levels 10%, 30%, 60% (dark, light, lighter gray) were employed.

Fig. 10. *η%-superconvergence regions for σ_{11} and σ_{12} for the class of "harmonic" solutions of the equations of plane elasticity: Triangular elements in the Criss-Cross pattern.* (a) $\mathcal{R}^{\eta\%}_{\sigma_{11}}(\mathcal{Q}^{\text{"}H\text{"}};\tilde{\tau},\tilde{T})$, $p=2$, $\min\limits_{\tau_1}\eta\%=5.53\%$, $\min\limits_{\tau_2}\eta\%=30.50\%$; (b) $\mathcal{R}^{\eta\%}_{\sigma_{12}}(\mathcal{Q}^{\text{"}H\text{"}};\tilde{\tau},\tilde{T})$, $p=2$, $\min\limits_{\tau_1}\eta\%=28.75\%$, $\min\limits_{\tau_2}\eta\%=24.51\%$; (c) $\mathcal{R}^{\eta\%}_{\sigma_{11}}(\mathcal{Q}^{\text{"}H\text{"}};\tilde{\tau},\tilde{T})$, $p=3$, $\min\limits_{\tau_1}\eta\%=10.77\%$, $\min\limits_{\tau_2}\eta\%=1.07\%$; (d) $\mathcal{R}^{\eta\%}_{\sigma_{12}}(\mathcal{Q}^{\text{"}H\text{"}};\tilde{\tau},\tilde{T})$, $p=3$, $\min\limits_{\tau_1}\eta\%=6.91\%$, $\min\limits_{\tau_2}\eta\%=6.07\%$. The η%-levels 10%, 30%, 60% (dark, light, lighter gray) were employed.

Fig. 11. *Superconvergence points for the class of "harmonic" solutions of the equations of plane elasticity: Cubic serendipity square elements.* The superconvergence points are located at the intersection of the contours $C^{0\%}_{\frac{\partial u_1}{\partial x_1}}(\mathcal{Q}_i^{\text{"}H\text{"}};\tilde{\tau},\tilde{T})$, $i=1,\ldots,4$. Superconvergence points for (a) $\dfrac{\partial u_1}{\partial x_1}$; (b) $\dfrac{\partial u_1}{\partial x_2}$; (c) σ_{11}; (d) ϵ_{12}. Note that for the components of the gradient there are four superconvergence points

and one superconvergence line. For the components of stress and the shear-strain there is only one superconvergence point located at the center of the element. The superconvergence points are shown in each Figure by a solid circle and are also superconvergence points for the class of general solutions and for all values of Poisson's ratio.

Fig. 12. *η%-superconvergence regions for the class of "harmonic" solutions of the equations of plane elasticity: Cubic serendipity square elements.* The regions $\widehat{\tilde{\mathcal{R}}}^{\eta\%}_{F(u)}(\mathcal{Q}^{"H"};\tilde{\tau};\tilde{T})$ are given for $F(u)$: (a) $\dfrac{\partial u_1}{\partial x_1}$; (b) $\dfrac{\partial u_1}{\partial x_2}$; (c) σ_{11}; (d) ϵ_{12} for Poisson's ratio $\nu = 0.30$. For $\dfrac{\partial u_1}{\partial x_1}$, $\dfrac{\partial u_1}{\partial x_2}$, ϵ_{12} the η%-levels 5%, 10%, 25% (dark, light, lighter gray) were employed; for σ_{11} the η%-levels 25%, 50%, 75% were employed.

Fig. 13. *η%-superconvergence regions for the class of "harmonic" solutions of the equations of plane elasticity: Quartic serendipity square elements.* The regions $\widehat{\tilde{\mathcal{R}}}^{\eta\%}_{F(u)}(\mathcal{Q}^{"H"};\tilde{\tau};\tilde{T})$ are given for $F(u)$: (a) $\dfrac{\partial u_1}{\partial x_1}$; (b) $\dfrac{\partial u_1}{\partial x_2}$; (c) σ_{11}; (d) ϵ_{12} for Poisson's ratio $\nu = 0.30$. The η%-levels 5%, 10%, 25% (dark, light, lighter gray) were employed.

Fig. 14. *Common 25%-superconvergence regions for all Poisson's ratios ν, $0 \leq \nu \leq 0.35$, for the class of "harmonic" solutions of the equations of plane elasticity: Quartic serendipity square elements.* The regions $\bigcap_{0\leq\nu\leq 0.35} \widehat{\tilde{\mathcal{R}}}^{\eta\%}_{F(u)}(\mathcal{Q}^{"H"};\tilde{\tau};\tilde{T})$ are given for $F(u)$: (a) $\dfrac{\partial u_1}{\partial x_1}$; (b) σ_{11}; (c) ϵ_{12}.

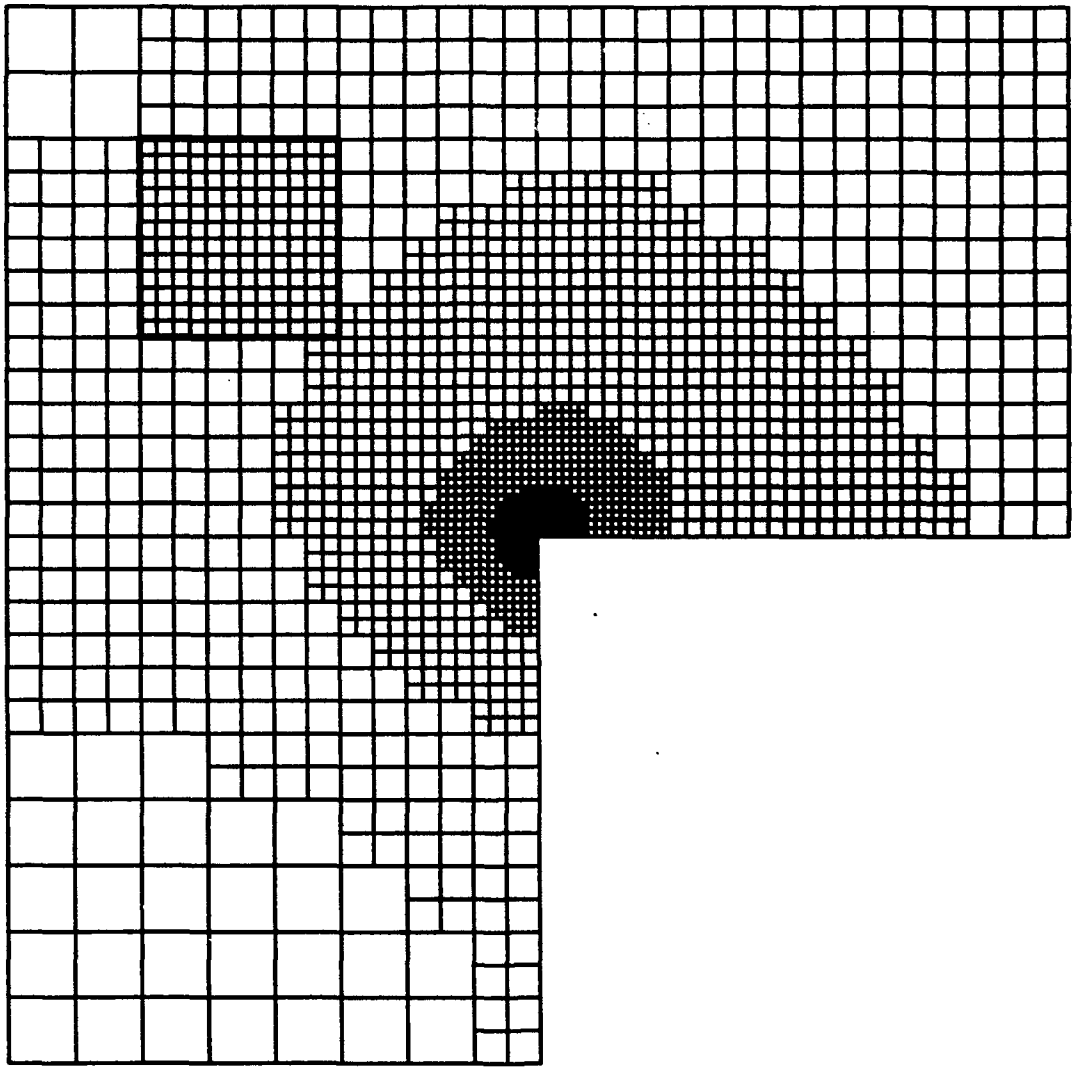

Fig. 1

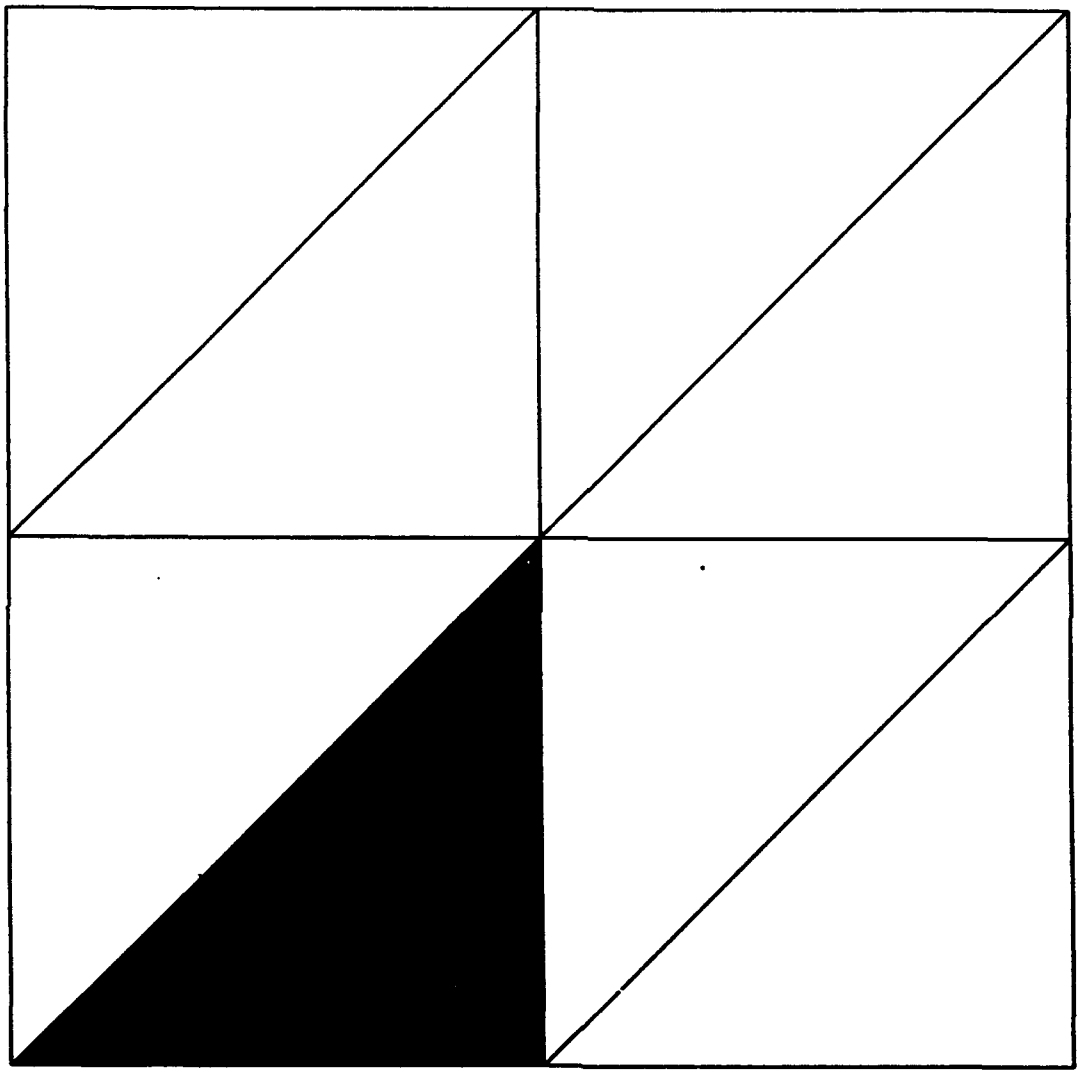

Fig. 2a

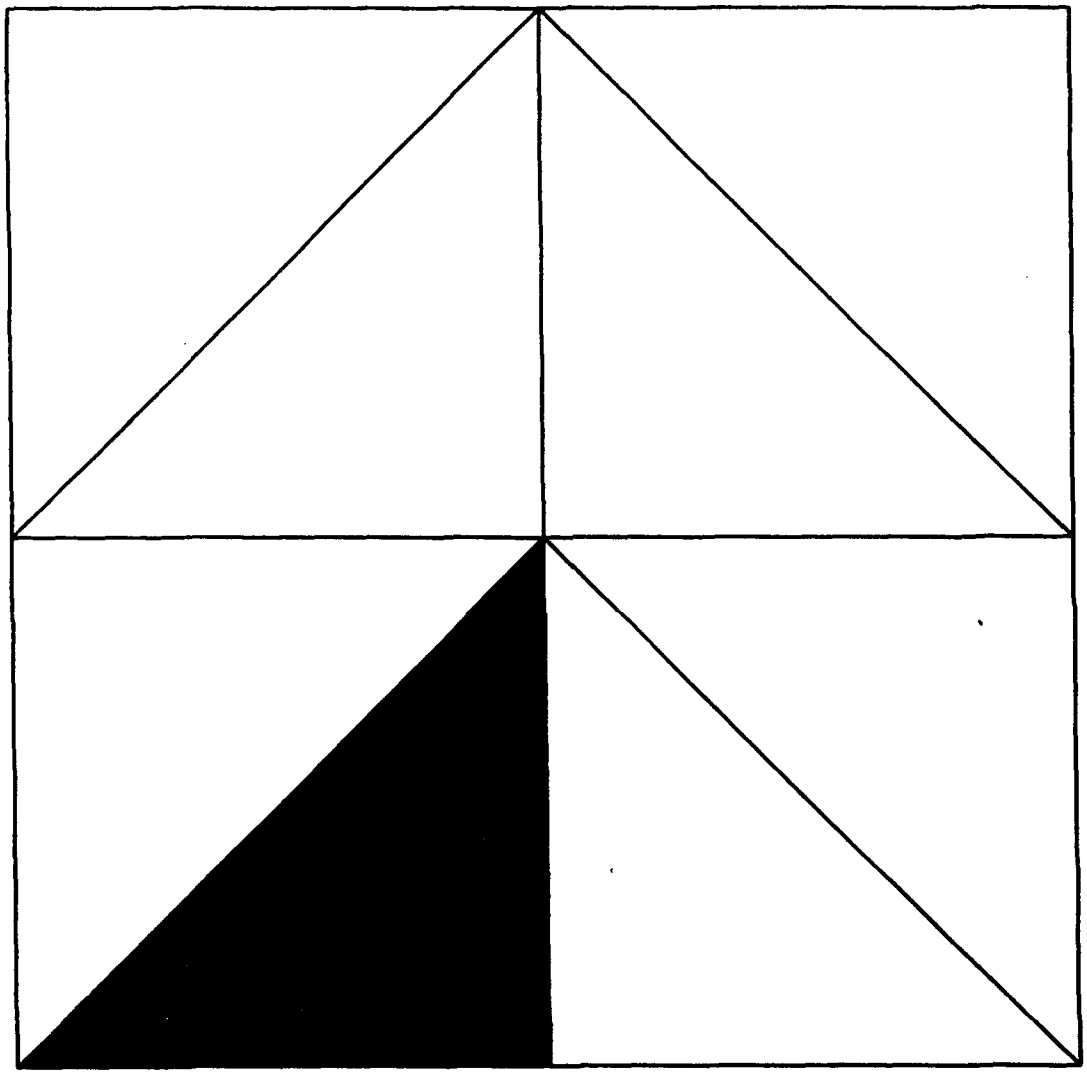

Fig. 2b

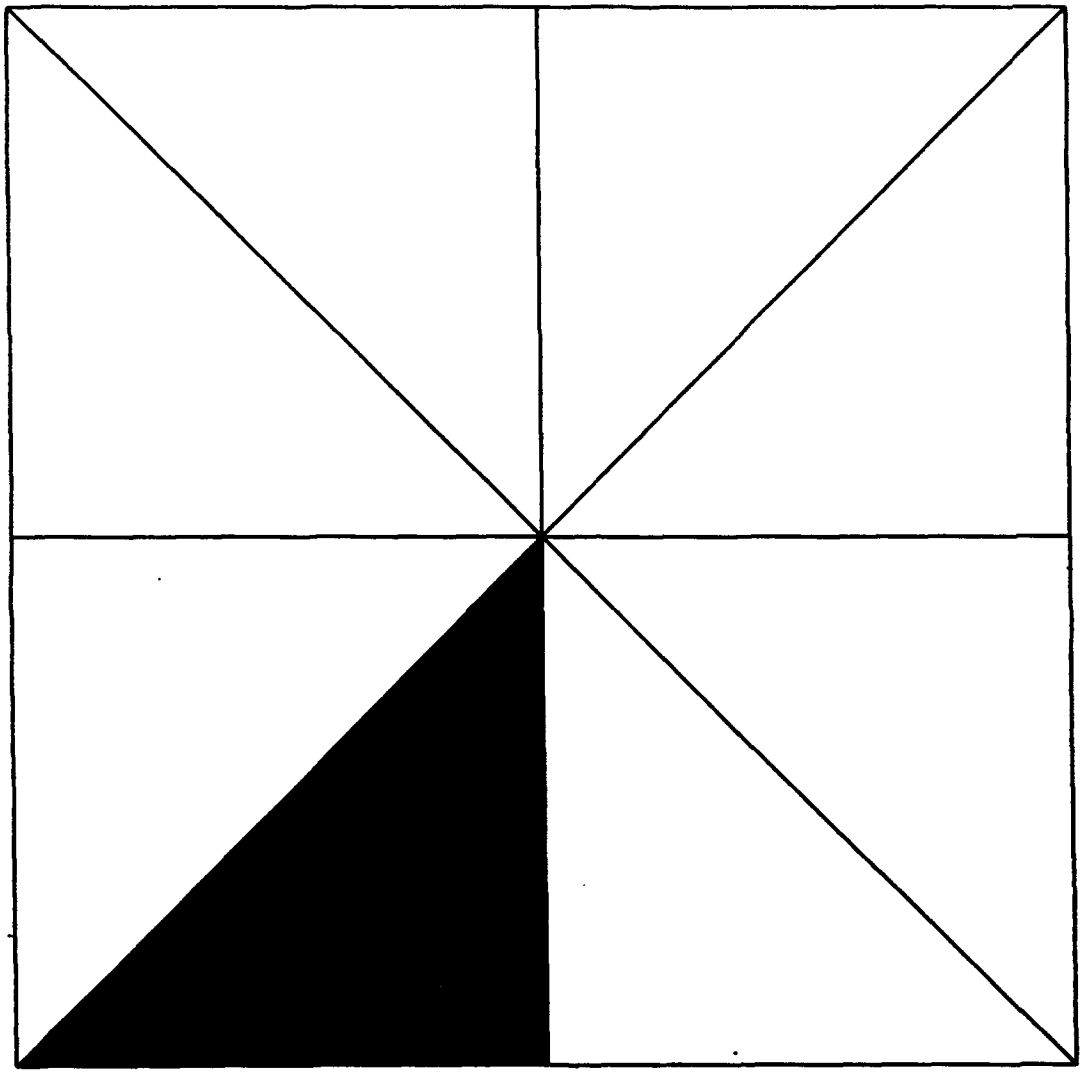

Fig. 2c

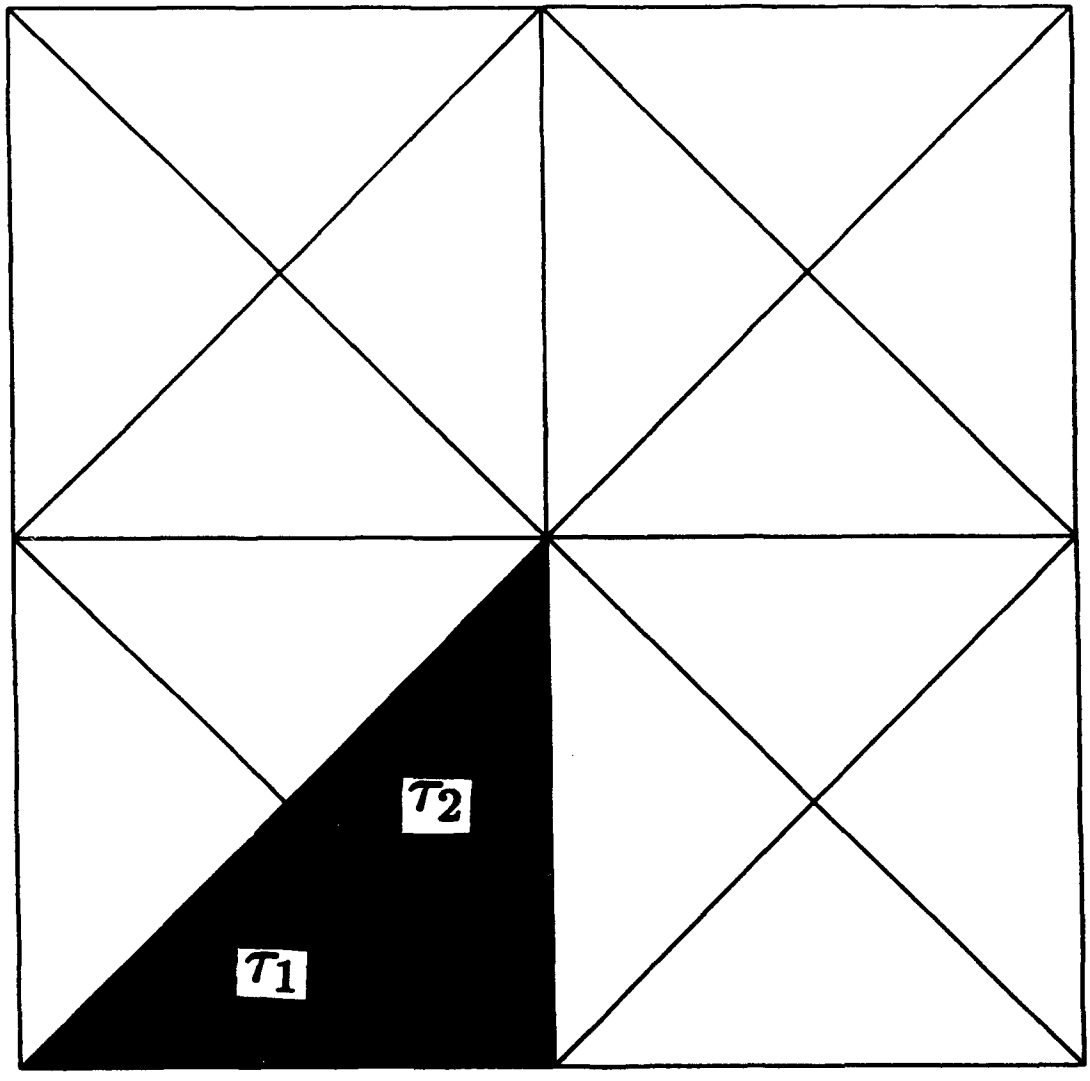

Fig. 2d

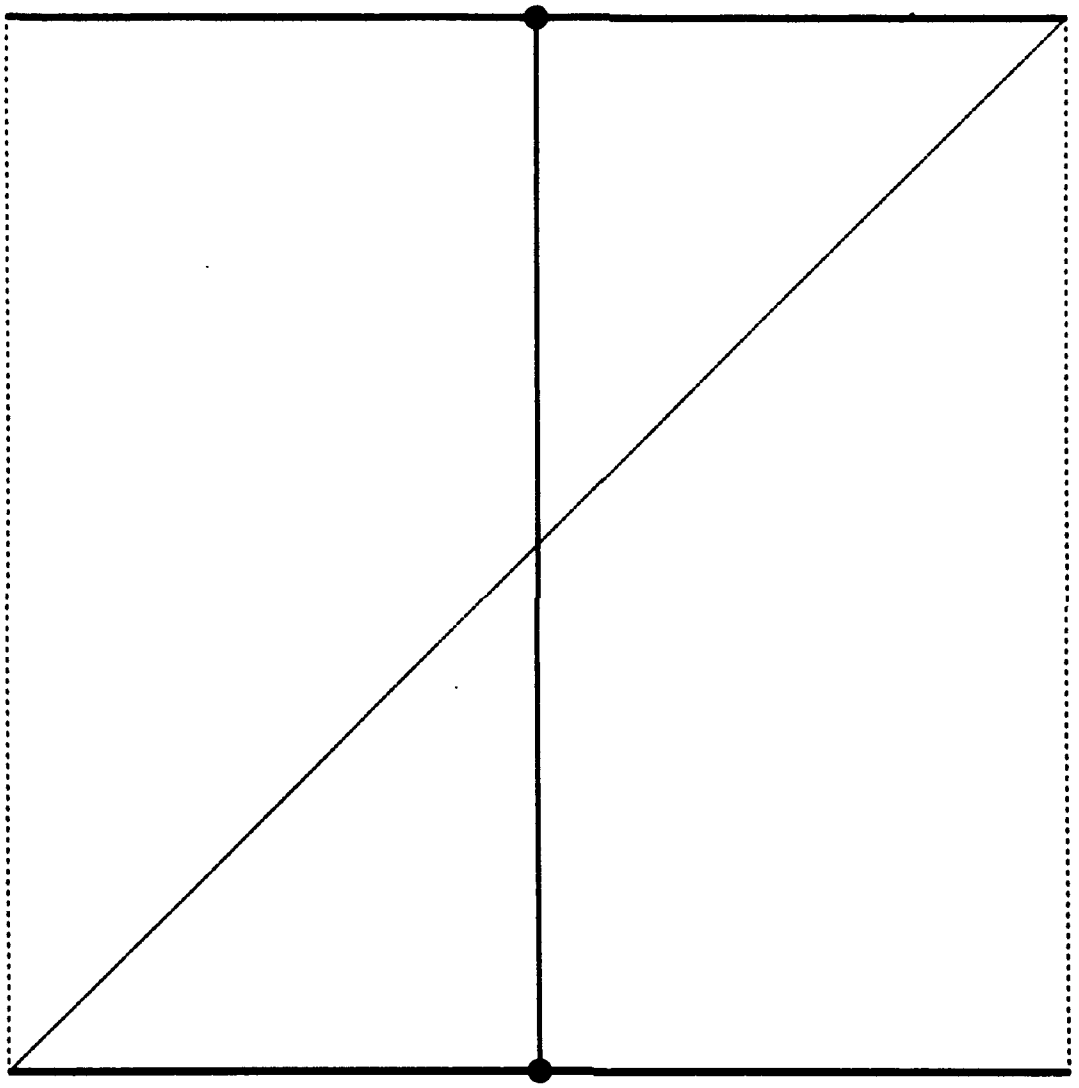

$\nu = .30$

f.e.m solution

Harmonic solution **P = 1**

Function Q1

Function Q2

Fig. 3a

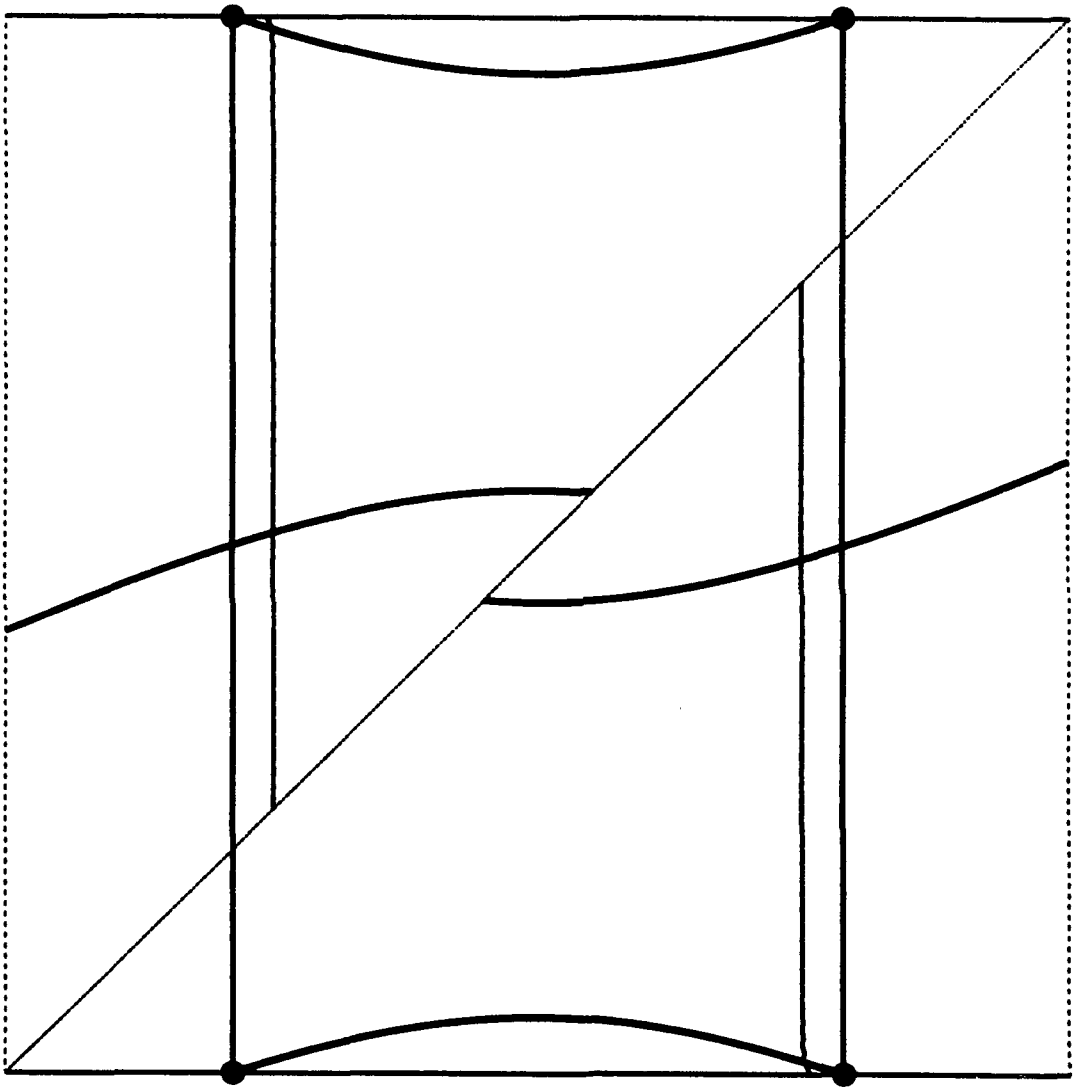

$\nu = .30$

f.e.m solution

Harmonic solution **P = 2**

— ***Function Q1***
— ***Function Q2***
— ***Function Q3***

Fig. 3b

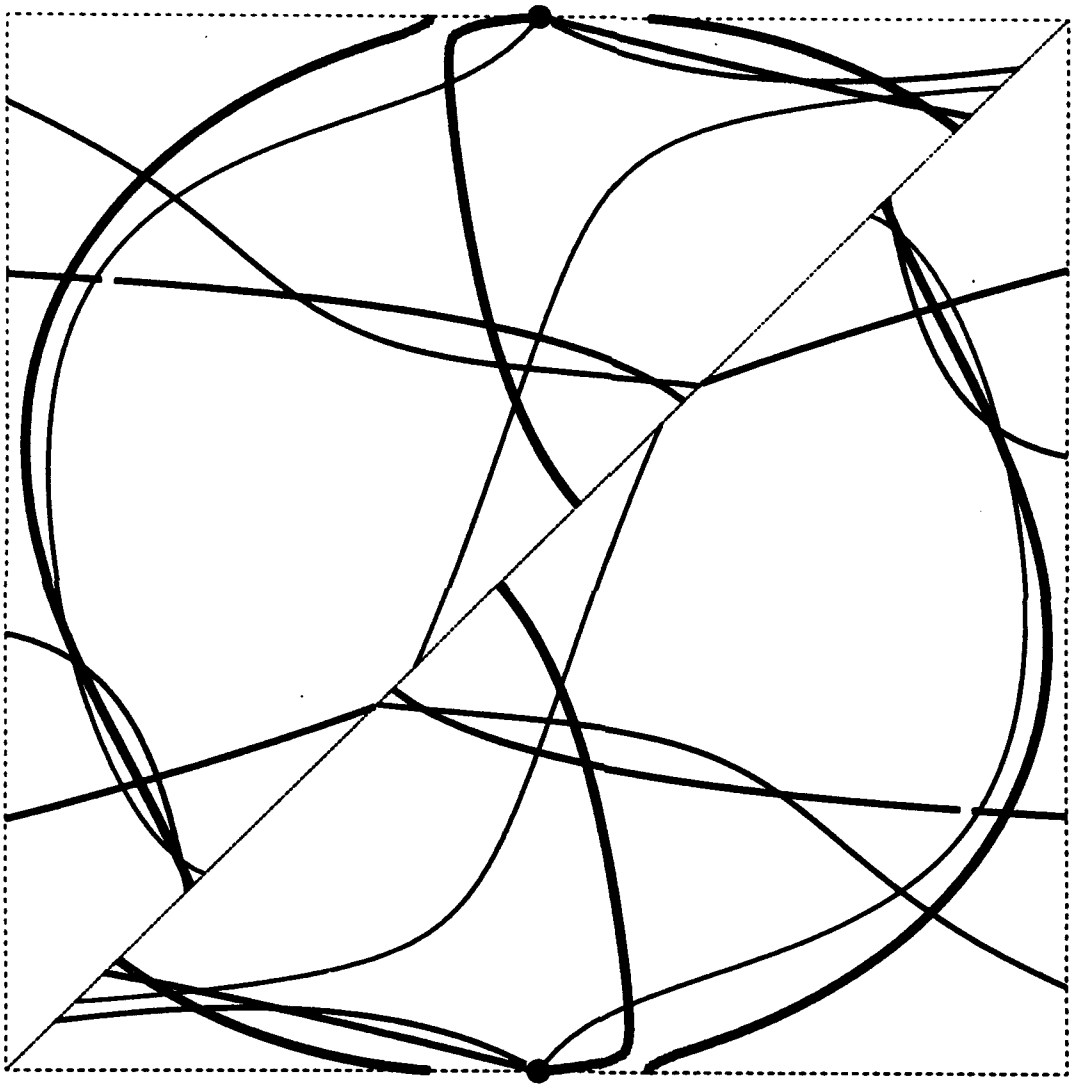

ν = .30

f.e.m solution

Harmonic solution **P = 3**

Function Q1
Function Q2
Function Q3
Function Q4

Fig. 3c

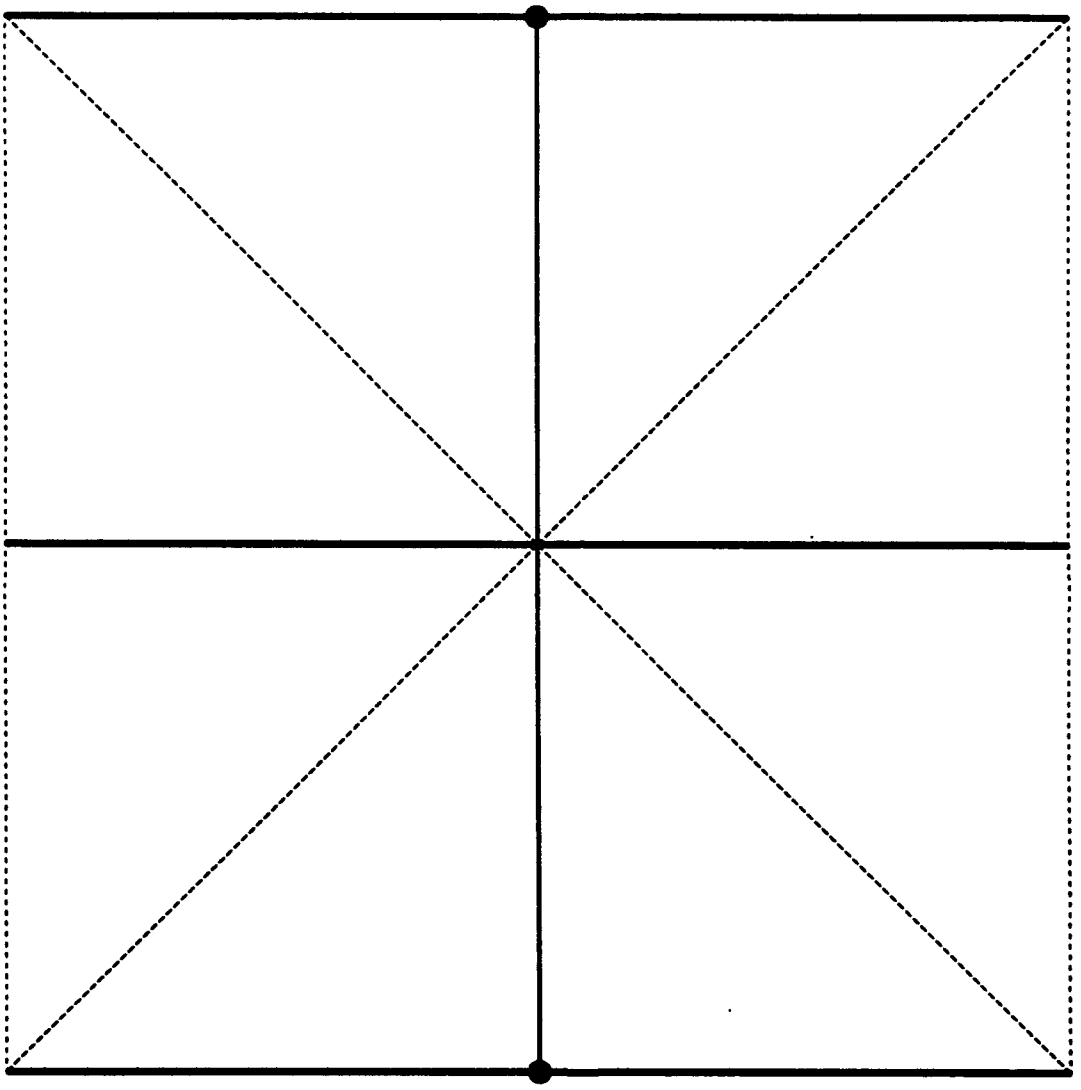

$\nu = .30$

f.e.m solution

Harmonic solution **P = 1**

— ***Function Q1***
— ***Function Q2***
— ***Function Q3***

Fig. 4a

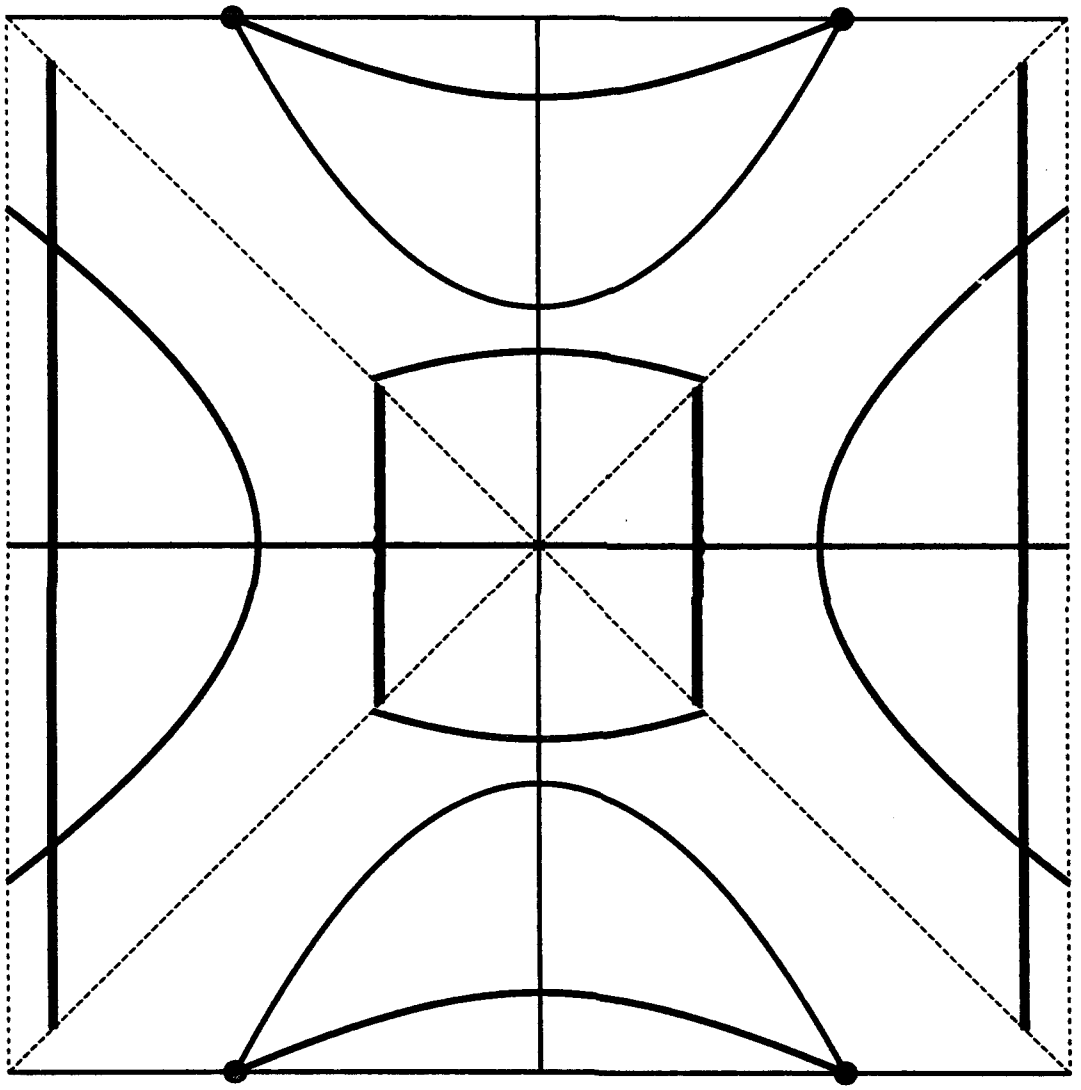

ν = .30

f.e.m solution

Harmonic solution **P = 2**

Function Q1
Function Q2
Function Q3
Function Q4

Fig. 4b

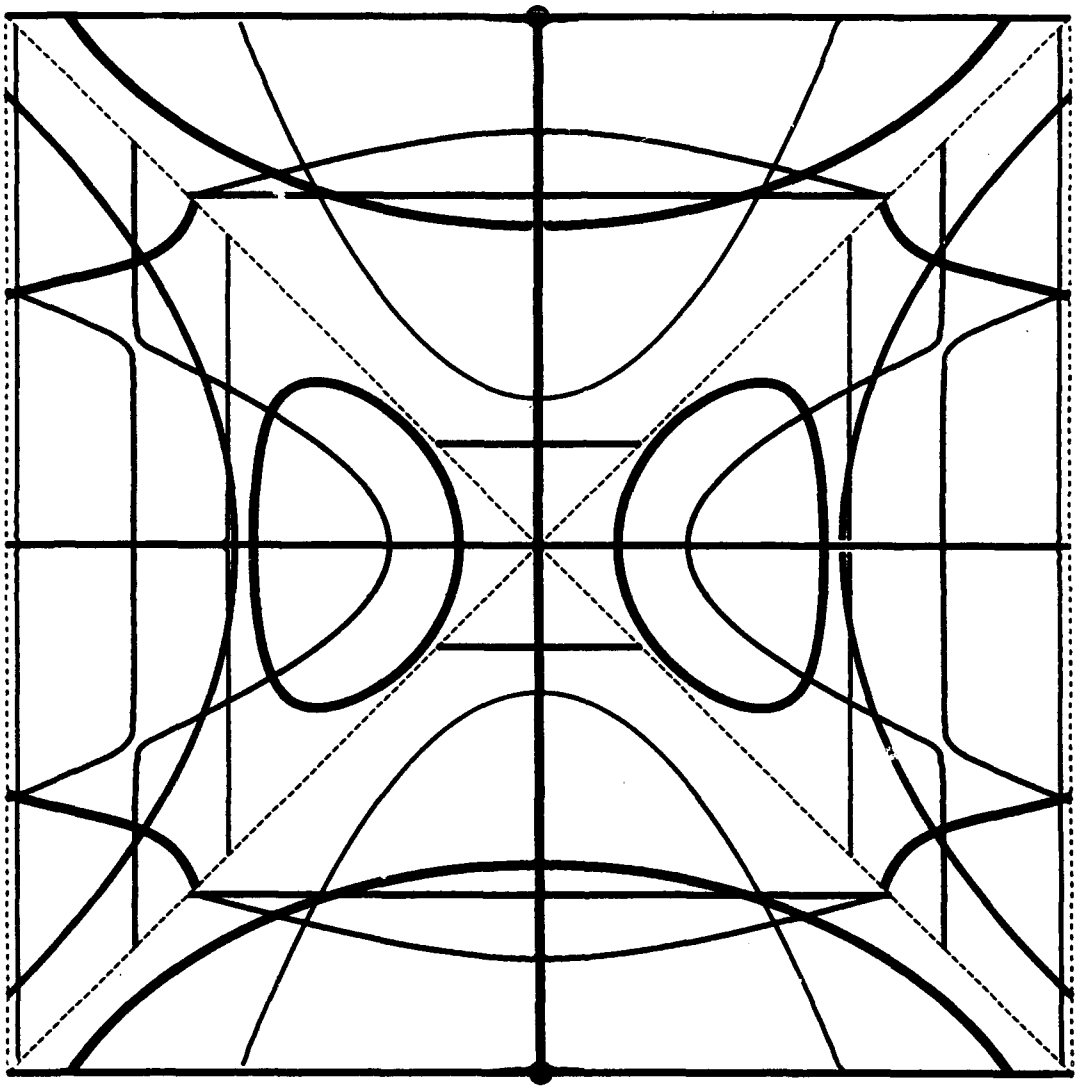

$\nu = .30$

f.e.m solution

Harmonic solution **P = 3**

— ***Function Q1***
— ***Function Q2***
— ***Function Q3***
— ***Function Q4***

Fig. 4c

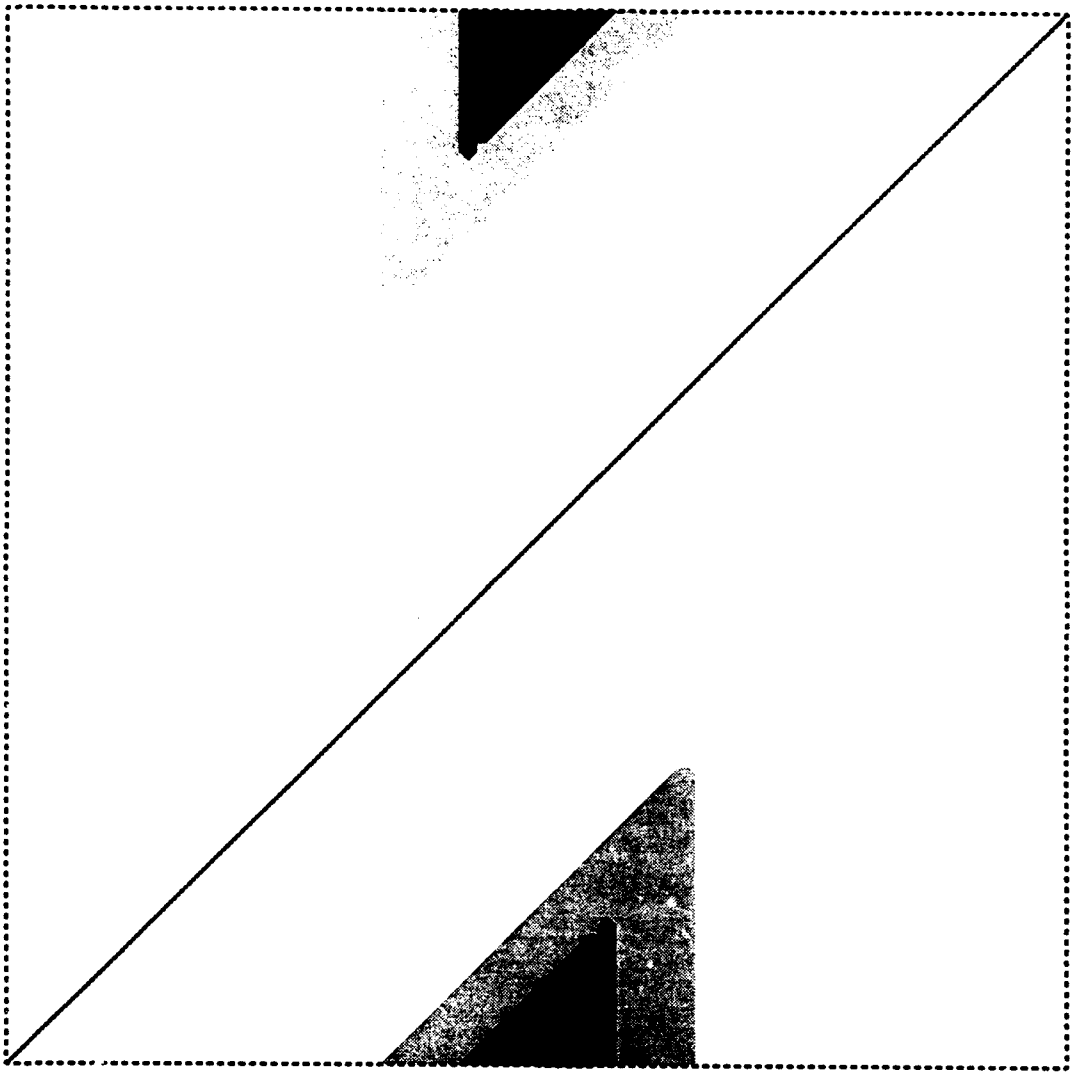

MAX ETA=100.00
MIN ETA= .00
0.0%
5.0%
15.0%
30.0%

ν = .30
f.e.m solution
Harmonic solution **P = 1**

Fig. 5a

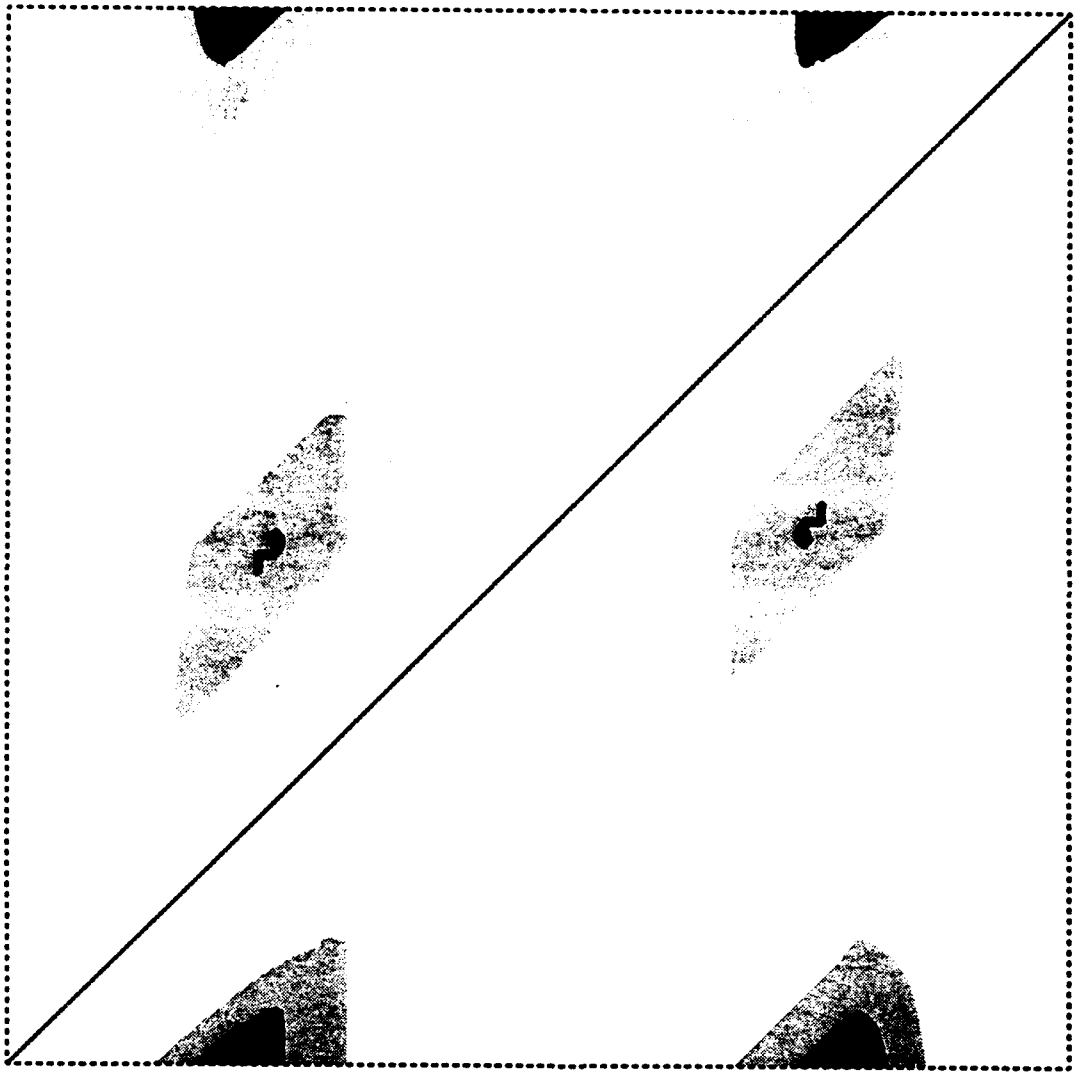

MAX ETA=100.00

MIN ETA= 1.83

0.0%

5.0%

15.0%

30.0%

ν = .30

f.e.m solution

Harmonic solution **P = 2**

Fig. 5b

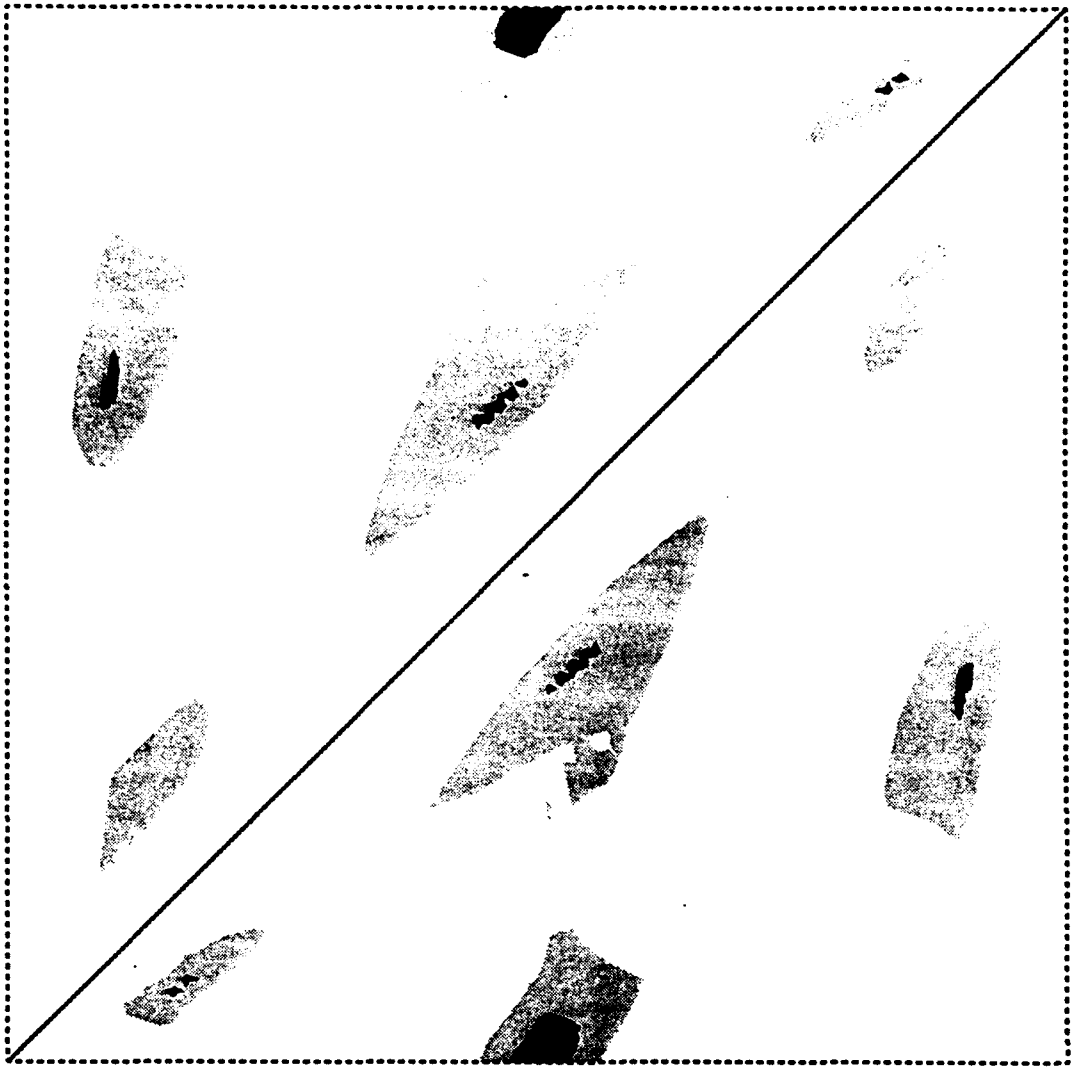

MAX ETA=100.00
MIN ETA= .00
0.0%
5.0%
15.0%
30.0%

ν = .30
f.e.m solution
Harmonic solution **P = 3**

Fig. 5c

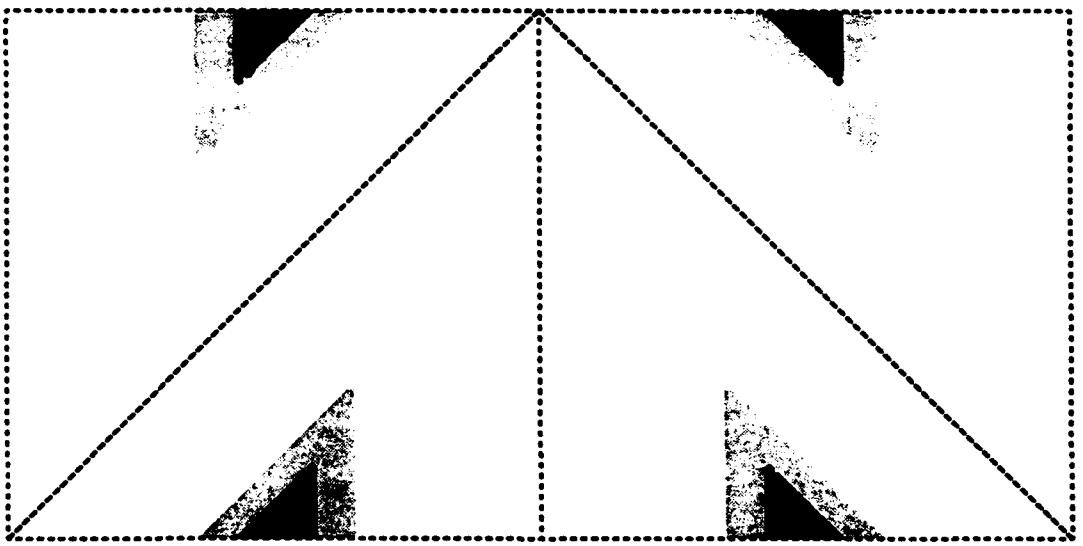

MAX ETA=100.00

MIN ETA= .00

0.0%

5.0%

15.0%

30.0%

ν = .30

f.e.m solution

Harmonic solution **P = 1**

Fig. 6a

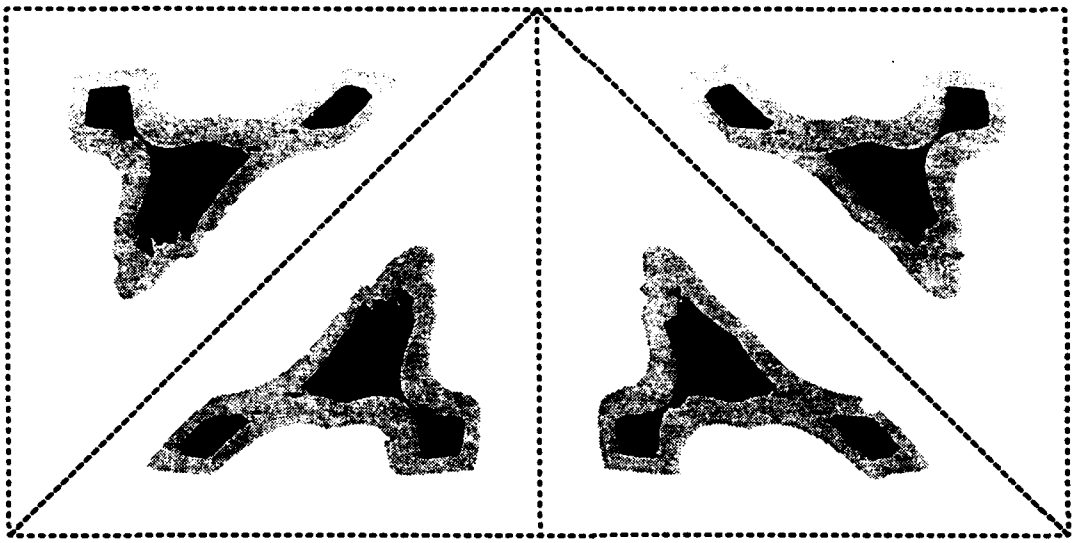

MAX ETA=100.00

MIN ETA= 33.33

0.0%

40.0%

50.0%

60.0%

ν = .30

f.e.m solution

Harmonic solution **P = 2**

Fig. 6b

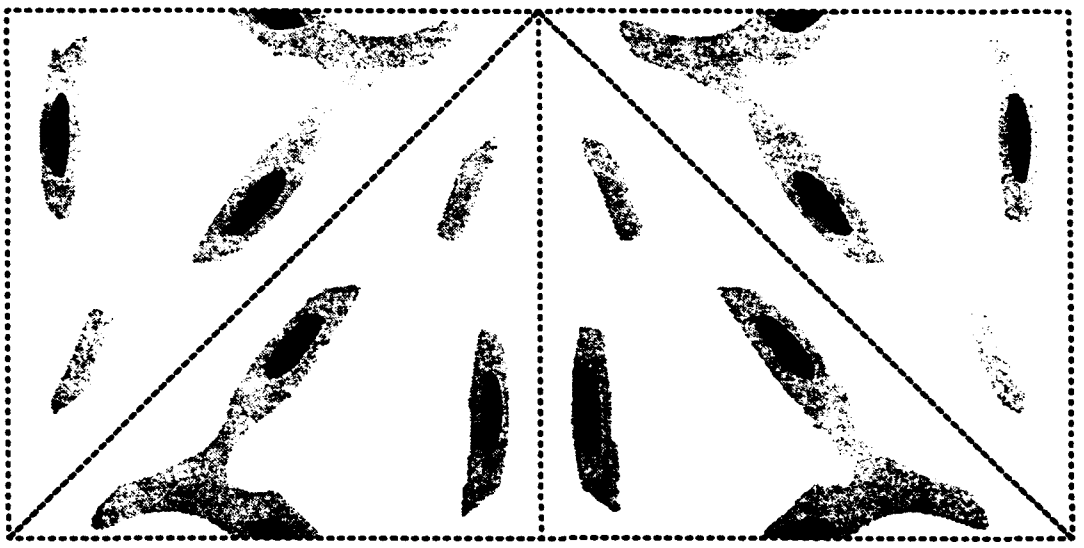

MAX ETA=100.00
MIN ETA= .00
0.0%
5.0%
15.0%
30.0%

ν = .30
f.e.m solution
Harmonic solution P = 3

Fig. 6c

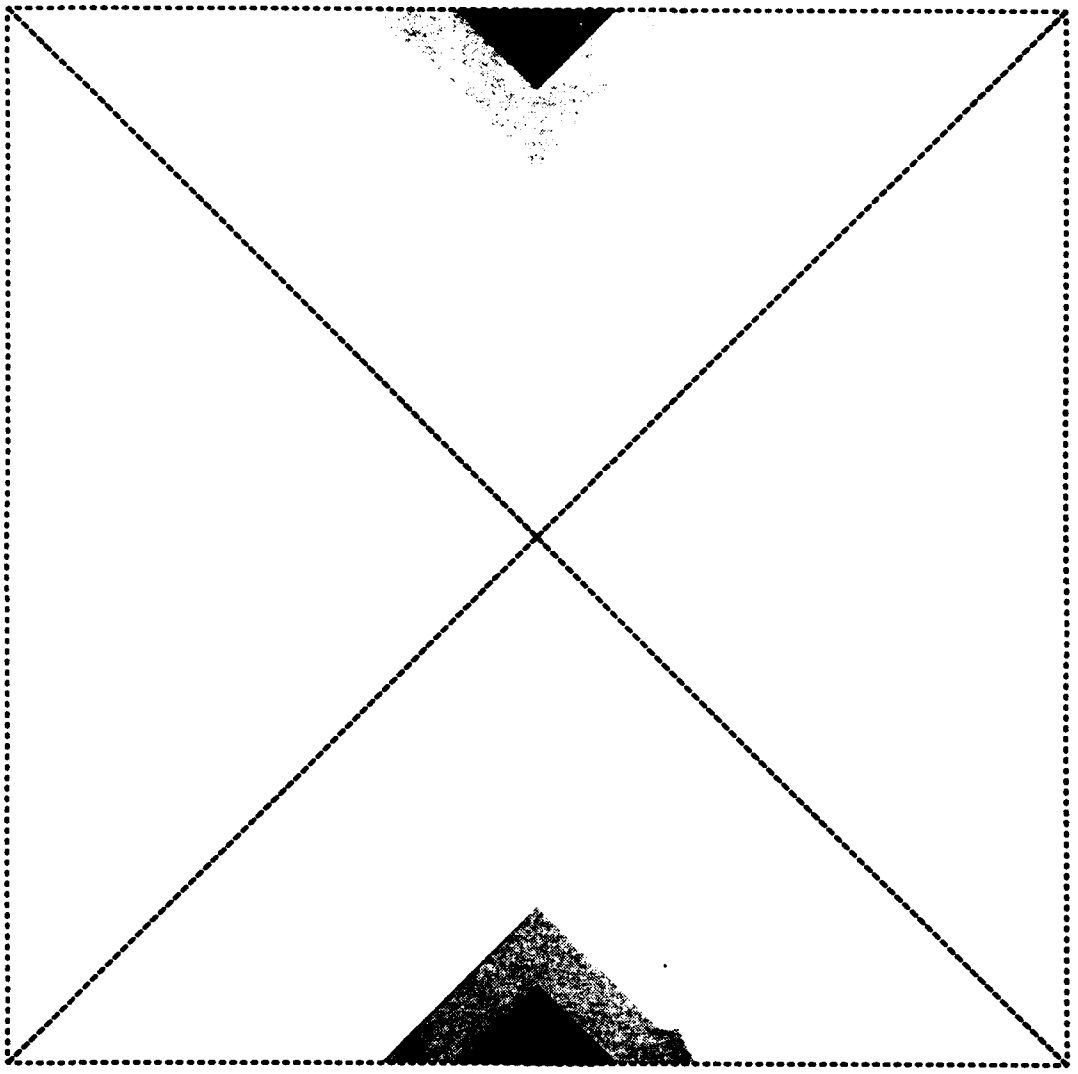

MAX ETA=100.00

MIN ETA1= .00 *MIN ETA2=100.00*

ν = .30

f.e.m solution

Harmonic solution **P = 1**

0.0%
5.0%
15.0%
30.0%

Fig. 7a

MAX ETA=100.00

MIN ETA1= 1.83 *MIN ETA2= 25.83*

ν = .30

f.e.m solution

Harmonic soluuion **P = 2**

0.0%
10.0%
30.0%
50.0%

Fig. 7b

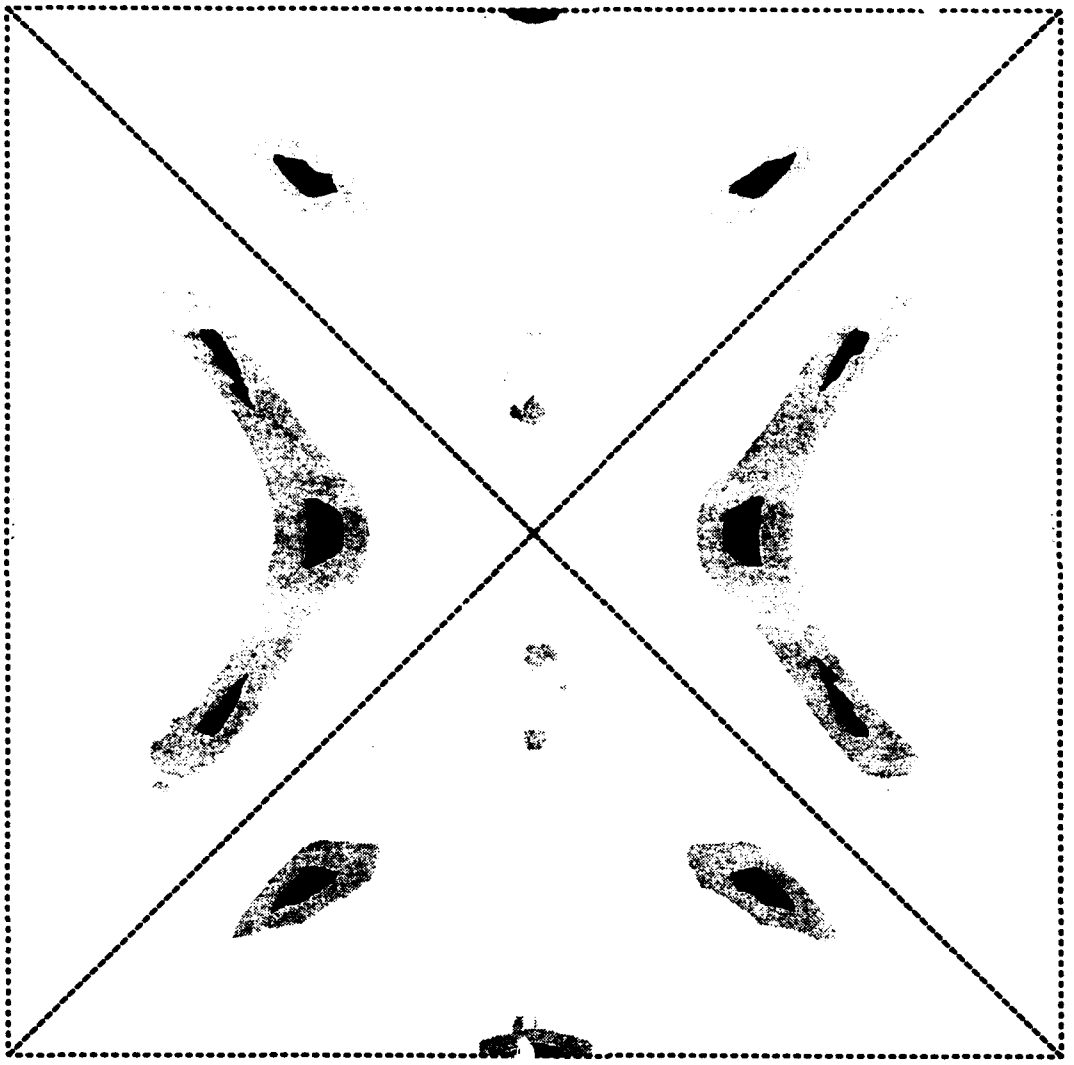

MAX ETA=100.00

MIN ETA1= .00 MIN ETA2= 6.77

ν = .30

f.e.m solution

Harmonic solution P = 3

0.0%
5.0%
15.0%
30.0%

Fig. 7c

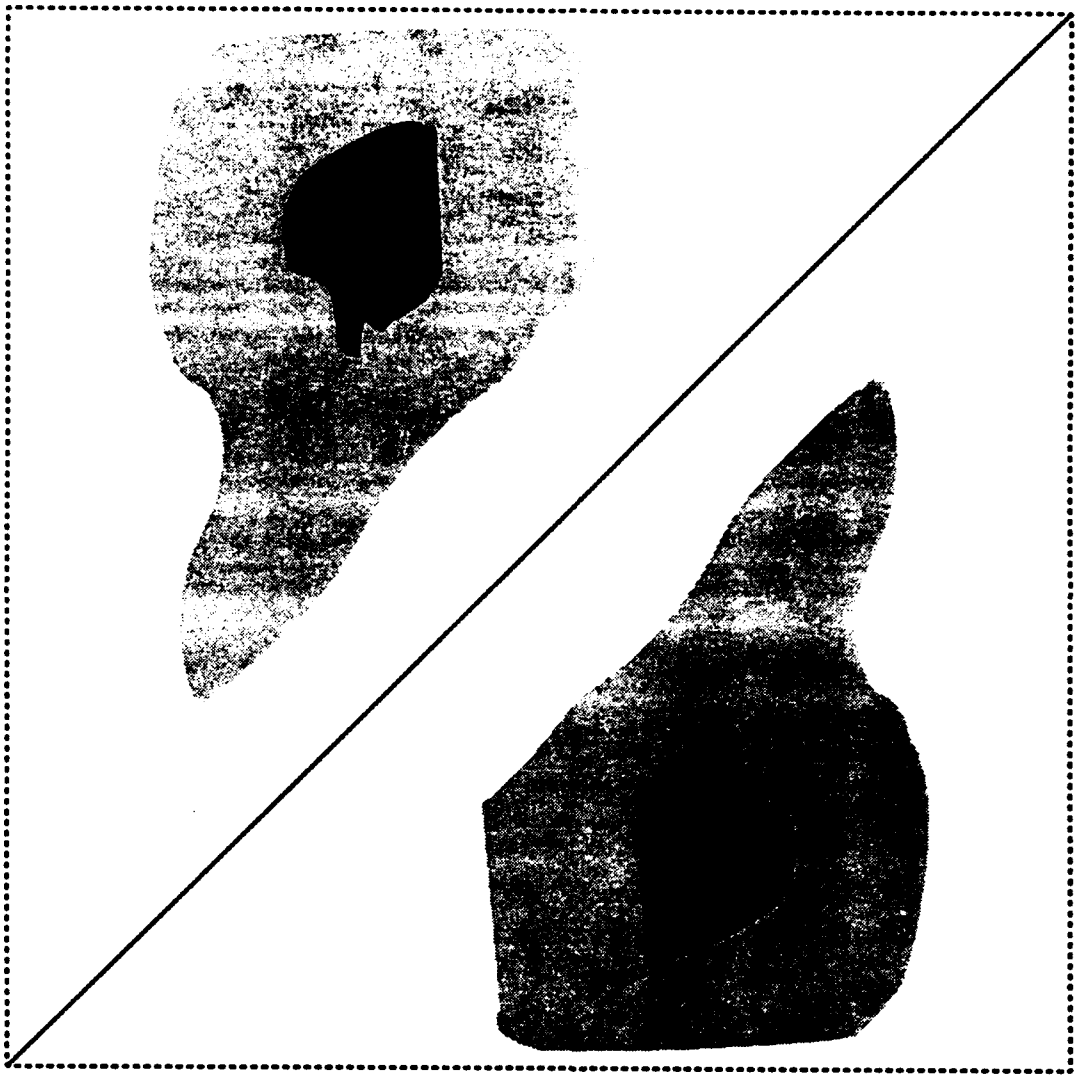

MAX ETA=100.00

MIN ETA= 18.17

0.0%

10.0%

30.0%

60.0%

ν = .30

f.e.m solution

Harmonic solution **P = 2**

Fig. 8a

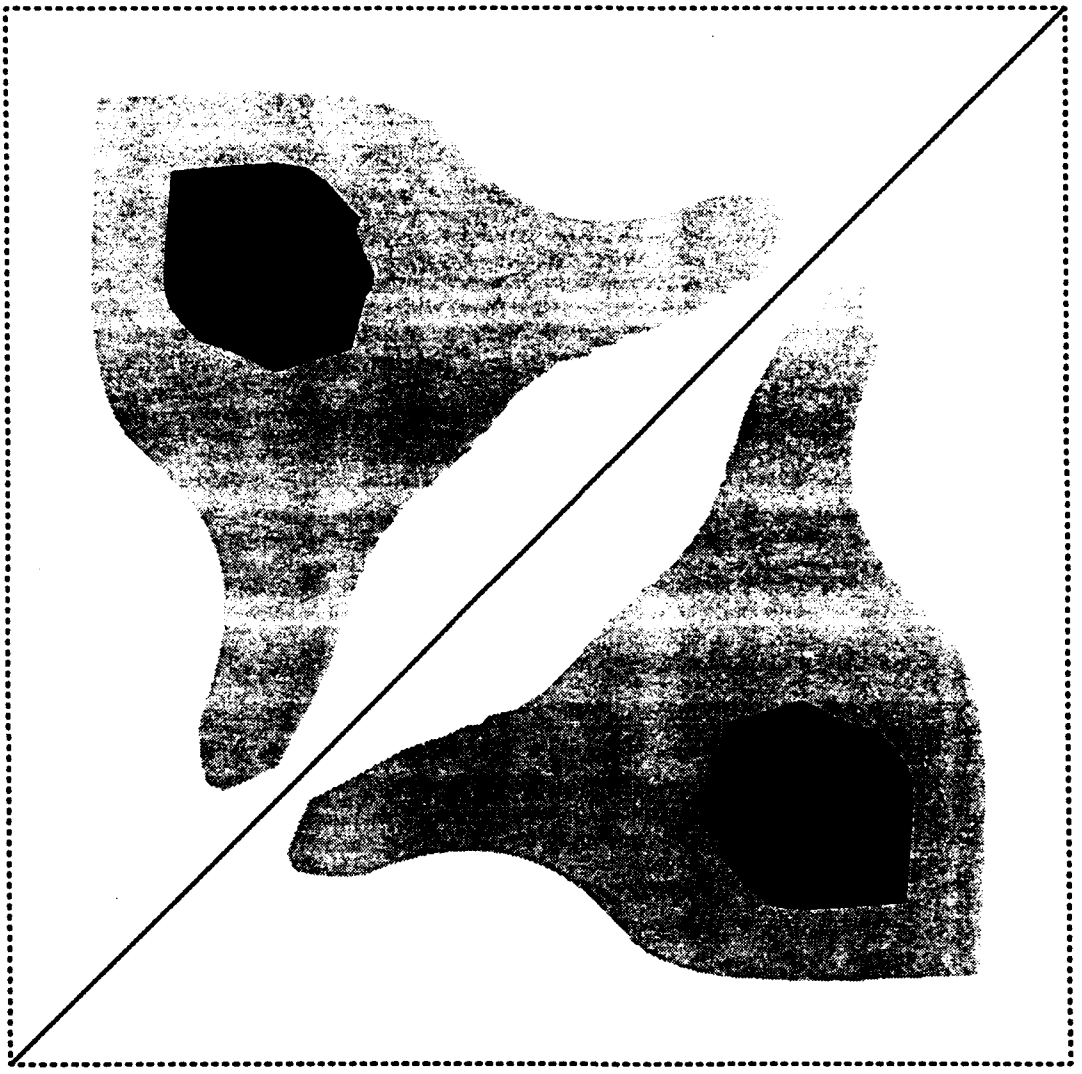

MAX ETA=100.00

MIN ETA= 5.75

0.0%

10.0%

30.0%

60.0%

ν = .30

f.e.m solution

Harmonic solution **P = 2**

Fig. 8b

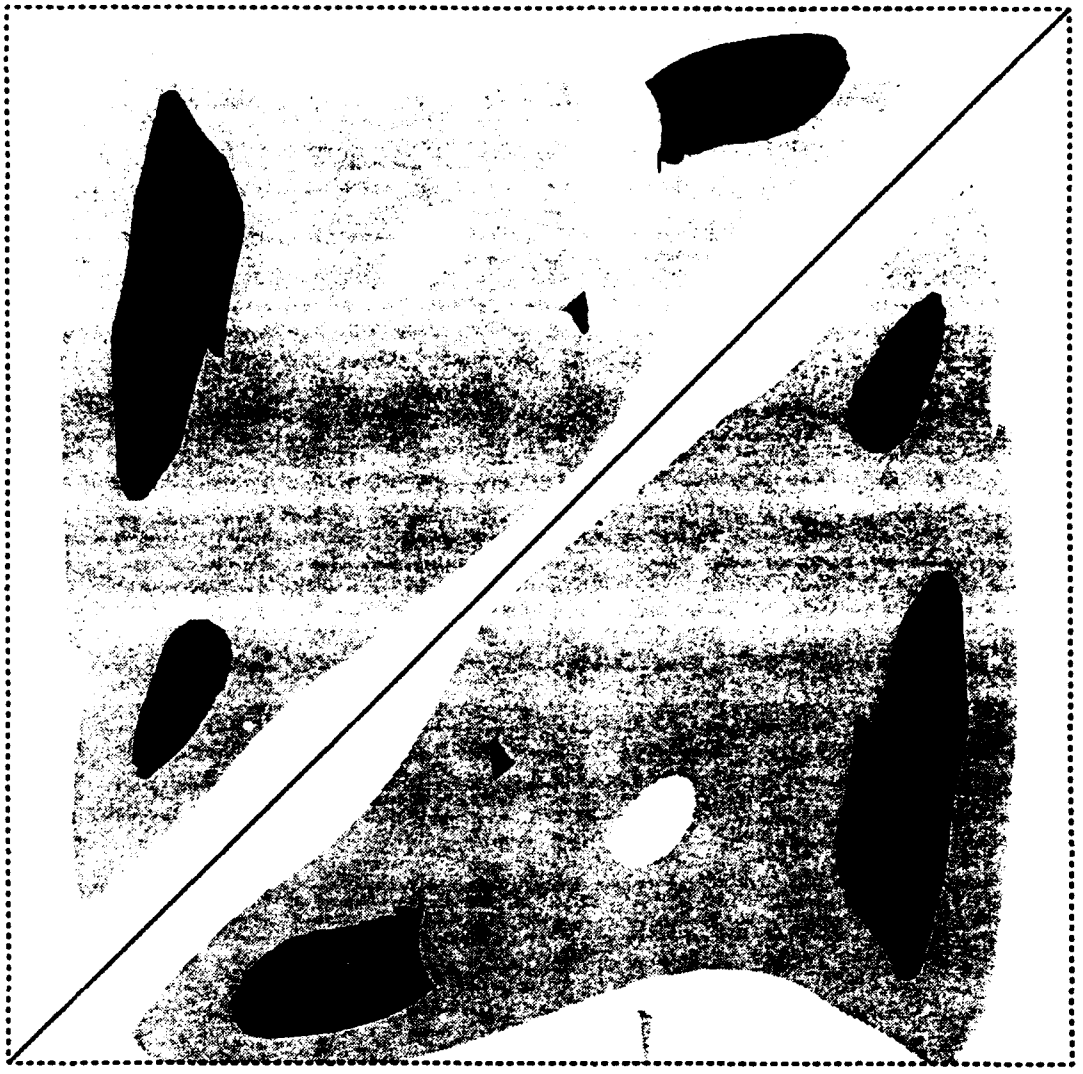

MAX ETA=100.00

MIN ETA= 8.71

0.0%

10.0%

30.0%

60.0%

ν = .30

f.e.m solution

Harmonic solution **P = 3**

Fig. 8c

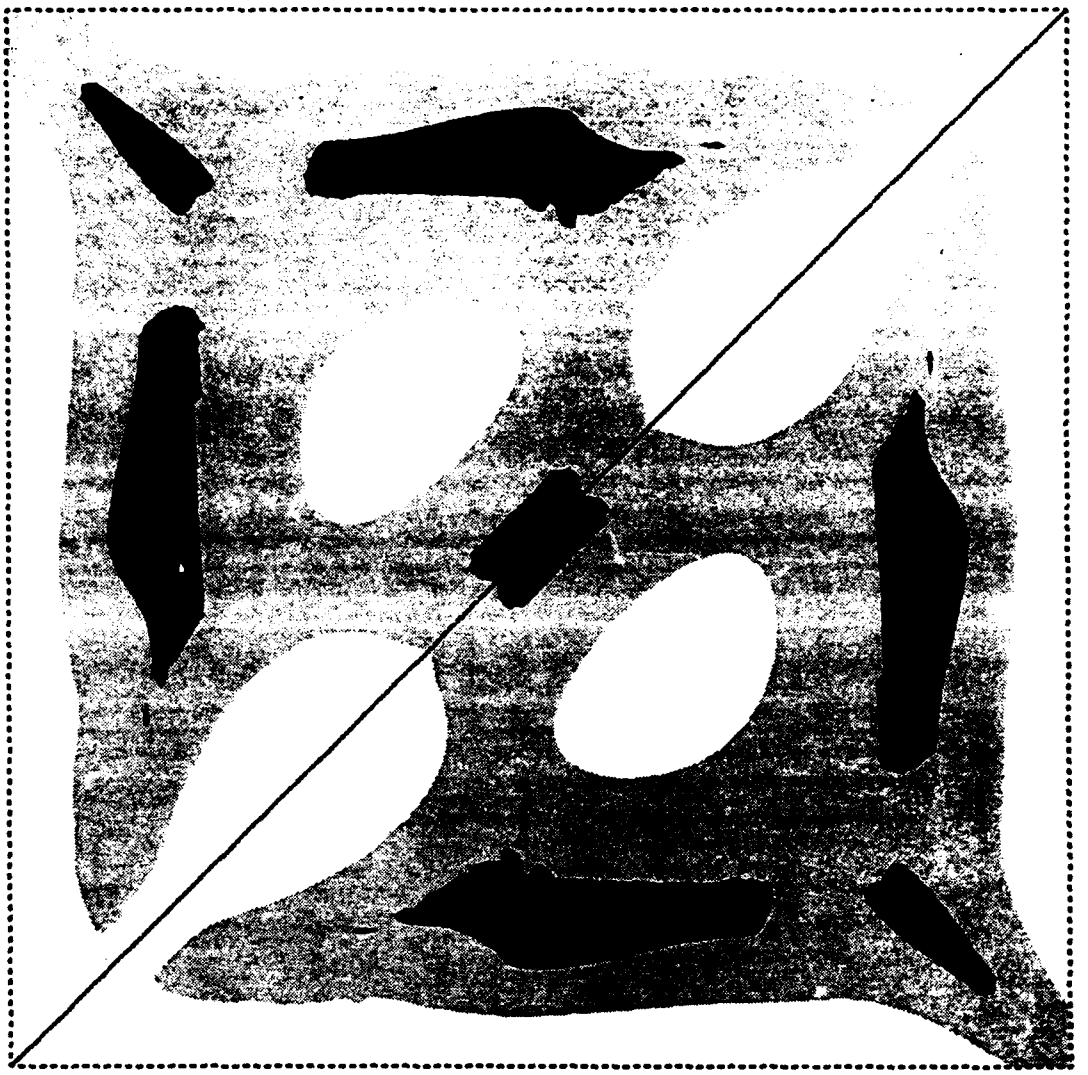

MAX ETA=100.00

MIN ETA= 13.33

0.0%

10.0%

30.0%

60.0%

ν = .30

f.e.m solution

Harmonic solution **P = 3**

Fig. 8d

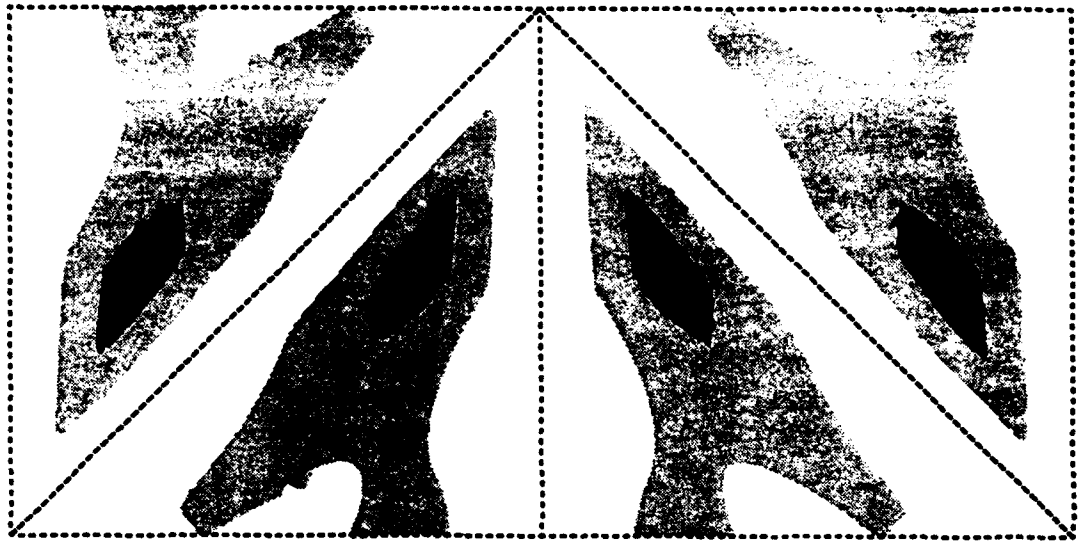

MAX ETA=100.00

MIN ETA= 11.79

0.0%

10.0%

30.0%

60.0%

ν = .30

f.e.m solution

Harmonic solution **P = 2**

Fig. 9a

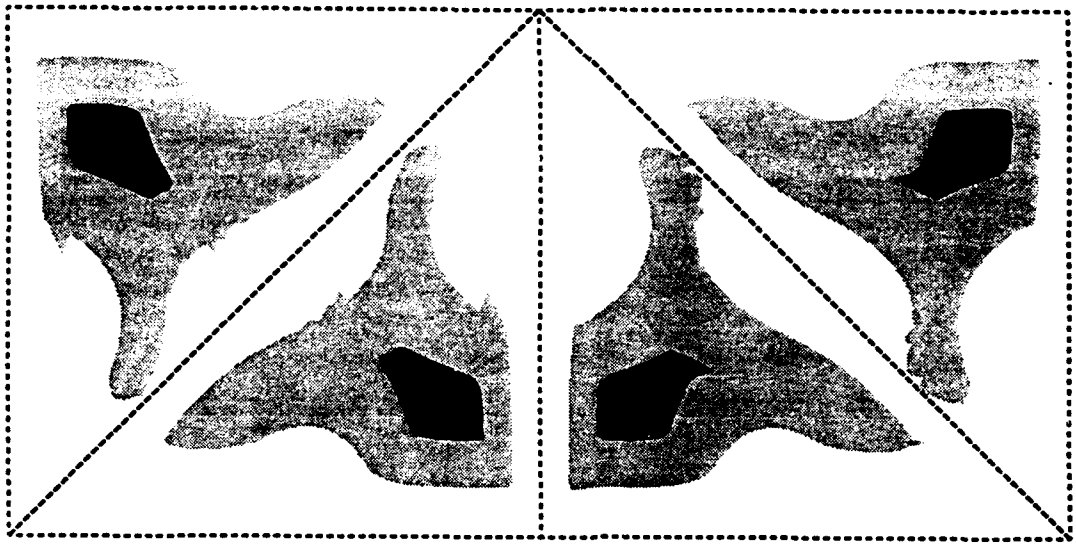

MAX ETA=100.00

MIN ETA1= 13.09 *MIN ETA2= 12.19*

ν = .30

f.e.m solution

Harmonic solution **P = 2**

0.0%
10.0%
30.0%
60.0%

Fig. 9b

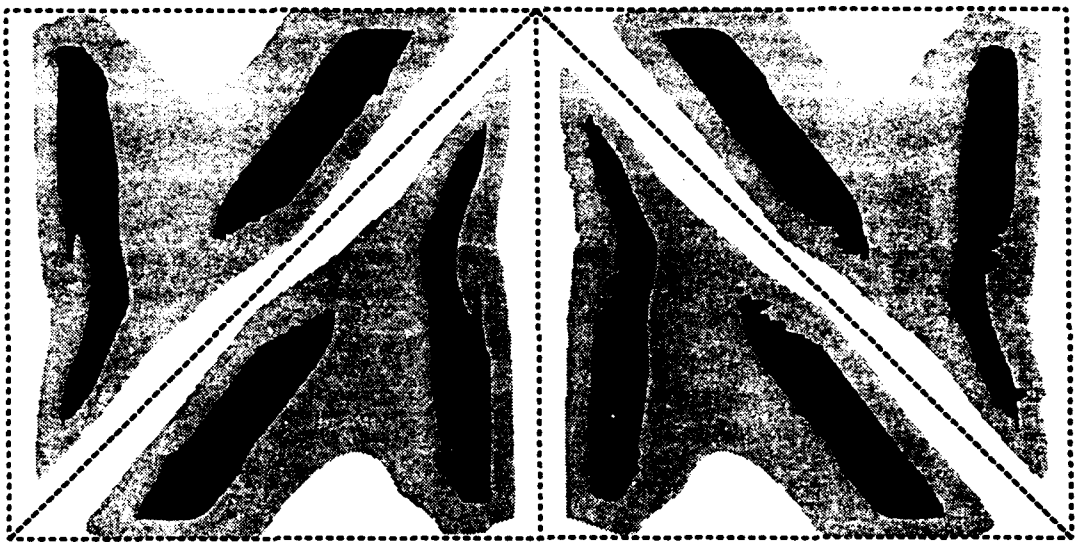

MAX ETA=100.00

MIN ETA= 11.50

0.0%

10.0%

30.0%

60.0%

ν = .30

f.e.m solution

Harmonic solution **P = 3**

Fig. 9c

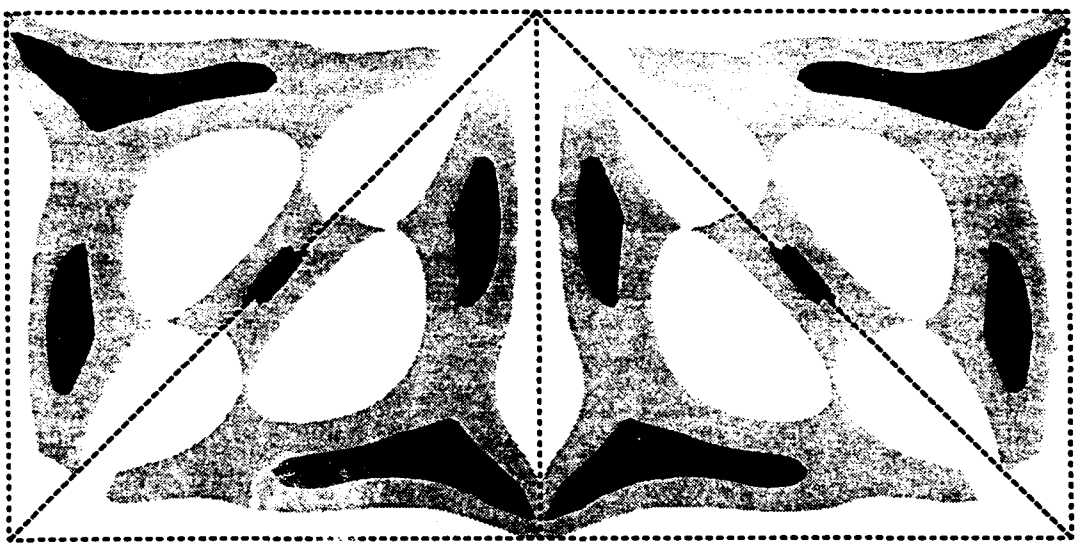

MAX ETA=100.00

MIN ETA= 3.88

0.0%

10.0%

30.0%

60.0%

ν = .30

f.e.m solution

Harmonic solution **P = 3**

Fig. 9d

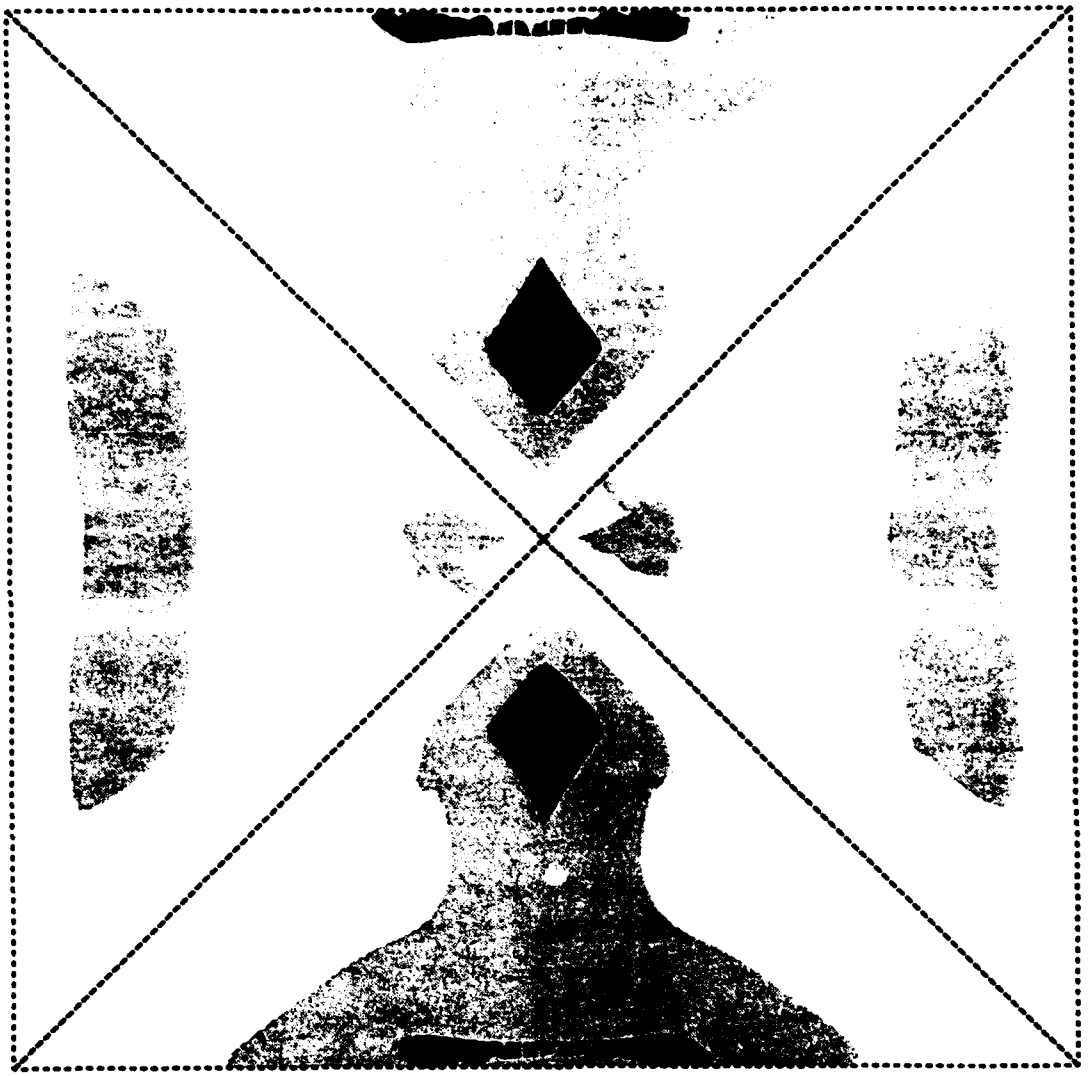

MAX ETA=100.00

MIN ETA1= 5.53 *MIN ETA2= 30.50*

ν = .30

f.e.m solution

Harmonic solution **P = 2**

0.0%
10.0%
30.0%
60.0%

Fig. 10a

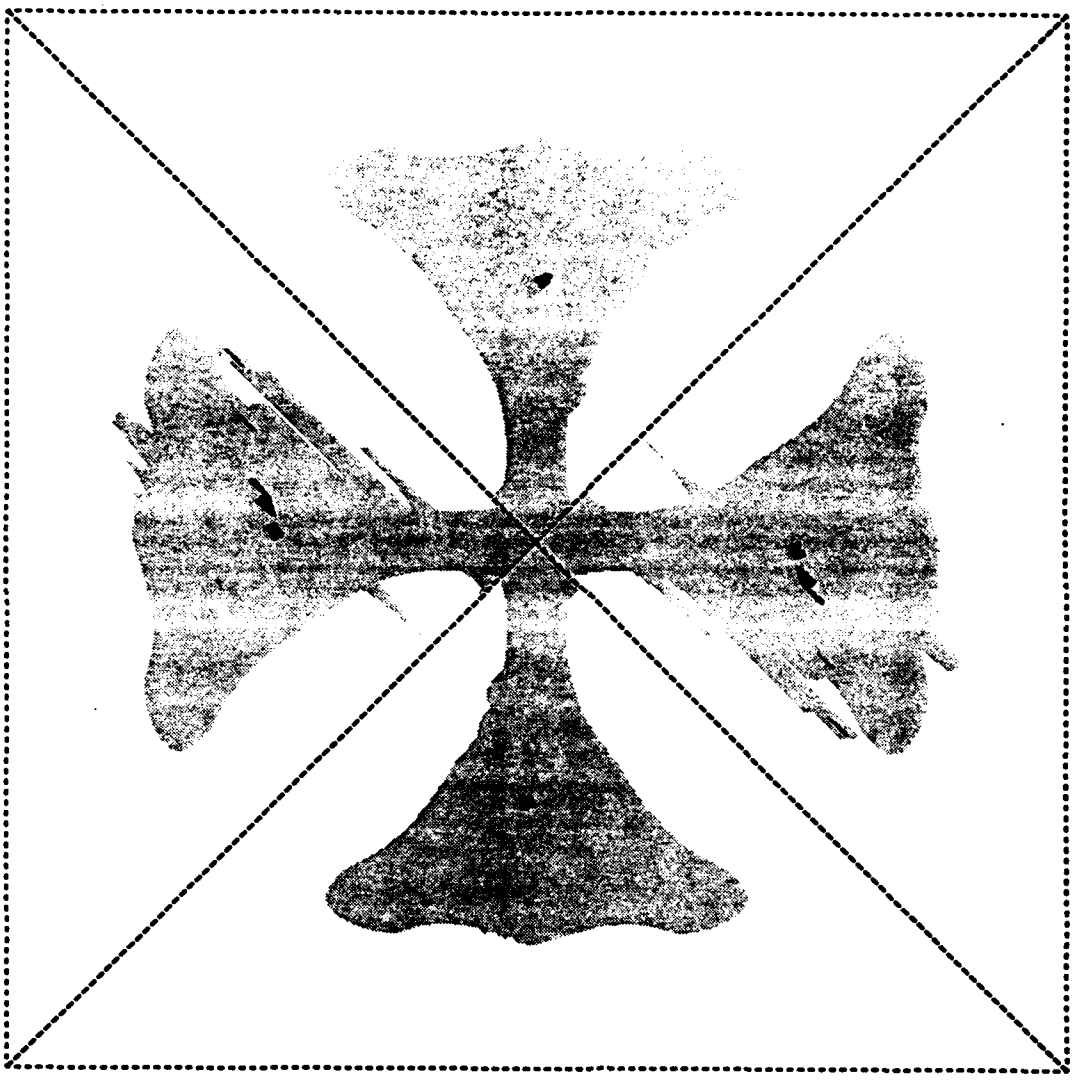

MAX ETA=100.00

MIN ETA1= 28.75 *MIN ETA2= 24.51*

ν = .30

f.e.m solution

Harmonic solution **P = 2**

0.0%
10.0%
30.0%
60.0%

Fig. 10b

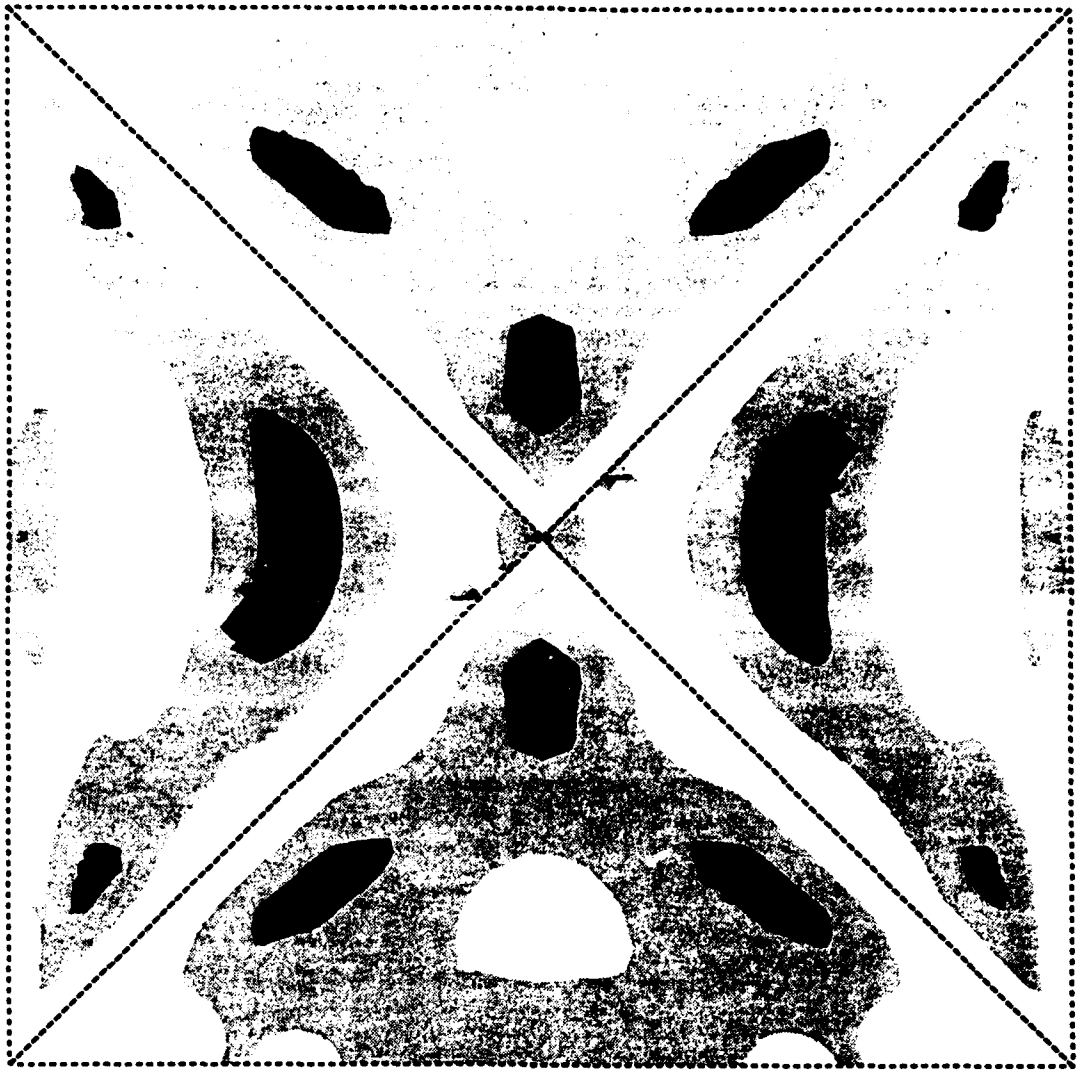
MAX ETA=100.00
MIN ETA1= 10.77
MIN ETA= 1.07
ν = .30
f.e.m solution
Harmonic solution
P = 3
0.0%
10.0%
30.0%
60.0%

Fig. 10c

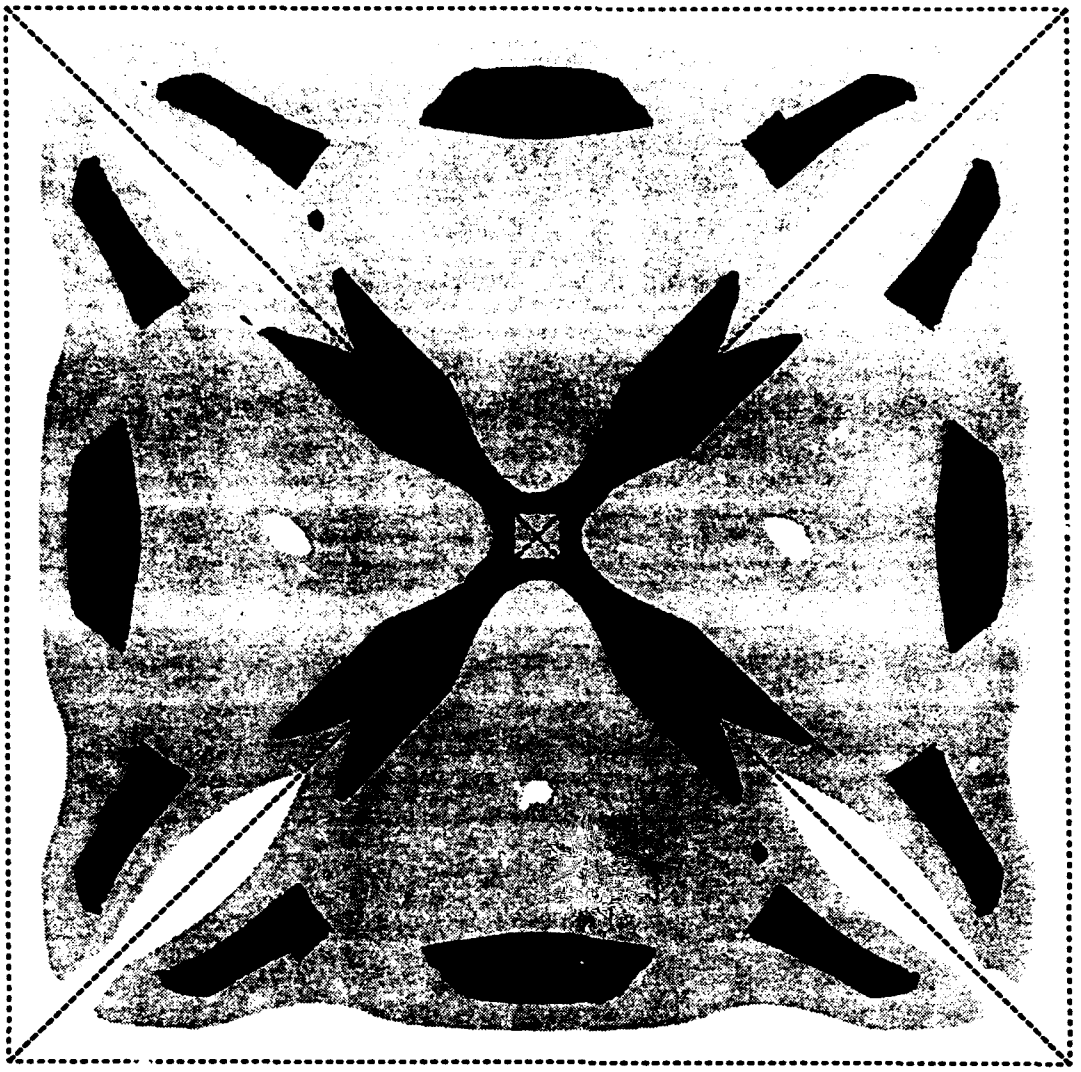

MAX ETA=100.00

MIN ETA1= 6.91 *MIN ETA2= 6.07*

ν = .30

f.e.m solution

Harmonic solution **P = 3**

0.0%
10.0%
30.0%
60.0%

Fig. 10d

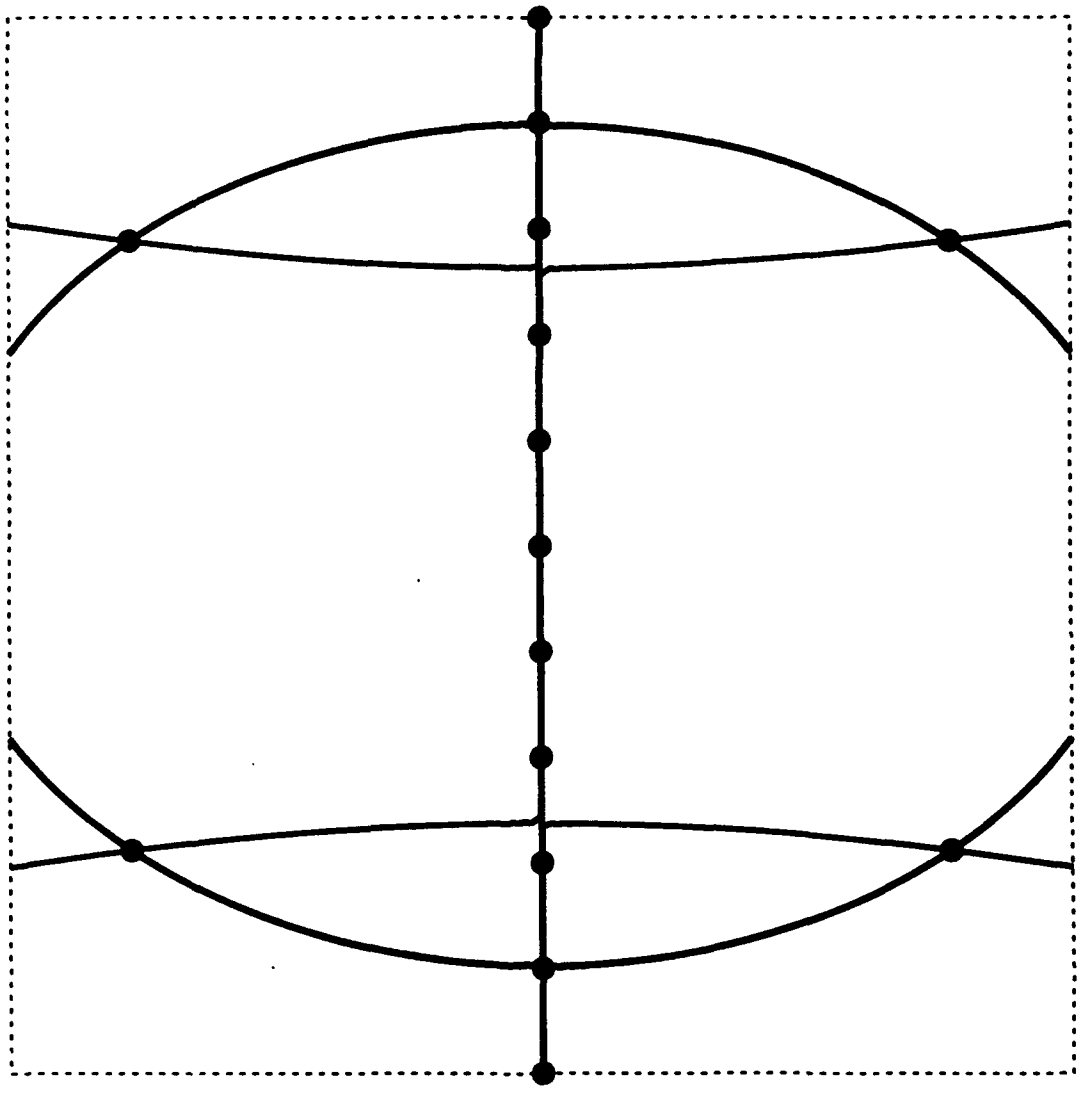

ν = .3000

Superconvergence of *u,x*

***Serendipity shape functions*, *p* = 3**

Fig. 11a

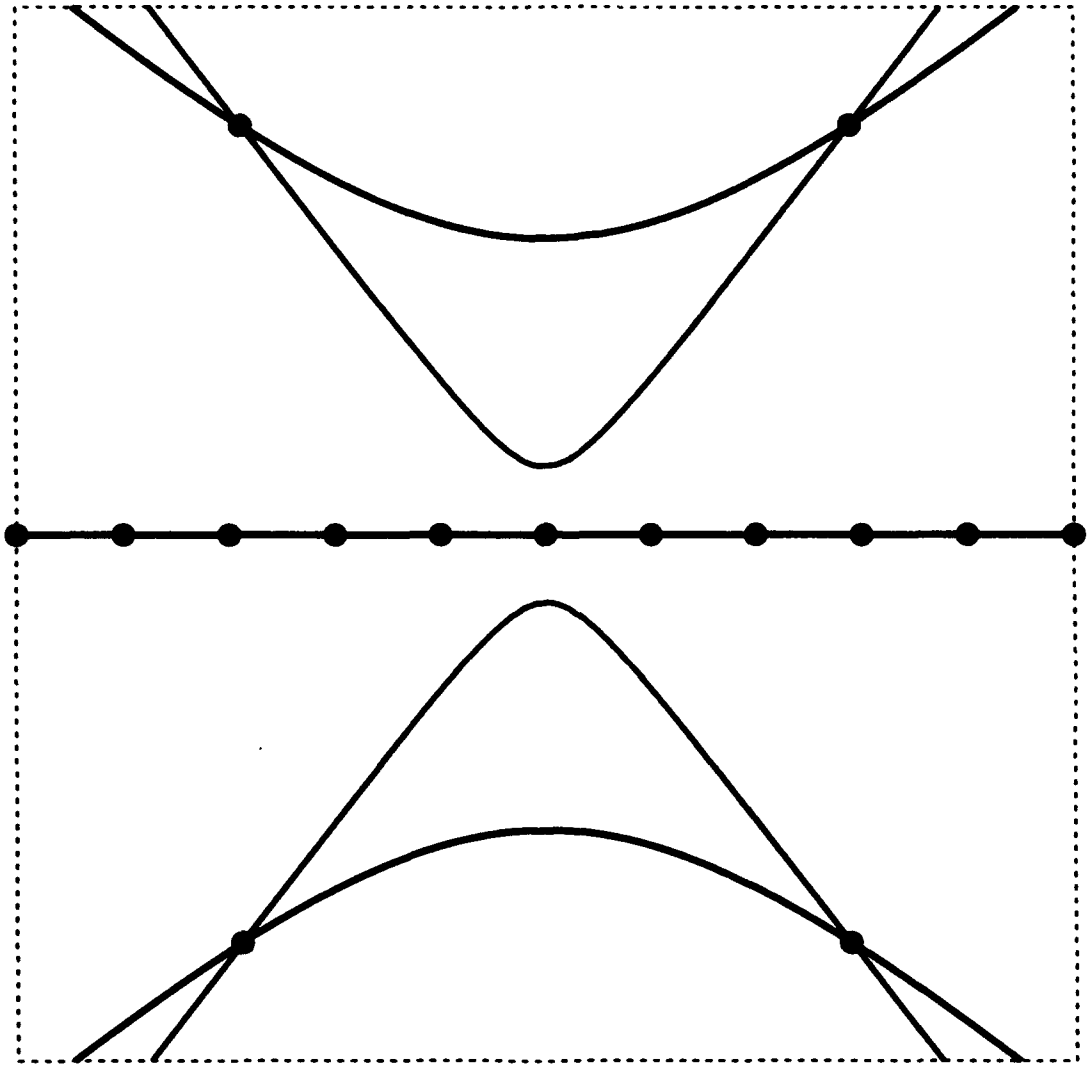

$\nu = .3000$

Superconvergence of u, y

Serendipity shape functions, $p = 3$

Fig. 11b

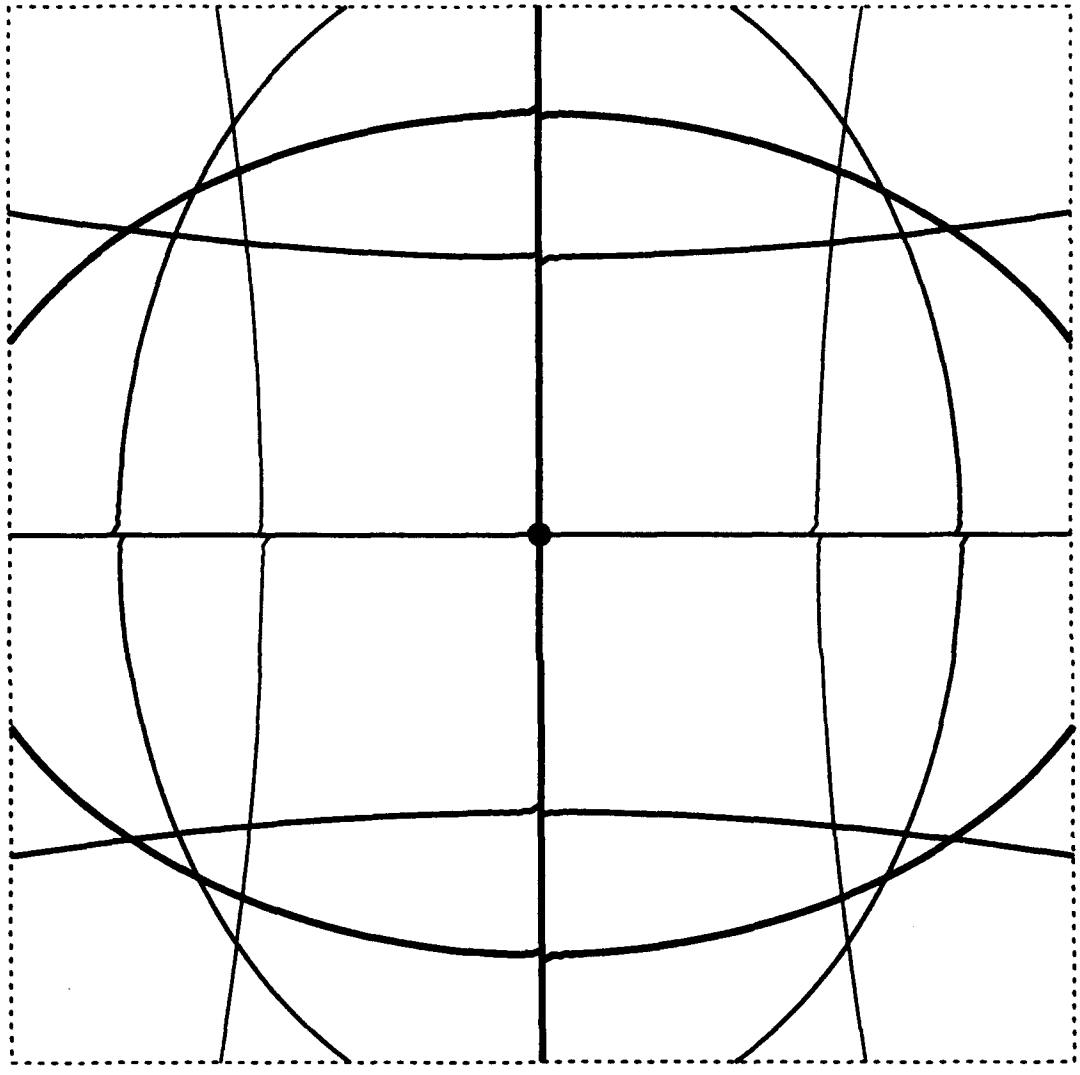

$\nu =$ .3000

Superconvergence for Stress σ_{xx}

Serendipity shape functions , p = 3

Fig. 11c

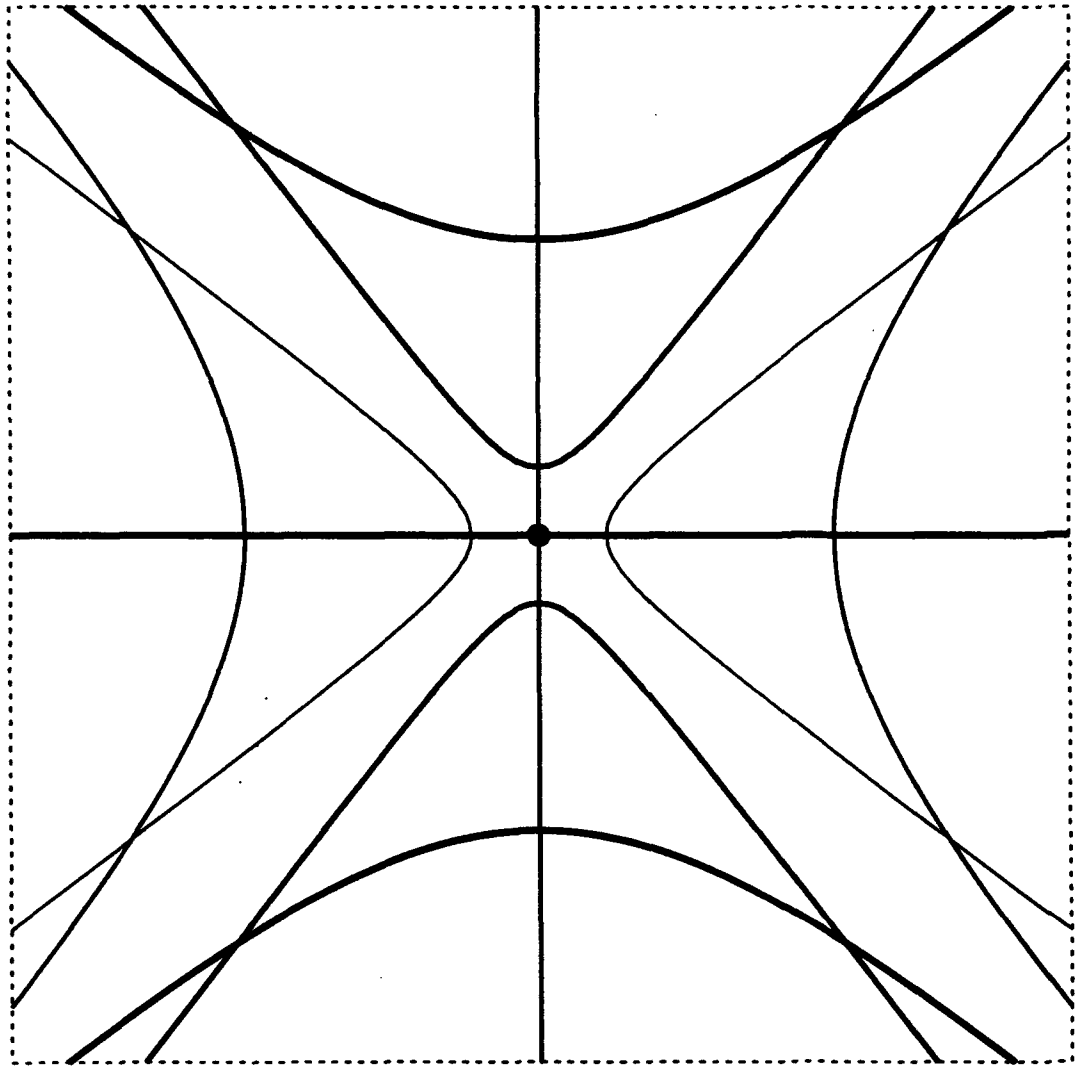

$\nu =$ .3000

Superconvergence for Strain ε_{xy}

Serendipity shape functions , p = 3

Fig. 11d

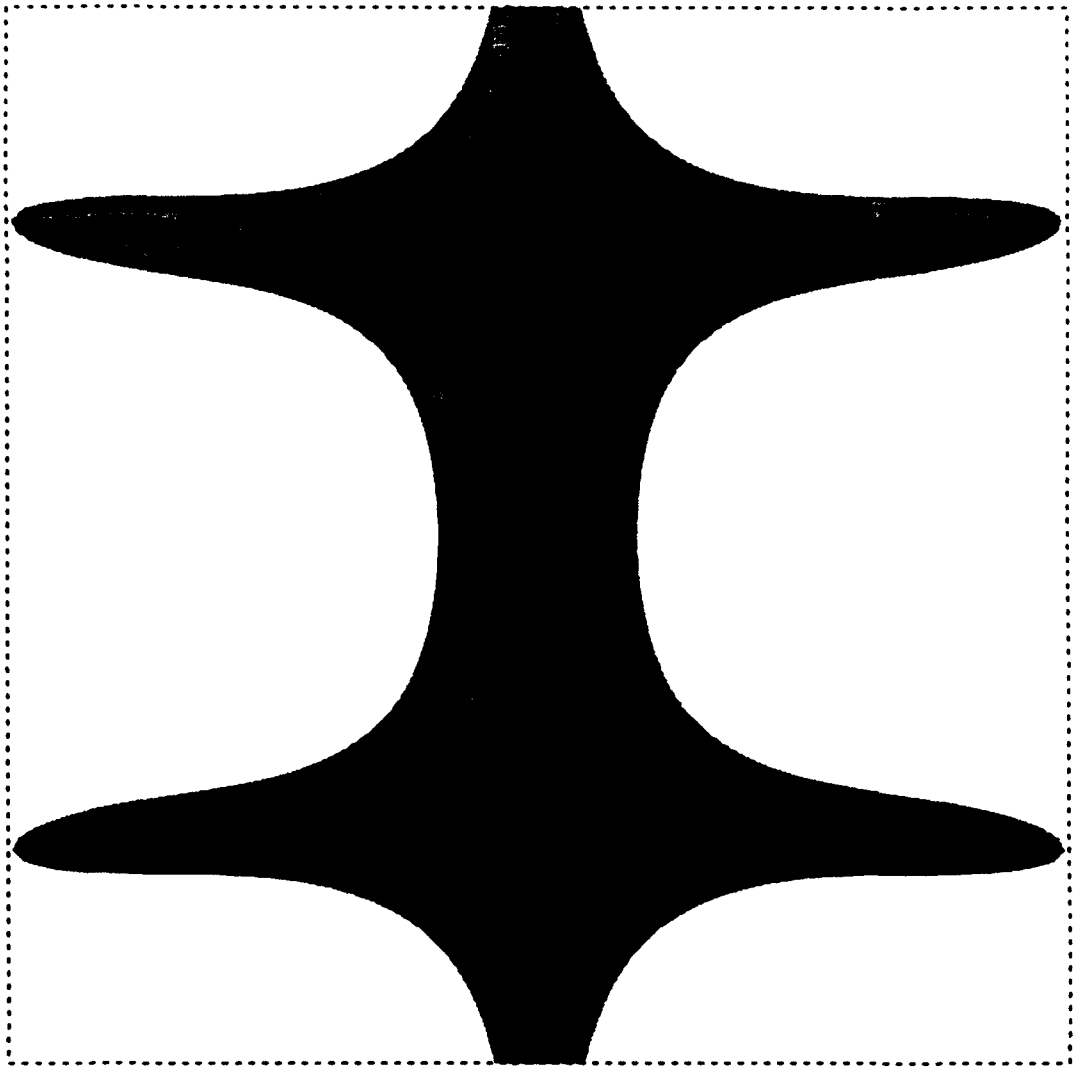

Minimum η % = .00

ν = .3000

Superconvergence of the *u,x*
Simplified approach with L-2 norm

Serendipity shape functions , p = 3

.0%
5.0%
10.0%
25.0%

Fig. 12a

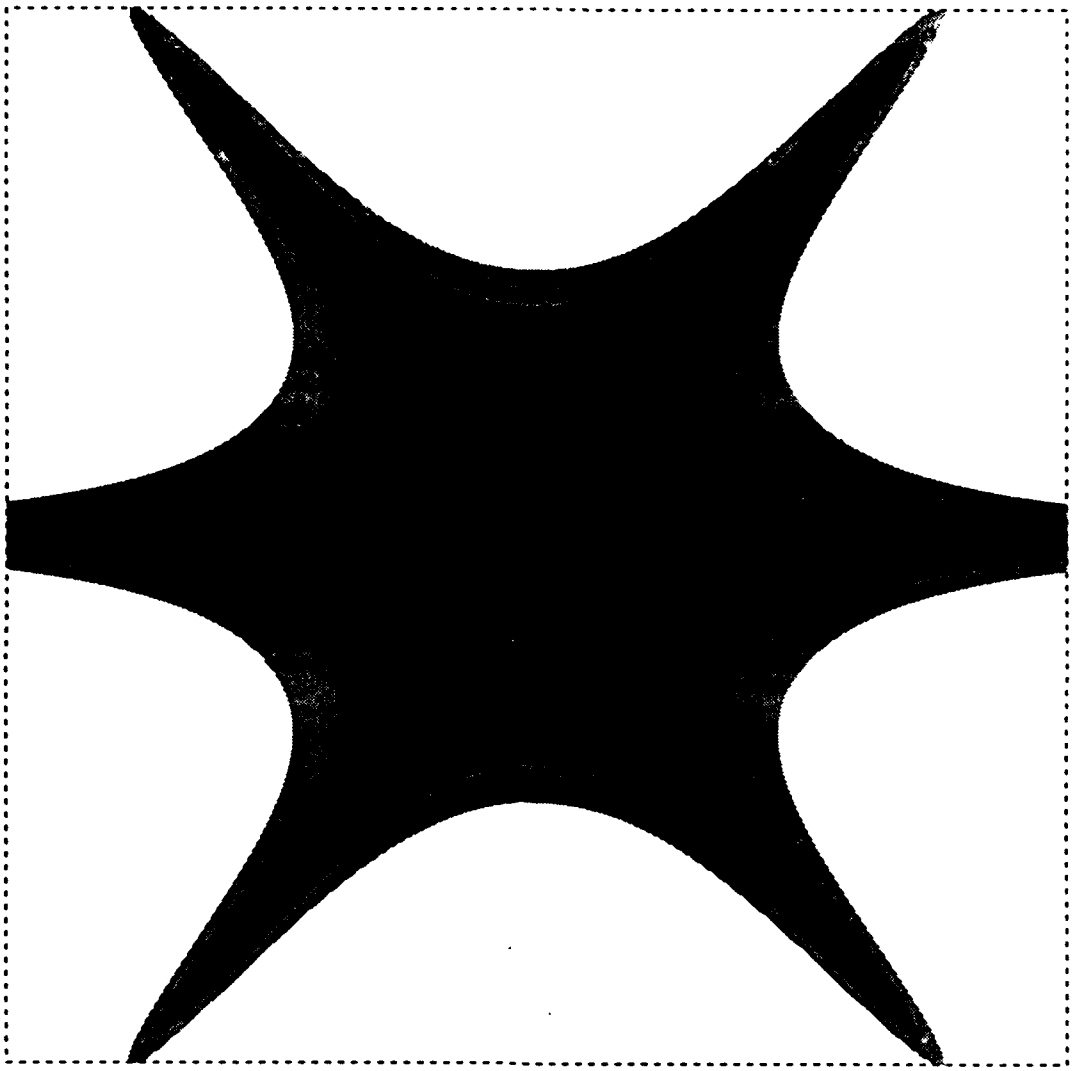

Minimum η % = .00

ν = .3000

Superconvergence of the *u,y*
Simplified approach with L-2 norm

Serendipity shape functions , p = 3

Fig. 12b

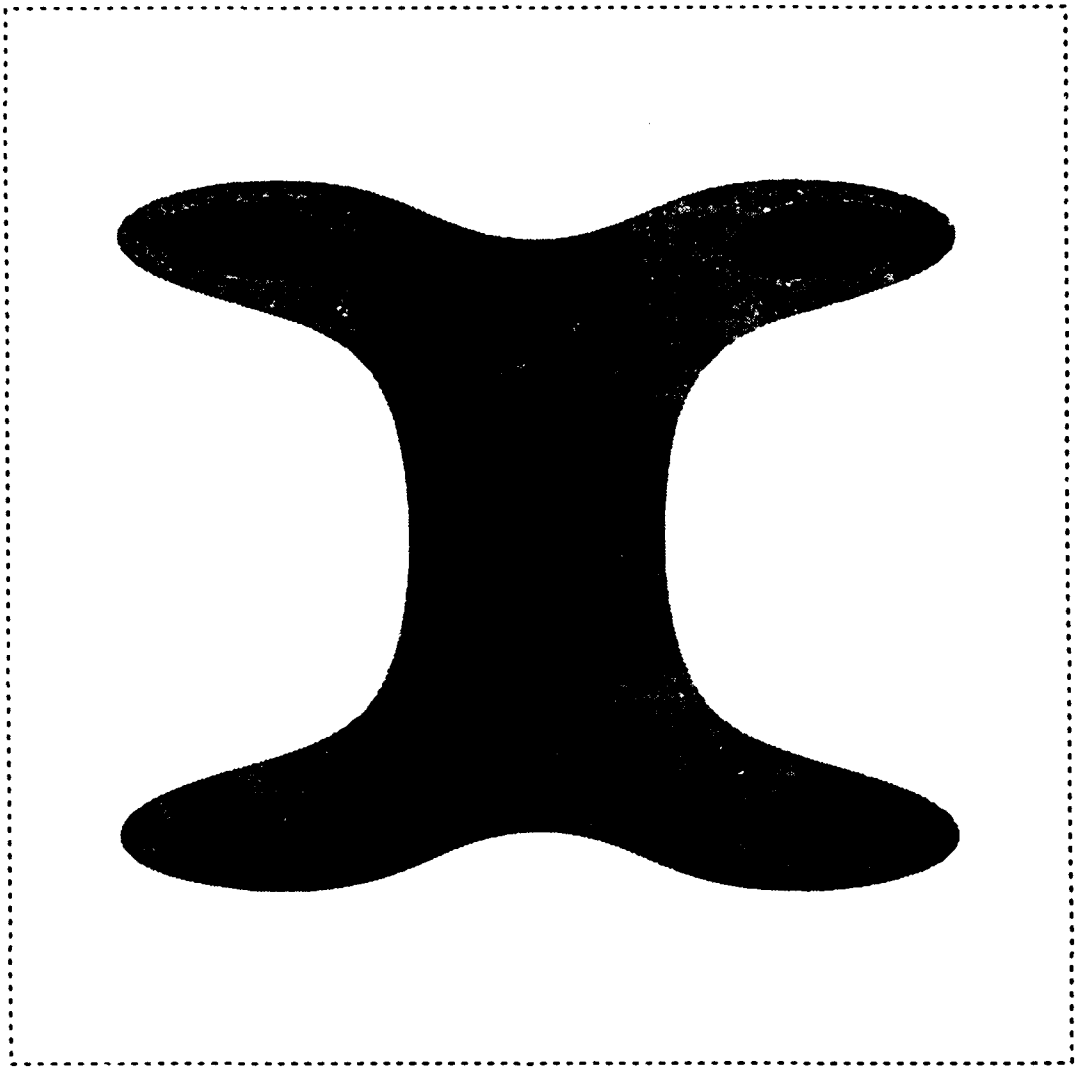

Minimum η % = .00

ν = .3000

Superconvergence for Stress σ_{xx}

Simplified approach with L-2 norm

Serendipity shape functions , p = 3

.0%

25.0%

50.0%

75.0%

Fig. 12c

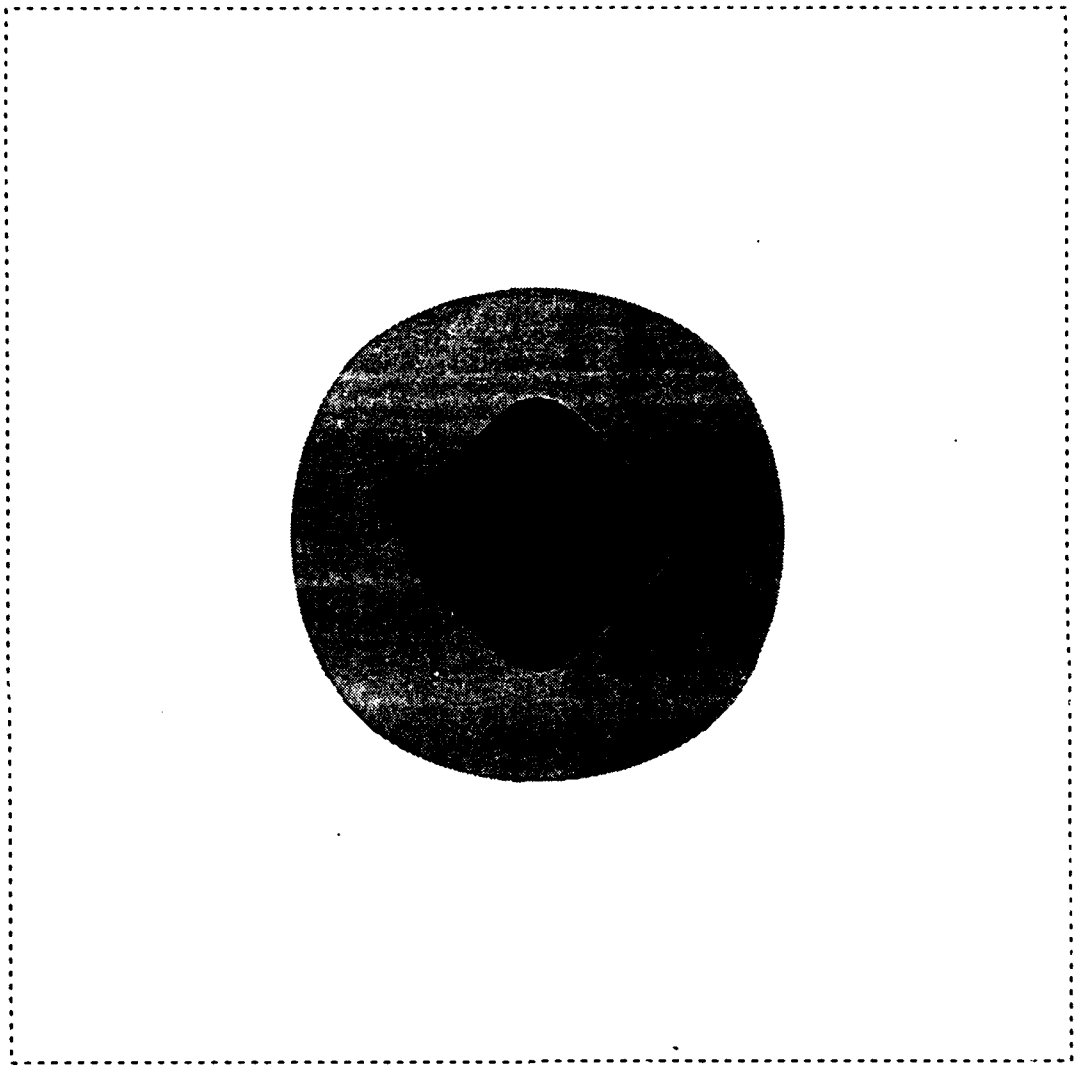

Minimum η % = .00

ν = .3000

Superconvergence for Strain ε_{xy}

Simplified approach with L-2 norm

Serendipity shape functions , p = 3

.0%
5.0%
10.0%
25.0%

Fig. 12d

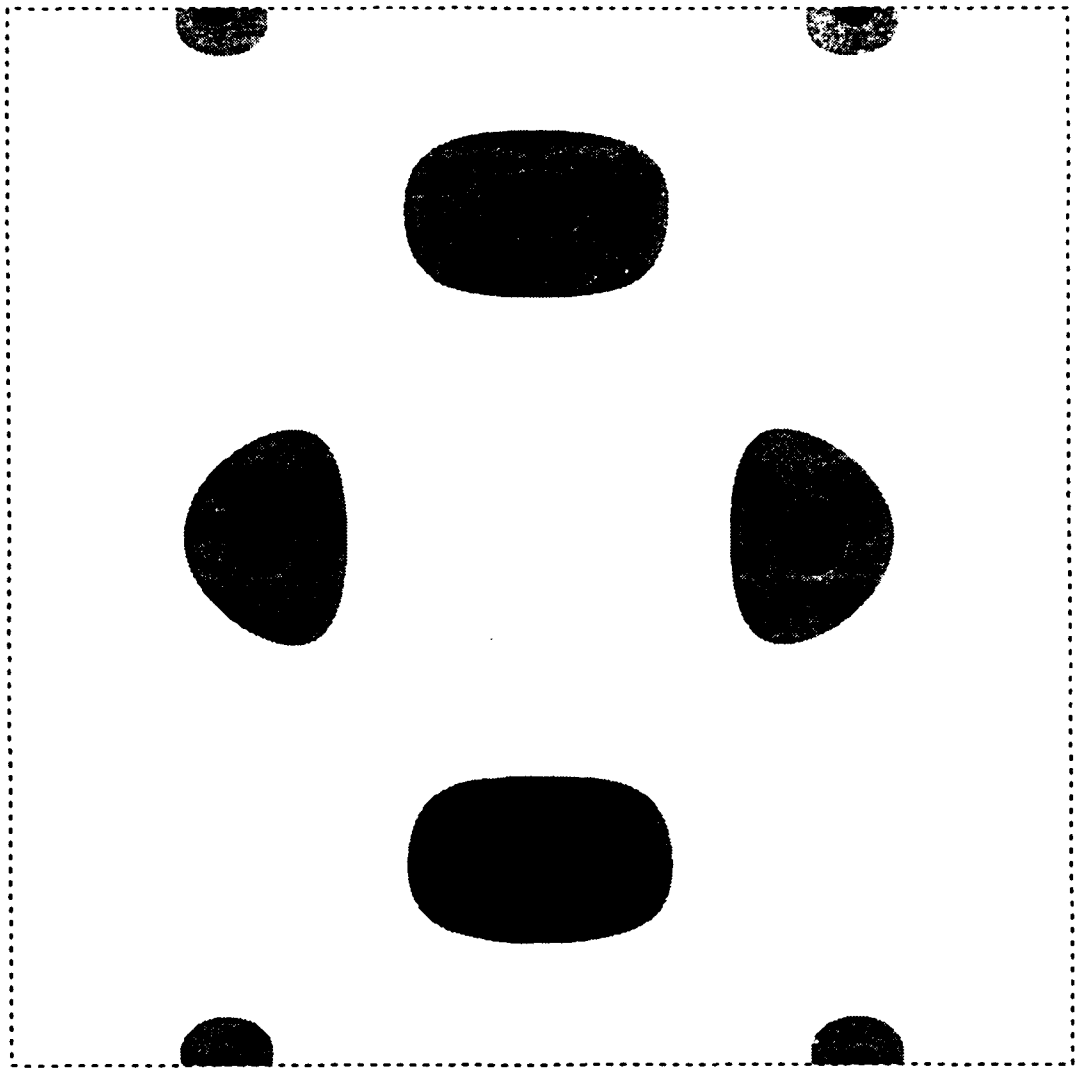

Minimum η % = .15

ν = .3000

Superconvergence of the *u,x*
Simplified approach with L-2 norm

***Serendipity shape functions*, p = 4**

.0%
5.0%
10.0%
25.0%

Fig. 13a

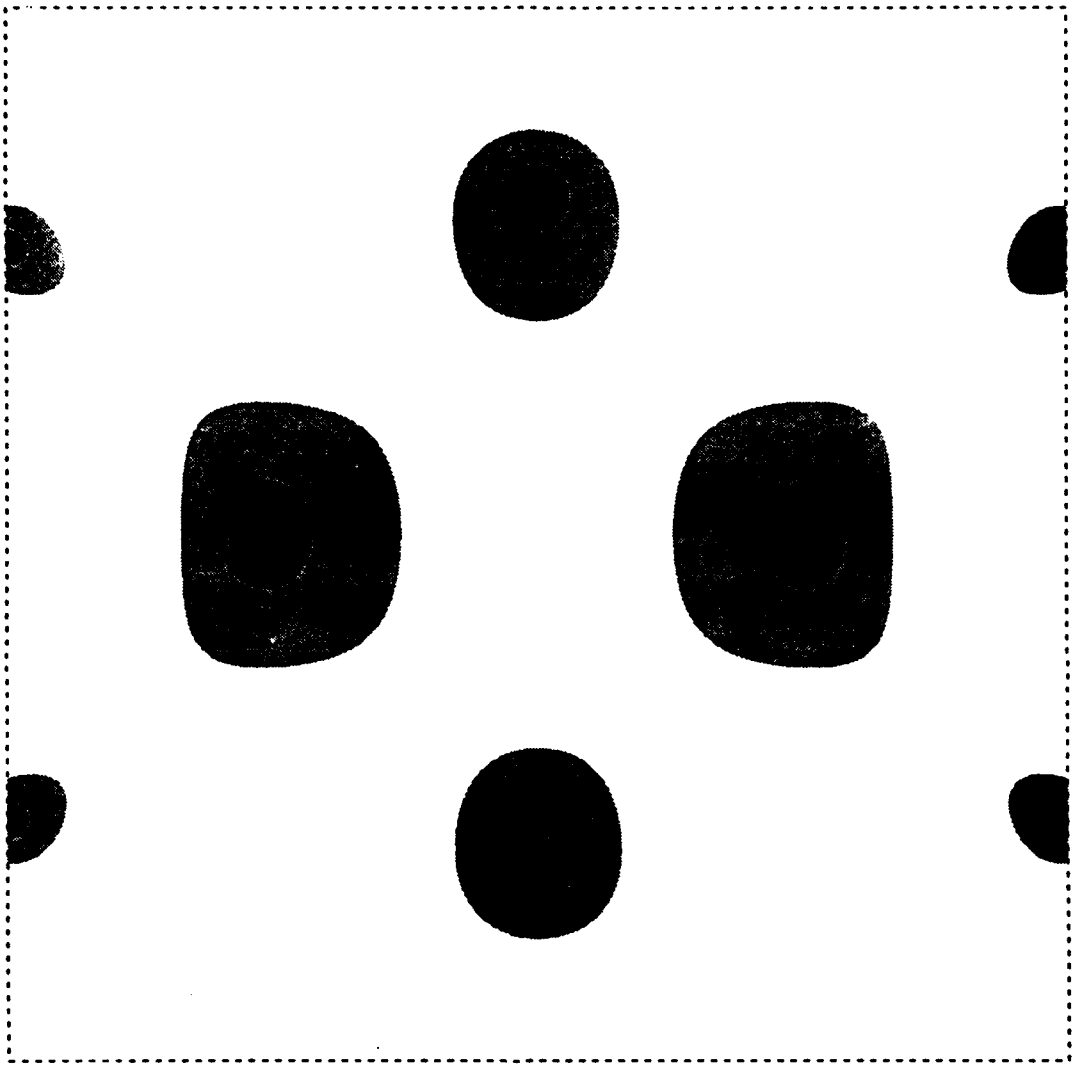

Minimum η % = .09

ν = .3000

Superconvergence of the u_y
Simplified approach with L-2 norm

Serendipity shape functions , p = 4

.0%
5.0%
10.0%
25.0%

Fig. 13b

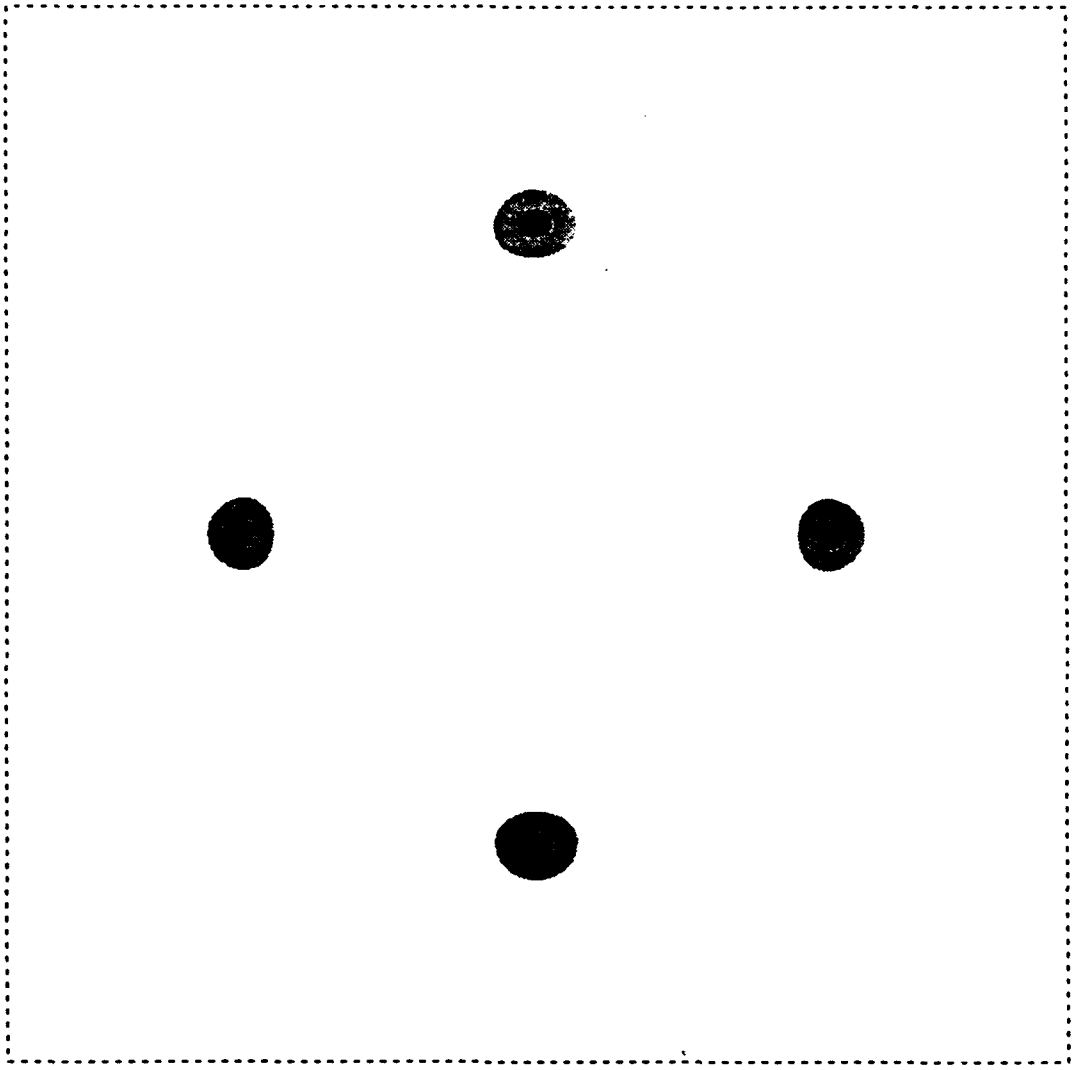

Minimum η % = .81

ν = .3000

Superconvergence for Stress σ_{xx}

Simplified approach with L-2 norm

Serendipity shape functions , p = 4

Fig. 13c

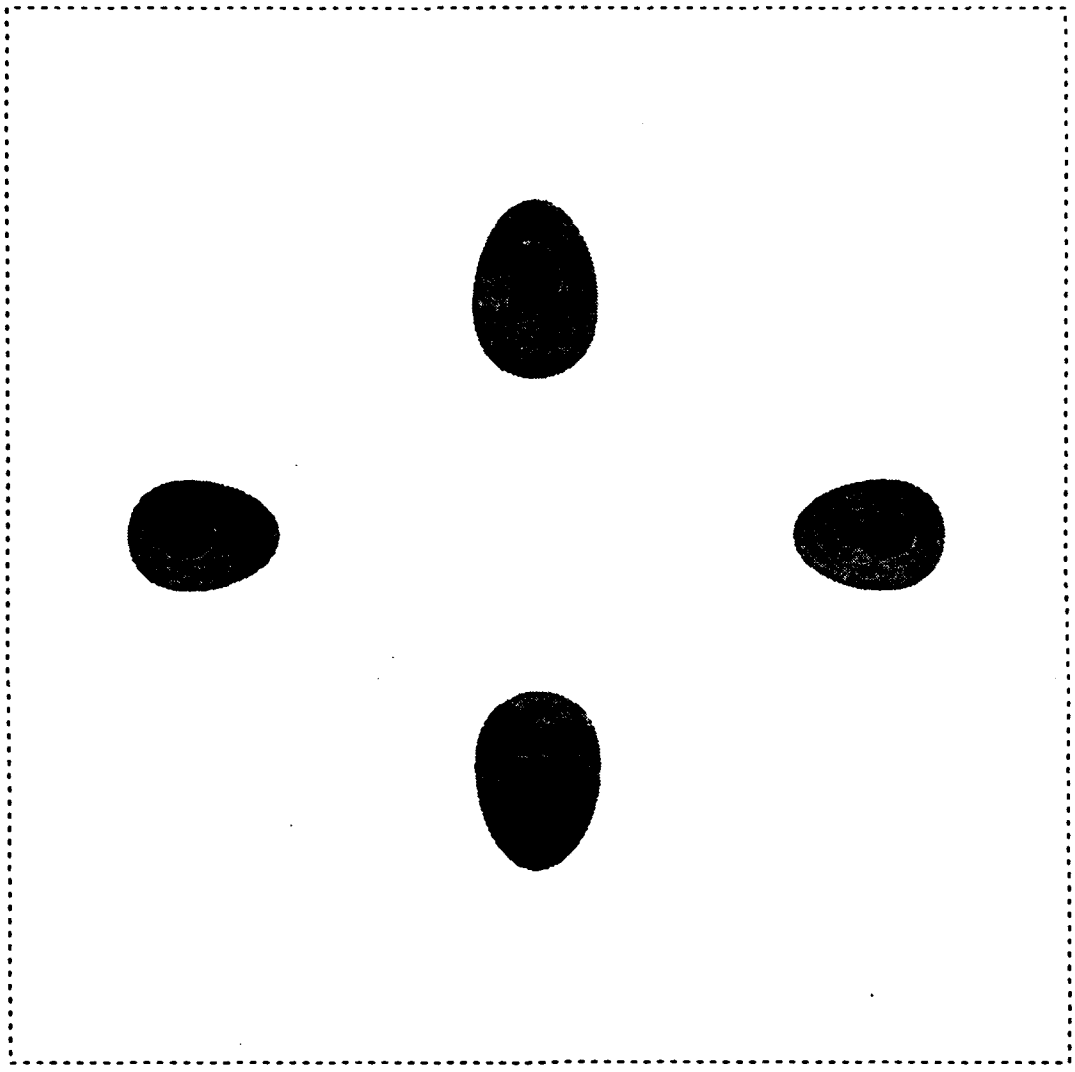

Minimum η % = .50

ν = .3000

Superconvergence for Strain ε_{xy}

Simplified approach with L-2 norm

Serendipity shape functions , p = 4

.0%
5.0%
10.0%
25.0%

Fig. 13d

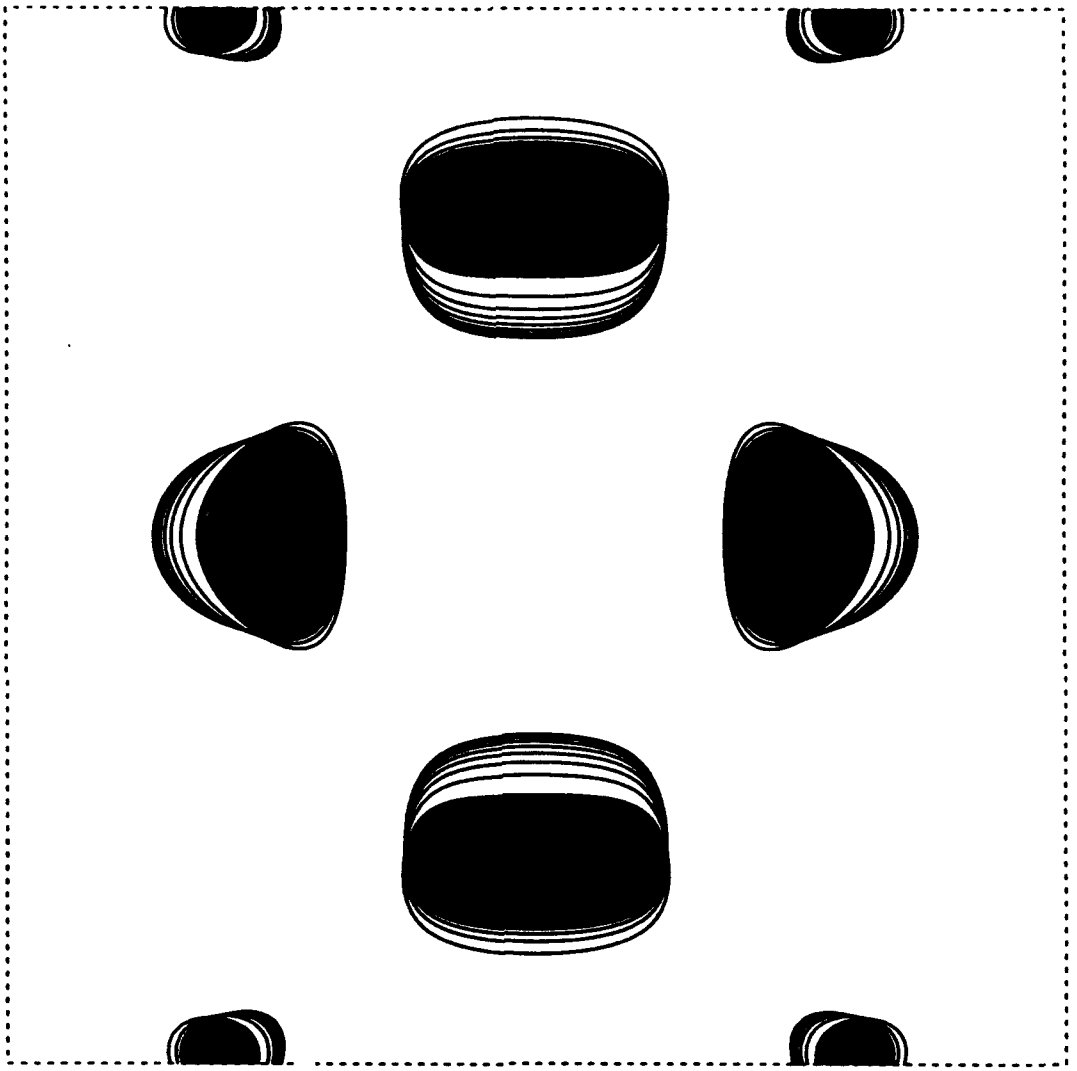

.0%
25.0%

Superconvergence of the $u_{,x}$
Simplified approach with L-2 norm

Serendipity shape functions , p = 4

Fig. 14a

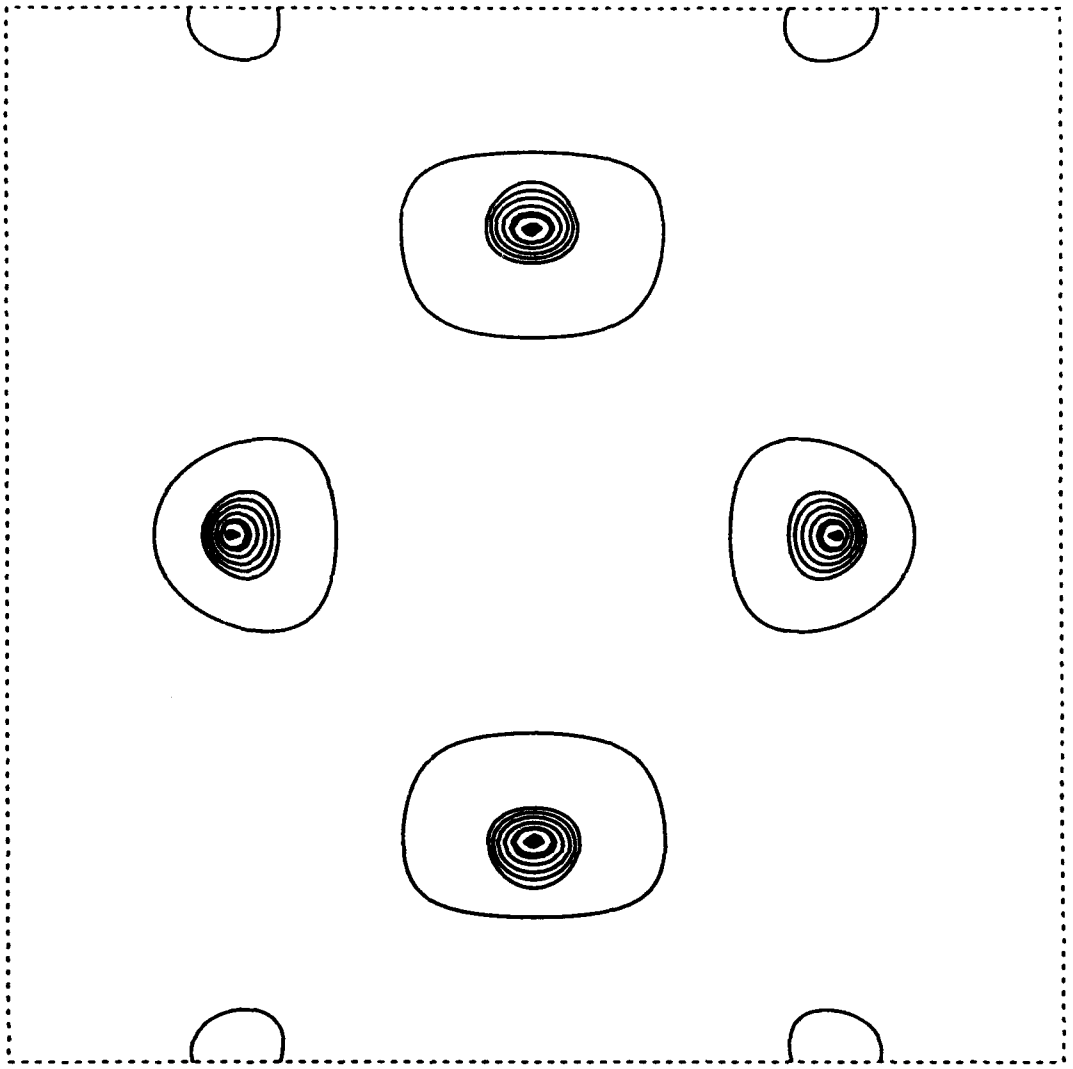

.0%
25.0%

Superconvergence for Stress σ_{xx}
Simplified approach with L-2 norm
Serendipity shape functions , p = 4

Fig. 14b

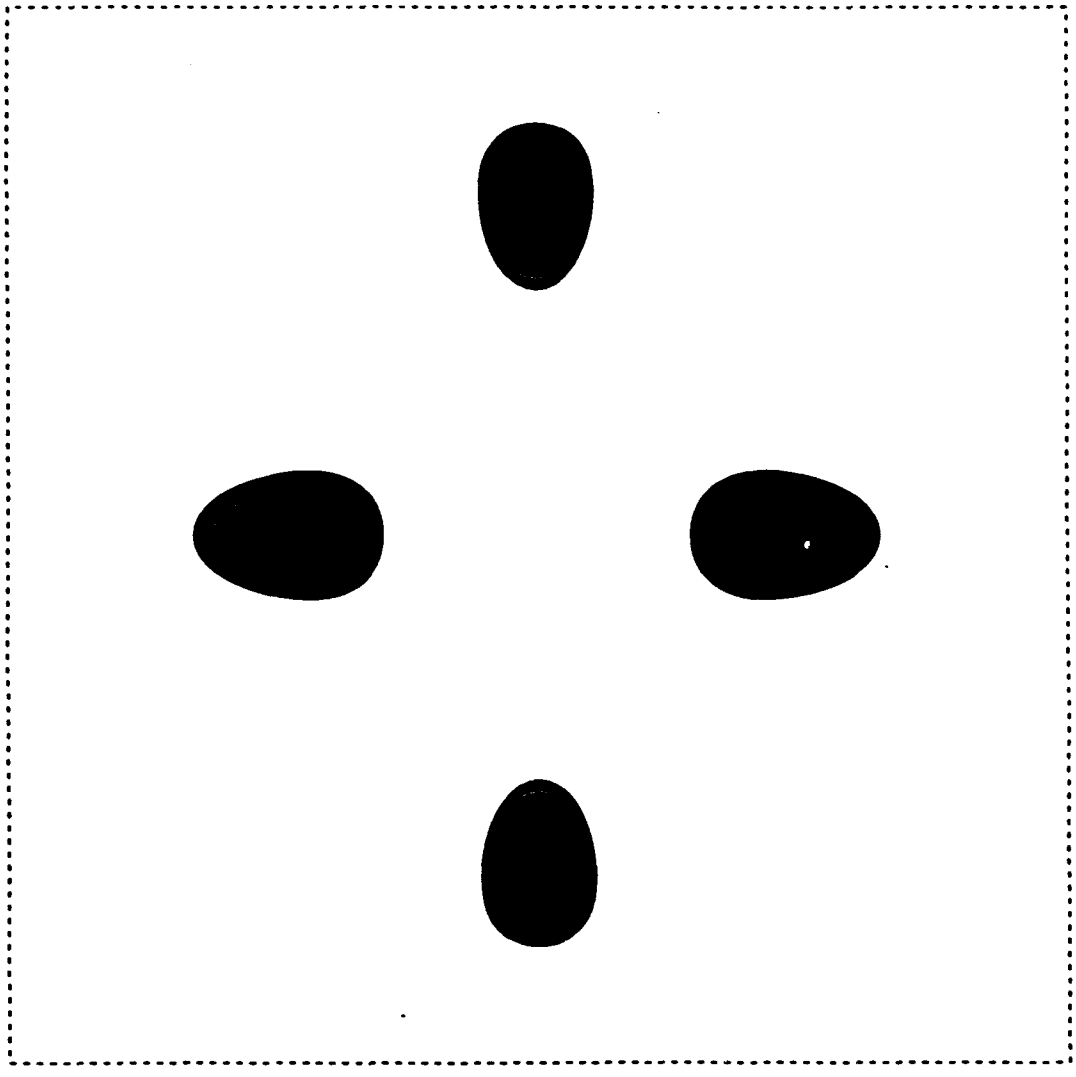

.0%
25.0%

Superconvergence for Strain ε_{xy}
Simplified approach with L-2 norm

Serendipity shape functions , p = 4

Fig. 14c

The Laboratory for Numerical Analysis is an integral part of the Institute for Physical Science and Technology of the University of Maryland, under the general administration of the Director, Institute for Physical Science and Technology. It has the following goals:

- To conduct research in the mathematical theory and computational implementation of numerical analysis and related topics, with emphasis on the numerical treatment of linear and nonlinear differential equations and problems in linear and nonlinear algebra.

- To help bridge gaps between computational directions in engineering, physics, etc., and those in the mathematical community.

- To provide a limited consulting service in all areas of numerical mathematics to the University as a whole, and also to government agencies and industries in the State of Maryland and the Washington Metropolitan area.

- To assist with the education of numerical analysts, especially at the postdoctoral level, in conjunction with the Interdisciplinary Applied Mathematics Program and the programs of the Mathematics and Computer Science Departments. This includes active collaboration with government agencies such as the National Institute of Standards and Technology.

- To be an international center of study and research for foreign students in numerical mathematics who are supported by foreign governments or exchange agencies (Fulbright, etc.).

Further information may be obtained from **Professor I. Babuška**,Chairman, Laboratory for Numerical Analysis, Institute for Physical Science and Technology, University of Maryland, College Park, Maryland 20742-2431.